ABSTRACT

Title of dissertation:	SYNTHESIS AND CONTROL OF MORPHOLOGY OF POLY(METHYL METHACRYLATE) AND POLY ACRYLIC ACID MICRO-PARTICLES BY THE MODIFIED SUSPENSION POLYMERIZATION TECHNIQUES
	Yunju Jung Kim, Doctor of Philosophy, 2015
Dissertation directed by:	Professor Kyu Yong Choi
	Department of Chemical and Biomolecular Engineering

This dissertation studied the synthesis and control of morphology of two kinds of polymers by modified suspension polymerization techniques. The first polymer, poly (methyl methacrylate), is a transparent thermoplastic polymer, which is typically used in diffusing film in the backlight unit of an LCD. Also, the synthesis of micron-sized polymer particles with complex internal morphologies such as hollows, multihollows, and multiporous structures is of growing interest in many technological applications such as microelectronic displays and microencapsulation. The direct synthesis of such materials is carried out in heterogeneous processes with controlled phase

separation mechanisms. In such systems, detailed knowledge of heterogeneous polymerization kinetics and phase separation phenomena is essential for investigating the process characteristics.

An *in situ* polymerization and phase separation technique has been used to construct a ternary phase diagram for the free radical precipitation polymerization of methyl methacrylate (MMA), *n*-hexane, and poly(methyl methacrylate) (PMMA) system. The onset of the phase separation point during polymerization is directly monitored in real time by laser light scattering (LLS) technique for a broad range of polymer concentrations. The presented method overcomes the difficulty of determining the cloud points by titrating unreactive blends of polymer and solvent at high initial monomer concentrations that lead to high polymer concentration and high viscosity of the mixture fluid at the system phase separation point.

We present the micro dispersive suspension polymerization (MDSP) process to produce complex particle morphologies in a single-stage process. MDSP is a hybrid of suspension and dispersion polymerizations. The micron-sized polymer particles are polymerized by suspension polymerization, and the internal morphology of particle is polymerized by dispersion polymerization inside the polymer particles. Varying the initial conditions for the phase separation in precipitation and dispersion polymerizations, final particles' morphology may change from solid polymer particles to complex porous polymeric structures. In this heterogeneous process, the system evolution depends on the composition and molecular characteristics of the coexisting phases and on the characteristics of the interface. Using MDSP, we were able to develop a phase diagram to show the regions of multi-hollow/porous and core-shell/pomegranate-like poly (methyl methacrylate) (PMMA) particles. We also show that controlling morphology of polymer particles by thermodynamic and kinetic variables is technically feasible.

The second polymer, poly (acrylic acid), is an absorbing polymer. Superabsorbent polymers (SAP) can absorb and retain extremely large amounts of water or aqueous solutions relative to their own mass. Partially neutralized sodium polyacrylate is industrially a very important polymer for many applications. However, in industry sodium polyacrylate is mostly manufactured by bulk polymerization, and the resultant bulk polymer is pulverized using a kneader to obtain small discrete polymer particles. It is environment-unfriendly process and the produced granules from bulk have irregular shapes, rather than a spherical shape. This study is aimed at investigating the inverse suspension polymerization of acrylic acid to make spherical polymer particles. In particular, the study is focused on how the resulting polymer morphology and characteristics are affected by the polymerization conditions.

A feasible and simple technique to obtain Na-polyacrylate microparticles with sizes below 10 μm was investigated using a high shear mixing device. To maintain the stability of submicron size of aqueous droplets in the oil medium, a co-surfactant system containing Span 80 and Tween 80 was used. Neutralization of acrylic acid was proved from EDX analysis. Na-polyacrylate submicron particles were characterized by size, surface morphology, swelling capacity, and conversion. When the speed of homogenization was lowered from 3000 rpm to 1000 rpm, particles over 10 μm were obtained, but more nano-sized particles were present outside.

We also developed the technique above to increase polymer particle size to tens of microns. In this process, a wrinkled and cracked surface of Na-polyacrylate particles was observed in the special environment of post treatment. Surface area, swelling capacity, and swelling speed of different morphologies and sizes were characterized and analyzed.

In order to synthesize spherical Na-polyacrylate particles with smooth surface regardless of post treatment, polymerization time was progressed longer than 20 hr. Na-polyacrylate particles

had a solid structure at high conversion over 0.996 after longer than 15 hrs of polymerization, which made particles maintain their shapes regardless of post treatment. When a high monomer concentration was used in this polymerization, perfectly smooth and spherical polymer particles were obtained after 9 hr, which was faster than when a lower monomer concentration was used.

SYNTHESIS AND CONTROL OF MORPHOLOGY OF POLY (METHYL METHACRYLATE) AND POLY (ACRYLIC ACID) PARTICLES BY THE MODIFIED SUSPENSION POLYMERIZATION TECHNIQUES

By

Yunju Jung Kim

Dissertation submitted to the Faculty of the Graduate School of the
University of Maryland, College Park, in partial fulfillment
of the requirements for the degree of
Doctor of Philosophy
2015

Advisory Committee:
Professor Kyu Yong Choi, Chair
Professor Namsun Wang
Professor Dongxia Liu
Professor Amy J. Karlsson
Professor Sang Bok Lee

Acknowledgements

I would like to express my deep and sincere appreciation to my advisor, Professor Kyu Yong Choi for his guidance and support throughout the study for ten years. He especially impressed me by encouraging and helping me to be able to restart the research again after maternity and childcare leave for three years. I would like to thank dissertation committee, Professors Namsun Wang, Dongxia Liu, Amy J. Karlsson, and Sang Bok Lee.

I'm thankful to my lab mates, Sangyool Lee, Woojic Yang, Lisa Wiest, Paul Han, and Heetae Jeon. They have never said "no" to me when I asked for them anytime. I want to say thank you to the alumni in my lab, Joongjin Han and Inhak Baick, who graduated few years ago. They helped me to initiate study abroad well. Also, Laleh Emdadi in Dr. Liu's lab helped me the BET analysis, and I really appreciate it. The supports from all the faculty and staff in the department of Chemical and Biomolecular Engineering are gratefully appreciated.

I really would like to give my gratitude to my parents who made me be here, my husband who always supports me unconditionally, my parents-in-law who are caring for my children instead of me even now, and my children I love most in the world who have to go to sleep every night without crying even though their mom could not be with them. Above all, I am pleased to get to know God during this PhD study.

Table of Contents

List of Tables

List of Figures

Chapter 1 Introduction of Control of Various Morphological Changes of Poly Methyl Methacrylate by Micro-Dispersive Suspension Polymerization

1.1. Introduction

1.1.1. Background and motivation

Design of polymer particles with specific morphologies are of both significant scientific and industrial importance. The most well-known polymer particle structures of complexity include core-shell, multi-porous, cage-like, hollow, and multi-hollow morphologies. Figure 1-1 illustrates schematics of these particles and the representative scanning electron microscopic (SEM) images reported in the literature [1-4].
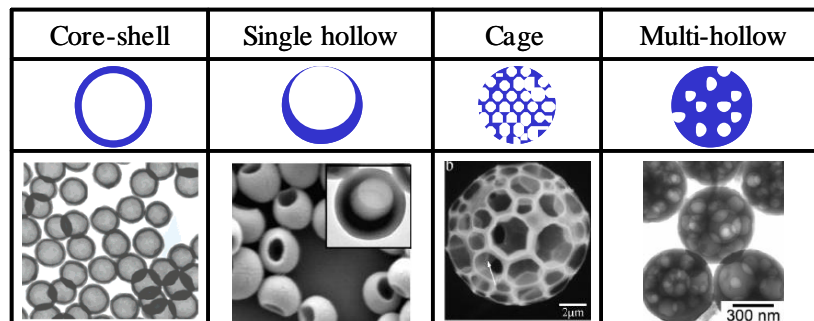
Figure 1-1. Schematic and SEM images of polymer particles of various morphological structures.

These polymer particles of different size ranges are used in a wide variety of applications such as microcapsules for drug delivery systems[5-9], protection of biologically active materials (e.g., enzymes, proteins, and DNAs) [1,10], weight-saving thermal insulation [11], hiding and opaquifying agents [12-14], floating materials for absorbing organic oils [15,16], fabrication of electromagnetic wave absorbing materials for the absorption or dispersion of the electromagnetic energy for stealth applications[17,18]. These polymer particles with voids can also be used for making magnetic composite particles for wastewater treatment, separation and purification of enzymes and cells [19], encapsulation of functional cosmetic compounds [20], temperature-responsive microspheres [21-23], phase change material for thermal energy storage[24,25], and thermally expandable microspheres [26,27] .

Among these particle morphologies, multi-hollow particles are of recent interest. A multi-hollow particle contains more than one cavity. The multi-hollow particles are differentiated from multi-porous particles where the void space is present as interconnected tortuous pores or channels instead of geometrically well-defined spherical cavities (hollows).

One of the interesting potential applications of micron-sized (5 ~ 30 μm) multi-hollow polymer particles is in light diffusing films for high luminance in the backlight unit (BLU) of LCD devices (Fig. 1-2). The most commonly used diffuser films in the electronics industry are polymer films coated with micron-sized solid poly (methyl methacrylate) (PMMA) particles onto a transparent polyester film. The multi-hollow polymer particles of 5 ~ 30 μm in diameter with controlled sizes of internal cavities can be a new means to provide increased light diffraction path lengths with minimal particle population, making the display brighter and reducing the power requirement for the backlight unit.
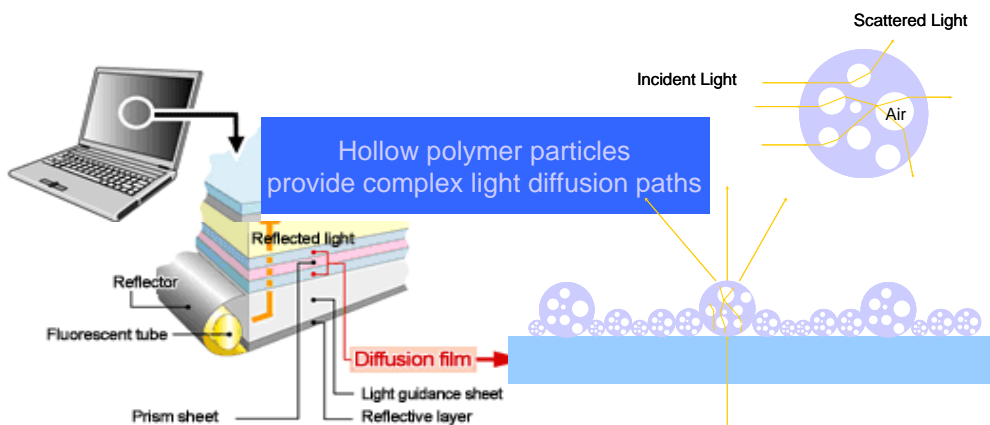
Figure 1-2. Description of light diffusion through hollow polymer particles applied in LCD devices.

1.1.2. Review of previous works

A variety of chemical and physical synthetic techniques have been reported in the scientific and patent literature to produce sub-micron sized hollow latex polymer particles. Most of these reported techniques employ a multi-stage process where seed polymer particles produced first by emulsion polymerization are swollen with solvent and with or without reactive components. Finally, the solvent is removed from the swollen particles by a subsequent evaporation process. For example, in a dynamic swelling method, polystyrene (PS) seed particles are dispersed in an ethanol/water mixture where divinylbenzene (DVB, crosslinking agent), toluene, and benzoyl peroxide (BPO) are dissolved. The dispersed oil phase is absorbed by the seed particles and the polymerization is carried out. As the polymerization proceeds, the PS moves towards the interior surface of the particles due to the crosslinking reaction of DVB, allowing the hydrophobic toluene to separate in the center of the particles. As a result, hollow particles are obtained after the toluene is removed [28,29]. In osmotic swelling methods, polymer particles (300-400 nm) with a

3

carboxylated polymer-core and a thermoplastic polymer-shell are first produced by emulsion polymerization. Then, the polymer-core ionized by the addition of an alkali is expanded by osmotic swelling, resulting in submicron-sized hollow particles with water and ionized polymer inside [13]. There are numerous variations of this seed particle/swelling/evaporation technique. Other techniques for hollow polymer particles include the interfacial cross-linking polymerization and precipitation in oil-in-water emulsion system [30]. In a layer-by-layer assembly techniques where a solid particle or oil droplet is used as a template, a polyelectrolyte of opposite charge is adsorbed, followed by the sequential adsorption of alternate layers of oppositely charged polyelectrolyes. As the solid core is dissolved out, water penetrates and swells the polymer shell [23,31]. Silica micro-particles can also be used as a template for surface functionalization: as the silica core is etched out by an HF solution, a core-shell structure is formed. Most of these reported methods offer effective means to synthesize submicron-sized hollow latex polymer particles. However, the preparation processes are mostly multi-step processes and they are complex and time consuming, especially in making micron-size particles. Also, very few techniques allow one to produce a wide variety of particle morphologies.

Most of the multi-stage synthetic methods to produce polymer particles with internal voids (hollows or cavities) utilize thermodynamic phase separation principles. For example, non-solvent for the polymer is mixed with the polymerization precursors or polymer solution. The subsequent reaction (e.g. cross-linking) and phase separation of the mixture from a fluid droplet leads to the formation of highly porous cross-linked network.

Single hollow or core-shell latex particles are perhaps the most extensively studied in the past two decades in developing functional polymer particles, mostly by emulsion polymerization techniques. To make micron-size core-shell particles, latex seed polymer particles are swollen with

monomer and polymerized. The removal of the polymer core by repeated centrifugation using a solvent yields a core-shell structure. Another technique to make hollow particles involves a stable emulsion of surface-sulfonated polystyrene particles mixed with monomer by mechanical stirring. The monomer droplet interface is adsorbed by the polymer latex particles. Then, the surface layer of emulsion particles is swollen by the monomer. The monomer present between the swollen latex particles is polymerized by γ-ray irradiation to form a thin and hard shell. With the gradual decrease of the internal monomer, a hollow core is formed. The polymeric shell shrinks and the swollen polystyrene particles disengage themselves from the polymeric shell, leaving behind a porous polymer shell [3,32-34]. Colloidosome [35] is another method to prepare hollow, elastic capsules, with sizes ranging from micrometers to millimeters. The capsule surfaces are composed of a close-packed layer of colloidal particles, linked together to form a solid shell. The interstices between the particles form an array of uniform pores. Surface functionalization is also a frequently used method to make submicrometer-sized single hollow polymeric particles. For example, the surface of silica particles is functionalized to contain polymerizable vinyl groups. Then, a polymer shell is attached to these modified silica particles through the copolymerization of styrene and divinylbenzene during a dispersion polymerization. The silica core in the composite particles is etched out with an HF/ethanol solution to produce 200 nm hollow polymeric particles [36]. Atom transfer radical polymerization (ATRP) has also been attempted to prepare hollow nano-spheres [37]. The ATRP initiator is immobilized on the silica particles of about 25 nm, and the particles are reacted with styrene and methyl methacrylate (MMA) to a thin shell of block copolymer. The exposure to UV results in cross-linking of the PS shell and decomposition of the PMMA outer layer. After removal of the silica core by HF etching, hollow nanospheres with cross-linked PS shell of 20-60 nm in thickness and void cores of about 20-30 nm in diameter are obtained. Non-

reactive preparation techniques have also been reported. For example, 200 nm solid PS beads are suspended in water and swollen by adding a good solvent (eg. toluene or styrene) of the polymer. Toluene diffuses into the beads and the particle size increases by swelling. The swollen particles are quickly frozen in liquid nitrogen. Because of the poor thermal conductivity of PS, a temperature gradient is formed in the radial direction and solidification of toluene starts from the surface. As toluene is solidified, toluene moves towards the surface creating a void at the center. The frozen sample is slowly warmed up to let toluene evaporate in a vacuum or under ambient pressure. Once the temperature reaches the melting point of toluene (-93ºC), the PS chains migrate towards the surface of each particle by the flux of the evaporating toluene, increasing the void size [1]. The foregoing techniques reported in the literature are certainly quite effective in synthesizing single hollow sub-micron sized latex particles, but most of these techniques involve complex multiple preparation stages and very long processing time [14]. Also, very few techniques allow one to produce a wide variety of particle morphologies.

Compared to many literature on the synthesis of single hollow or core-shell polymer particles of sub-micron sizes, the preparation of micron-sized multi-hollow or core-shell polymer particles has not been studied well. One reported method to synthesize micron-sized multi-hollow polymer particles is a multi-stage process of the water-in-oil-in-water (W/O/W) emulsion technique [38-40]. In such a method, water-in-oil (W/O) emulsion is prepared and redispersed in water containing a polymeric stabilizer (polyvinyl alcohol, PVA) to form a stable water-in-oil-in-water (W/O/W) emulsion which is then polymerized for 10 hr. As the particles are washed by decantation in water and ethanol and dried under vacuum, multi-hollow particles are formed. The major drawback of this method is that obtaining a stable W/O/W emulsion is very difficult and only one type of particle morphology (multi-hollow) is obtainable.

Table 1-1. Previous works to synthesize hollow polymer particles
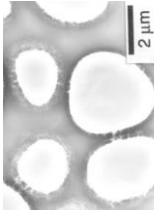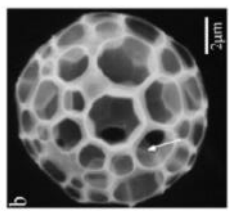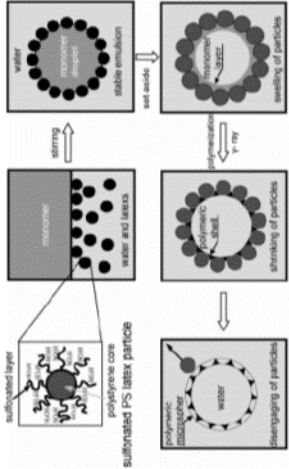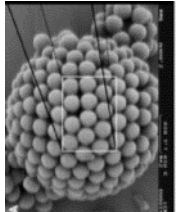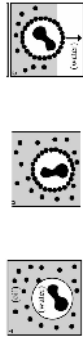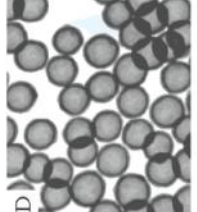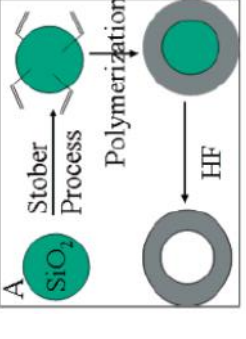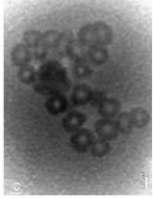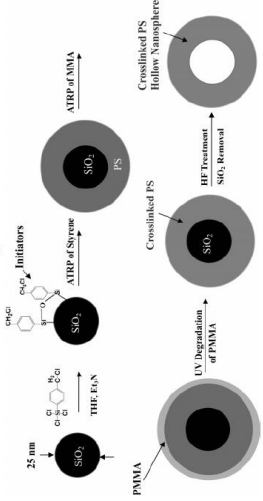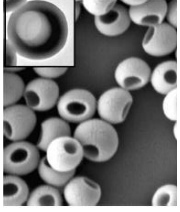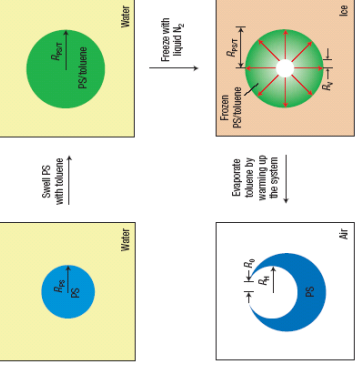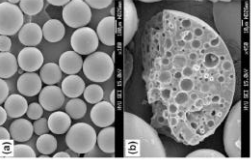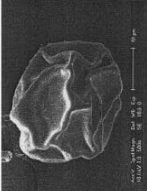
Method	Morphology	Procedure	Results & Limitations
Dynamic swelling method [28]		• Preparation of PMMA seed particles by dispersion polymerization (1.91microns) • Preparation of PMMA/PS composite particles • Extraction of PS from PMMA/PS composite particles • Toluene treatment of the PMMA/PS composite particles • Extraction of PMMA from the ultrathin crosssections of PMMA/PS composite particles	• Particle size:2~4 microns • Thickness: ~100 nm
Self-assembly of latex particles at the emulsion droplet interface [3]			• average diameter: 9.3~ 19 microns • PMMA particle -pore size: 1.92 microns -Shell thickness:172nm • PVA particle -pore size: 450nm -Shell thickness:38nm • This makes just one hole in one particle • It takes too long time
Selectively permeable capsules composed of colloidal particles [35]		• Adsorption of colloidal particles onto the interface of emulsion droplets • Locking together of the adsorbed particles to form an elastic shell • Making uniform holes in an elastic shell: heating above Tg of PS and making the 'necks' (sintering) • Removing the fluid interface by exchanging the external fluid with one that is miscible with the fluid inside the colloidosome • Transfer the capsules into the new fluid by gentle centrifugation	• Sintering: increasing the sintering time leads to smaller pores • after 20 min, the particles coalesced completely and the holes were fully closed • by using particles with different T_g, the sintering temperature can be adjusted over a wide range
Monodisperse polymer-shell-SiO$_2$ core particles by dispersion polymerization [2]			• Core size and shell thickness can be controlled. -outside diameters:200~700 nm -shell thickness:20~90nm • At a high monomer/silica ratio: thick shells, the hollow polymeric particles are robust and maintain their spherical shape. • at low monomer/silica ratios (<0.5) : shell is thin and flexible, and the hollow particles tend to deform • It takes too long time(at lease 6hr) • Particle size is too small

Table 1-1. Previous works to synthesize hollow polymer particles (continued)

Method	Morphology	Procedure	Results & Limitations
Surface-initiated Polymerization [37]			• Thickness: 20-60 nm • diameter of void cores: about 20-30 nm • It takes too long time(about 40hr) • Particle size is too small
Polymer hollow particles with controllable holes in their surfaces [1]			• Size of PS particle: 200nm • Size of hollow particle: -toluene: 269nm with an opening of 224 nm in radius Ro (evaporation under vacuum) -styrene: 290nm with an opening of 50 nm in radius Ro (evaporation under vacuum) -evaporation under ambient pressure and at a temperature higher than the melting point of styrene : Ro=126 nm • A stronger flux of solvent evaporation is involved in the toluene case, leading to the formation of holes with larger openings. • The enlargement of the opening is probably related to the magnitude of evaporation flux: as the temperature is increased, the flux of styrene evaporation becomes stronger leading to a larger opening at the surface. to the formation of holes with larger openings. • The temperature was controlled below 0 °C by surrounding the sample with a cooling bath or keeping the sample in a freezer
Water-in-oil-in-water emulsion polymerization [40]		• Preparation of the W/O/W emulsion -Aqueous solution was dropped into an oil phase(composed of MMA, EGDMA, Arlacel P135, and ADVN) -Water/oil mixture was homogenized at 10000 rpm for 5 min at room temperature. -W/O emulsion was redispersed by homogenizing it mildly again at 500 rpm for 5 min in PVA aqueous solution, obtaining finally a stable W/O/W emulsion • Polymerization at 60 C for 10 h while agitating it at a speed of 250rpm • Washing and Drying	• the size of the final W/O/W emulsions was rather affected by the concentration of PVA, resulting from the hydrophobic association of unsaponificated parts in PVA molecules in the interface between monomer and continuous water • Size:100 microns • the microcapsules contained a large number of small voids in their inner phase • W/O/W emulsions must retain their stability during polymerization
Suspension polymerization in the presence of a porogen [41]		• MMA suspension polymerization in the presence of cyclohexane: H₂O, MMA, cyclohexane, benzoyl peroxide, and HPMC(Hydropropyl methylcellulose) as a suspending agent	Particle collapsed and had a thick surface layer • The formation of primary particles in suspension polymerizations was caused by the insolubility of PMMA in the oil phase It is similar to our particle with $M_{CH}/M_{MMA} = 1$ • They tried only $M_{H2O}/M_{oil} < 1$ and $M_{CH}/M_{MMA} > 1$

8

1.1.3. Motivations for the current research

Suspension, dispersion, and precipitation polymerization techniques can be used to make micron-sized particles. In suspension polymerization, stable monomer droplets (20-100 µm) are generated by mechanical mixing in an aqueous medium containing water-soluble polymeric stabilizers such as poly (vinyl alcohol) (PVA). The monomer droplet contains an oil-soluble initiator and each droplet acts as a micro-polymerization reactor. When a monomer-soluble polymer such as poly (methyl methacrylate) (PMMA) or polystyrene (PS) is made by suspension polymerization, polymer particles with no internal morphology are produced. In dispersion polymerization, monomer is mixed with a solvent that is a poor solvent for the polymer. In many previous studies, polar solvents such as alcohol have been used as a dispersion medium. The polymer particle nucleation and precipitation occur in the liquid phase, while particle agglomeration is prevented by steric stabilizers dissolved in the monomer-solvent mixture. Small micron-sized polymer particles obtained in suspension polymerization and the polymer particles produced by dispersion polymerization have no internal morphology. Precipitation polymerization is used for the synthesis of a polymer that does not dissolve in its own monomer (e.g., vinyl chloride and acrylonitrile).

In this study, we investigated the heterophase polymerization process to produce complex particle morphologies in a single-stage process. Here, free radical polymerization, thermodynamically-driven phase separation and particle precipitation occurred simultaneously in a geometrically confined reaction space suspended in an aqueous medium. The heterogeneous polymerization in this study is a hybrid of suspension and dispersion polymerizations. Here, the polymerization occurs in the geometrically confined reaction space of a suspended liquid droplet.

The droplet contains monomer, initiator, nonsolvent, and steric dispersion stabilizers. The polymerization begins as a homogeneous phase, but as the concentration of polymer increases with monomer conversion inside the droplet, the volume fraction of nonsolvent in the polymerizing droplet increases, creating a less favorable thermodynamic environment for the solubility of polymer. As the composition of the reaction mixture reaches that of the binodal point, phase separation starts. Depending upon the specific thermodynamic conditions, the behavior of precipitated discrete polymer particles may change. Under certain reaction conditions, the mass of polymer precipitates increases sufficiently to induce the polymer agglomeration and the phase inversion occurs; the liquid phase containing unreacted monomer and solvent becomes a dispersed phase, which will eventually become hollows. We named this heterophase polymerization 'micro dispersive suspension polymerization'. No emulsifiers are used and hence the current invention differs from the emulsion polymerization technique that can produce multi-hollow particles of less than one micron.

1.2. Research objectives

Chapter 2 and 3 are concerned with the synthetic technique where precipitating of polymer particles and intra-particle phase separation phenomena are controlled simultaneously in a single-stage process. As phase separation occurs with a progress of polymerization, complex particle morphologies evolve. We aim to develop a fundamental understanding of underlying chemical and physical phenomena through experimentation.

This study is divided into two parts. In the first part, ternary phase diagram is constructed through an *in situ* polymerization technique. The ternary phase diagram is needed to understand the effects of thermodynamic and polymerization conditions on the evolution of morphological structures. The second part is on the development of fundamental understandings of chemical and physical phenomena at the particle-water interface and inside a polymer particle. Through these studies, we develop a design map for the synthesis of PMMA microparticles of various morphologies.

Chapter 2 Polymerization of Methyl Methacrylate in the Presence of Nonpolar Hydrocarbon Solvent – Construction of a Ternary Phase Diagram Through *In Situ* Polymerization

2.1. Introduction

In polymer science and engineering, detailed knowledge of phase diagrams is essential for investigating a variety of heterogeneous processes that involve phase separation phenomena. For instance, the final properties of asymmetric polymer membranes produced by the "wet inversion method" (i.e., immersion of a polymer solution in a coagulation bath) is determined by the thermodynamics and kinetics of the phase separation process [42-47]. Similarly, reaction-induced phase separation that occurs in the production of several polymers such as poly(vinyl chloride), polyacrylonitrile, and high-impact polystyrene strongly affects the evolution of monomer conversion, polymer molecular structure, and material's final morphology [48-50]. Also, in precipitation and dispersion polymerizations, the construction of an accurate phase diagram is one of the critical requirements to design the polymerization conditions that yield desired morphologies.

Conventional methods to construct ternary phase diagrams of polymer/solvent/nonsolvent systems consist in either titrating polymer/solvent solutions or preparing a series of polymer/solvent/nonsolvent blends. In the first method, clear polymer/solvent solutions of known

compositions are prepared and the nonsolvent is slowly doled into the solutions until they turns turbid as the polymer starts to precipitate [44,46,47,50-53]. This technique is hard to apply when the polymer content increases because the growing viscosity of the mixture prohibits the mixing of the added nonsolvent with the polymer/solvent solution and generates the appearance of local turbidity [50]. In the second method, a series of polymer/solvent/nonsolvent blends of known compositions are prepared to determine which of them undergo a phase separation process [43, 45,54,55]. Typically, a mixture is first heated at a relatively high temperature until a clear solution is observed, and the sample is then cooled to a desired temperature. This technique requires the preparation of numerous samples to obtain a good representation of the ternary diagram, and it cannot be used when one of the species reacts at high temperatures (e.g., monomer).

One of the most challenging problems related to the techniques described above is the detection of the onset of turbidity (cloud point). Certainly, visual examination of the samples is the most widely used method [43-47,50-54]. An alternative to the visual examination technique in determining the cloud point of a polymer solution is to use a light scattering technique [56]. For example, methacrylic acid monomer was polymerized in a light scattering cell in the presence of water and 2,2'-azobis(2-amidonopropane)-dihydrochloride as an initiator. Samples were irradiated with a laser beam, and the scattered light at 0 degree angle was recorded. Cloud points containing 3 and 15 wt. % of polymer were assumed to occur when a sharp decrease in the recorded intensity was observed.

In this chapter, we used a laser light scattering (LLS) technique to determine the cloud points for a system with methyl methacrylate (MMA), poly(methyl methacrylate) (PMMA), and a non-polar nonsolvent (for the polymer) such as n-hexane. For this purpose, MMA is polymerized in an LLS cell in the presence of the nonsolvent, and lauroyl peroxide (LPO) as the initiator. The

onset of turbidity was determined by recording the scattered light at a single angle. Visual examination method was also employed, though limited to low PMMA concentrations, and its results were compared with those by the LLS technique. A mathematical model for the ternary phase equilibrium has been adjusted using the experimental data to estimate the binodal curve, the spinodal curves, and the system tie lines. We show that the method has been successfully used to construct a ternary phase diagram for a wide range of polymer concentration.

2.2. Experimental

2.2.1. Materials

MMA (Sigma-Aldrich), n-hexane (Fisher), and lauroyl peroxide (LPO) (Atochem) were used as the monomer, nonsolvent, and initiator, respectively. Both the monomer and nonsolvent were purified by ion-exchange columns, while the initiator was used as received. PMMA standards of polydispersity below 1.09 and weight-average molecular weights of 625,500; 138,500; 60,150; 30,530; 10,290; and 3,810 g/mol were purchased from Polymer Laboratories. Methacryloxypropyl-terminated polydimethylsiloxane (PDMS) of molecular weight between 4000 and 6000 g/mol was purchased from Gelest.

Methyl methacrylate | Poly (methyl methacrylate) | Lauroyl peroxide

Methacrlyoxypropyl-terminated Poly(dimethly siloxane)

Figure 2-1. Chemical structures used in the micro dispersive suspension polymerization of MMA [111].

2.2.2. Determination of cloud points by *in situ* polymerization

In this study, cloud points for the PMMA/MMA/n-hexane system were determined by conducting *in situ* polymerization experiments of MMA in the presence of n-hexane. The proposed technique is aimed at overcoming the drawbacks of the conventional titration method in the region of high polymer contents caused by the high viscosity of the reactive mixture, the inadequate dissolution of the polymer, the poor mixing of the added nonsolvent, and the appearance of local turbidity.

A schematic representation of the reaction path is shown in Figure 2-2. Since n-hexane is not consumed during the polymerization, the reaction path is represented by a simple straight line. Initially, the monomer/n-hexane mixture is a single homogeneous phase (point A in Fig. 2-2). The

reaction proceeds homogeneously until the amount of PMMA in the system is high enough to induce the system phase separation (point B in Fig. 2-2). At that point, the mixture turns turbid and such turbidity can be detected to construct the ternary phase diagram. To determine the onset of turbidity, two techniques are applied: (1) visual examination; and (2) LLS. In what follows, a description of the proposed techniques is provided.
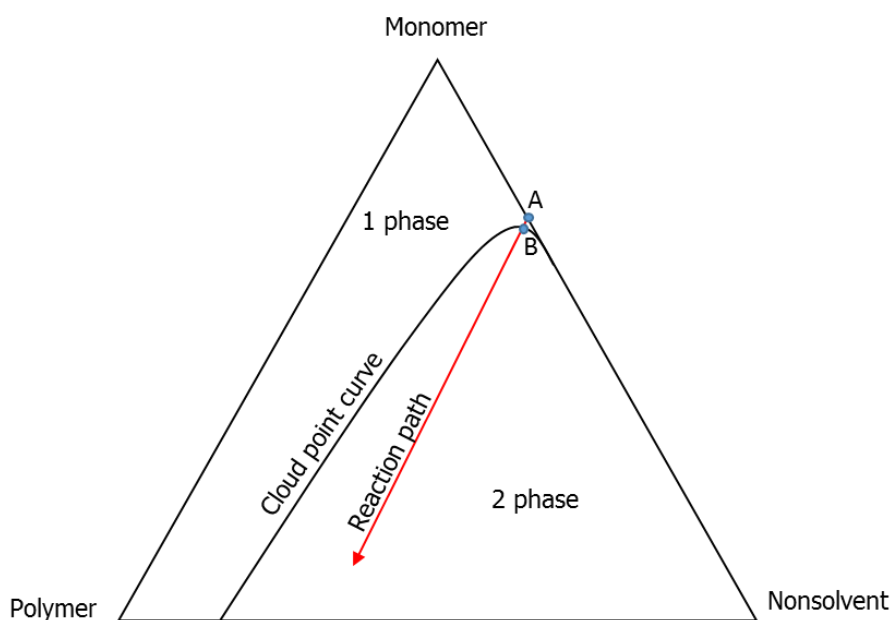
Figure 2-2. Schematic representation of an *in situ* polymerization on the ternary phase diagram: A, initial ''homogeneous'' solution of monomer/nonsolvent; B, polymerization cloud point [47].

Onset of turbidity by visual examination of polymerizing mixtures

Solutions of MMA/n-hexane/LPO of varying compositions were prepared, as shown in Table 2-1 (samples V1-V6). First, a LPO/MMA solution was prepared at room temperature and loaded into 4-mL glass vials. The initial concentration of LPO was 0.07 mol/L-MMA. Different

amounts of n-hexane were added into the mixtures, and the vials were sealed and immersed in a clear water bath at 70°C to start the polymerization. The reaction mixtures in the vials reached the bath temperature in less than 3 min. The vials were taken from the bath as soon as their contents turned visually turbid. To stop the reaction after the contents became turbid, the vials were quenched in a cold ice-water bath, and hydroquinone inhibitor was added. Since the vial content was quite small, the temperature of the mixture was reduced very fast, and the amount of polymer produced during the quenching period was negligible. Also, hydroquinone dissolved easily in the polymer solution sample because of the relatively low monomer conversion reached at the cloud points. The amount of PMMA at the cloud point was determined by a standard gravimetric technique that consists of precipitating the polymer with methanol, filtering, and drying under vacuum until constant weight. Since the vials were sealed, it was assumed that the mass of n-hexane remained constant during the polymerization experiments.
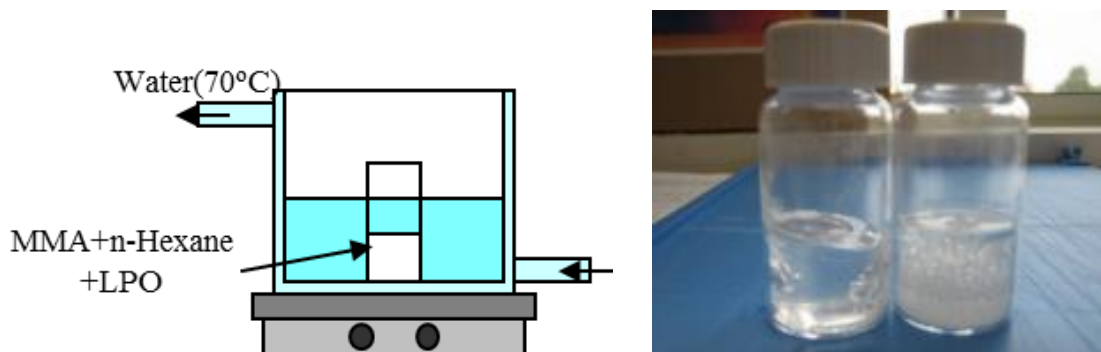
Figure 2-3. Illustration of visual examination of polymerizing mixtures and polymerized PMMA at high monomer concentration.

Table 2-1 illustrates the measured compositions for the investigated mixtures at the cloud points. Also presented in Table 2-1 are the reaction times required to reach the cloud point and the

corresponding monomer conversion, calculated as the ratio between the mass of PMMA at the moment of phase separation and the initial mass of MMA. At high n-hexane contents, the transition from a clear solution to a turbid solution occurred very fast, and the visual examination of the polymerizing monomer/n-hexane mixtures was quite accurate and reproducible. However, when using low nonsolvent contents, a significant amount of polymer was produced before reaching the cloud point (see Fig. 2-2), and the technique reproducibility was very poor. Specifically, the reaction mixtures in the vials exhibited partial turbidity because of high viscosity and hence, it was difficult to pinpoint the exact cloud point. For that reason, the results of recipes containing initial weight fraction of n-hexane lower than 0.379 are not reported in Table 2-1.

Table 2-1. Initial and final compositions (wt. fractions) in in-situ polymerization and phase separation experiments with visual detection (V) and on-line laser light scattering technique (LS).

Blend	Initial composition			Final composition at the cloud point				
	n-hexane	MMA	PMMA	n-hexane	MMA	PMMA	conversion	time
	[-]	[-]	[-]	[-]	[-]	[-]	[-]	[min]
V1	0.379	0.621	-	0.379	0.601	0.020	0.033	5.4
V2	0.443	0.557	-	0.443	0.540	0.017	0.031	8.3
V3	0.511	0.489	-	0.511	0.473	0.016	0.032	10.3
V4	0.582	0.418	-	0.582	0.405	0.013	0.031	13.4
V5	0.657	0.343	-	0.657	0.332	0.011	0.032	20.5
V6	0.819	0.181	-	0.819	0.175	0.006	0.032	36.3
LS1	0.098	0.902	-	0.098	0.271	0.630	0.699	28.0
LS2	0.151	0.849	-	0.151	0.209	0.640	0.753	33.7
LS3	0.207	0.793	-	0.207	0.448	0.345	0.435	35.3
LS4	0.233	0.767	-	0.233	0.583	0.184	0.240	32.8
LS5	0.375	0.625	-	0.375	0.608	0.017	0.027	11.8
LS6	0.514	0.486	-	0.514	0.472	0.014	0.029	8.6
LS7	0.651	0.349	-	0.651	0.338	0.011	0.032	12.9
LS8	0.819	0.181	-	0.819	0.176	0.005	0.028	17.9

Onset of turbidity by LLS technique

To improve the accuracy in determining the cloud points along the in situ polymerizations, and to overcome the experimental difficulties of the visual examination technique in the region of

high polymer contents, LLS was used to detect the nascent polymer precipitation. For this purpose, several MMA/n-hexane/LPO mixtures of known compositions were prepared in LLS cells (samples LS1-LS8 in Table 2-1). The initial concentration of LPO was 0.07 mol/L-MMA. Cells were placed in the sample holder of a Photocor-FC light scattering instrument (Photocor) equipped with a 5 mW laser light source (JDS Uniphase, He-Ne laser, laser wavelength = 632.8 nm) (Figure 2-4).
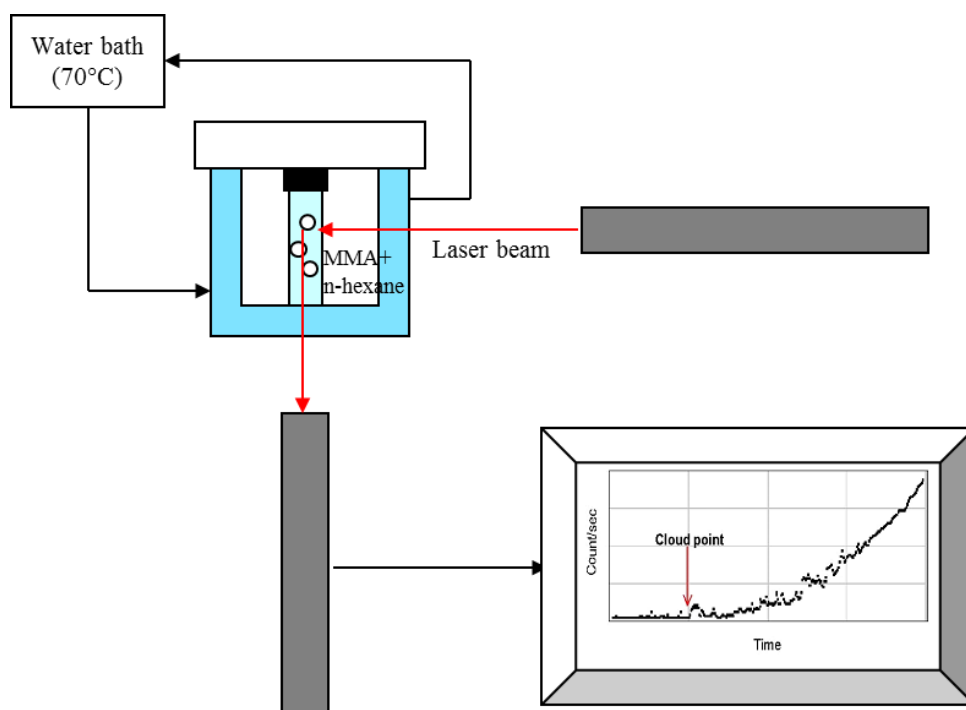
Figure 2-4. A Photocor-FC light scattering instrument (Photocor) [57] and schematic of LLC technique.

19

The temperature was controlled by circulating water at 70^oC through the sample holder jacket. The intensity of the scattered light at $90\ ^oC$ was recorded during the polymerization. At the cloud point, an abrupt increase in the scattered light intensity was observed (see Fig. 2-4 and 2-5). Note that ordinates of Figure 2-5 exhibit arbitrary units because actual values are not required to detect the onset of polymer precipitation. After detecting the onset of turbidity, samples were quickly taken from the holder. LLS cells were immersed in a cold ice-water bath, after adding hydroquinone as inhibitor. The compositions of the final mixtures shown in Table 2-1 were gravimetrically determined as explained in the "Onset of Turbidity by Visual Examination of Polymerizing Mixtures" section. However, when the amount of polymer produced at the cloud point was too high (i.e., samples LS1-LS3), it was necessary to first dissolve the polymer in acetone before precipitating it with methanol. Note that the content of polymer at the cloud points of samples LS1 and LS2 are over 60%. As far as we are aware, this region of the ternary diagram has not been investigated before for solvent/nonsolvent/polymer systems due to the limitations of the conventional nonreactive titration technique.
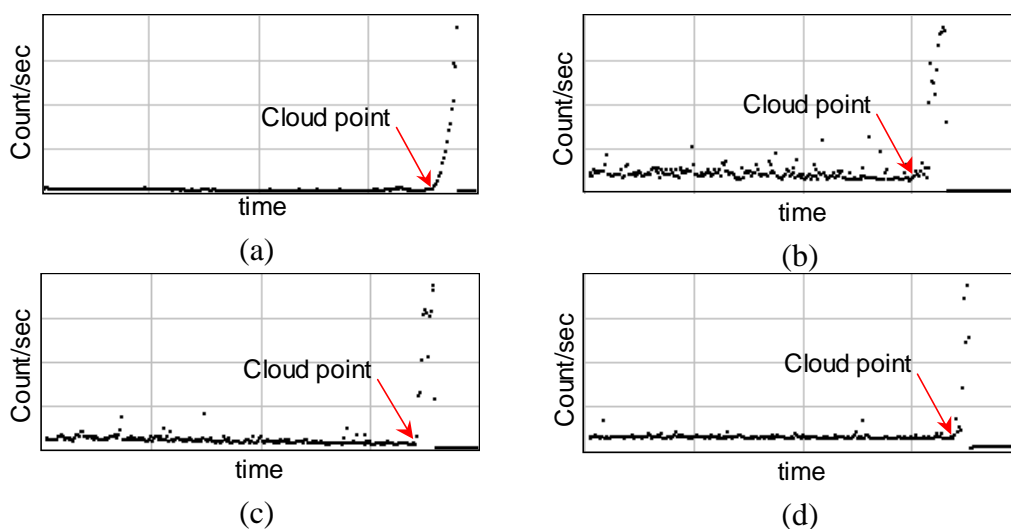
Figure 2-5. Number of photons scattered per second at an angle of 90° along the polymerization: (a) LS1, (b) LS5, (c) LS6, and (d) LS8.

Based on the determined cloud points for the samples of different compositions, a ternary phase diagram has been constructed (Fig. 2-6), and the following can be observed: (a) cloud points determined by visual examination of mixtures containing weight fractions of n-hexane between 0.379 and 0.819 almost overlap with the results obtained by LLS technique. This is a good indication of the accuracy of visual examination for determining cloud points in the region of relatively low polymer content; (b) as mentioned before, for n-hexane contents below 0.379, the reproducibility of visual examination technique was very poor and only the LLS technique could be applied.
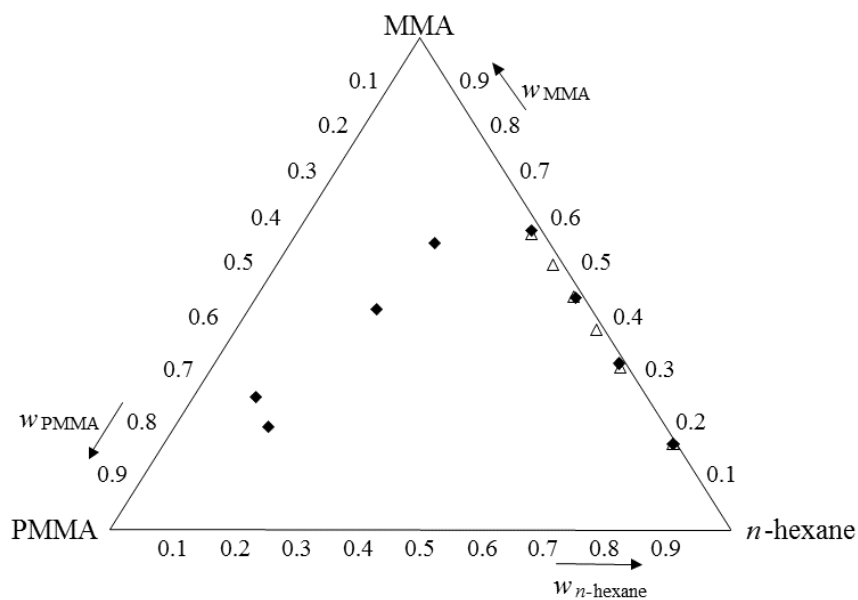
Figure 2-6. Cloud points measured along the polymerization of MMA in the presence of n-hexane at 70 °C. (◇) Visual examination; (◆) light scattering method.

Some of the polymer samples taken at the system cloud points were analyzed to determine their molecular weights by gel permeation chromatography (GPC), using a UV detector and PLgel

10 lm MIXED-B columns (Polymer Laboratories). Chloroform was the mobile phase and PMMA

standards of narrow molecular weight distribution were used to calibrate the column. Resulting

average molecular weights are presented in Figure 2-7. It can be seen that molecular weights of

the polymer produced in the LLS cells do not vary too much when comparing different samples.

For instance, samples LS1-LS4 exhibit number-average molecular weights between 30,000 and

55,000 g/mol, and polydispersities in the order of 1.7 (Fig. 2-7).
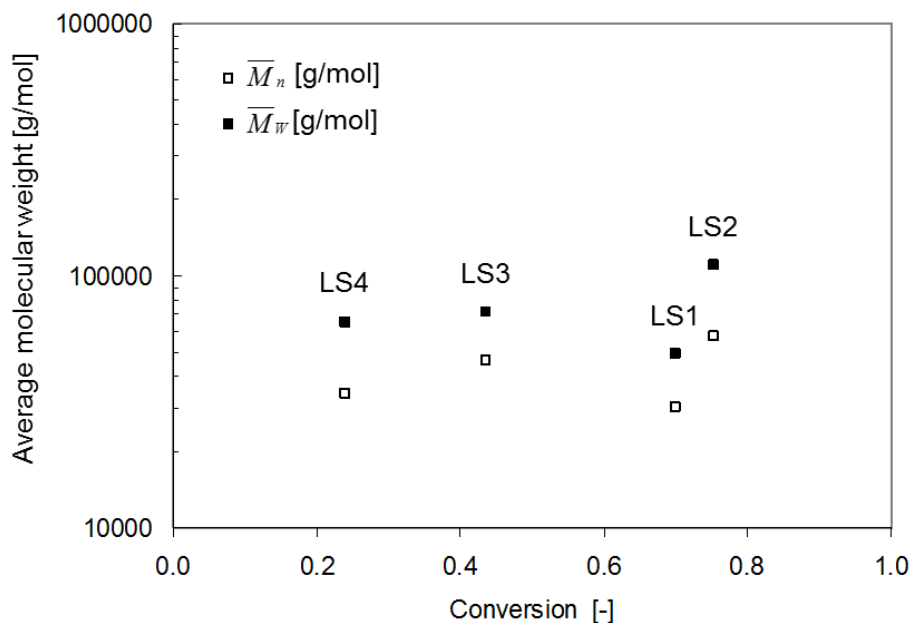
Figure 2-7. Average molecular weights of PMMAs produced in LLS cells at the cloud points.

2.2.3. Construction of the theoretical ternary phase diagram

The Flory-Huggins (FH) theory of polymer solutions [58] is used to construct a theoretical binodal curve for the investigated MMA/PMMA/n-hexane system. For a ternary system at equilibrium, the Gibbs free energy of mixing (ΔG_m) can be expressed as follows:

$$\frac{\Delta G_m}{RT} = \sum_{i=M,P,S} n_i \ln(\phi_i) + \chi_{S,P} n_S \phi_P + \chi_{M,P} n_M \phi_P + \chi_{S,M} n_S \phi_M \tag{2.1}$$

where n_i and ϕ_i are the number of moles and the volume fractions of species (with $i = $ M (monomer), P (polymer), S (nonsolvent) indicating MMA, PMMA, and n-hexane, respectively), $\chi_{i,j}$ is the interaction parameter between species i and j, R is the gas constant, and T is the absolute temperature. The effect of polymer molecular structure on the ternary diagram was neglected [63]. Therefore, cloud points and binodal points were assumed to be the same. Also, it was assumed that $\chi_{i,j}$ is independent from the phase composition.

From Eq. (2.1), the chemical potential for each species referred to the standard state ($\Delta\mu_{i,j}$) can be written as follows [44]:

$$\frac{\Delta\mu_{S,k}}{RT} = \ln(\phi_{S,k}) + 1 - \phi_{S,k} - s\phi_{M,k} - r\phi_{P,k} + (\chi_{S,M}\phi_{M,k} + \chi_{S,P}\phi_{P,k})(\phi_{M,k} + \phi_{P,k}) - s\chi_{M,P}\phi_{M,k}\phi_{P,k} \tag{2.2}$$

$$s\frac{\Delta\mu_{M,k}}{RT} = s\ln(\phi_{M,k}) + s - \phi_{S,k} - s\phi_{M,k} - r\phi_{P,k} + (\chi_{S,M}\phi_{S,k} + s\chi_{M,P}\phi_{P,k})(\phi_{S,k} + \phi_{P,k}) - \chi_{S,P}\phi_{S,k}\phi_{P,k} \tag{2.3}$$

$$r\frac{\Delta\mu_{P,k}}{RT} = r\ln(\phi_{P,k}) + r - \phi_{S,k} - s\phi_{M,k} - r\phi_{P,k} + (\chi_{S,P}\phi_{S,k} + s\chi_{M,P}\phi_{M,k})(\phi_{S,k} + \phi_{M,k}) - \chi_{S,M}\phi_{S,k}\phi_{M,j} \tag{2.4}$$

where subscript k indicates the phase (1 = nonsolvent-rich phase, 2 = polymer-rich phase); s and r are the molar volume ratios of solvent/monomer and solvent/polymer, respectively. In order to calculate the molar volume of the polymer, the number-average molecular weight ($\overline{M}_n$) was used.

At equilibrium, $\left.\dfrac{\partial^2 \overline{\Delta G}_m}{\partial \phi_i \partial \phi_j}\right|_{P,T}$ equals 0 and the binodal curve (coexisting curve) can be calculated. This calculation was conducted by Luciani [63] and the obtained binodal curve is in Fig. 2-8.
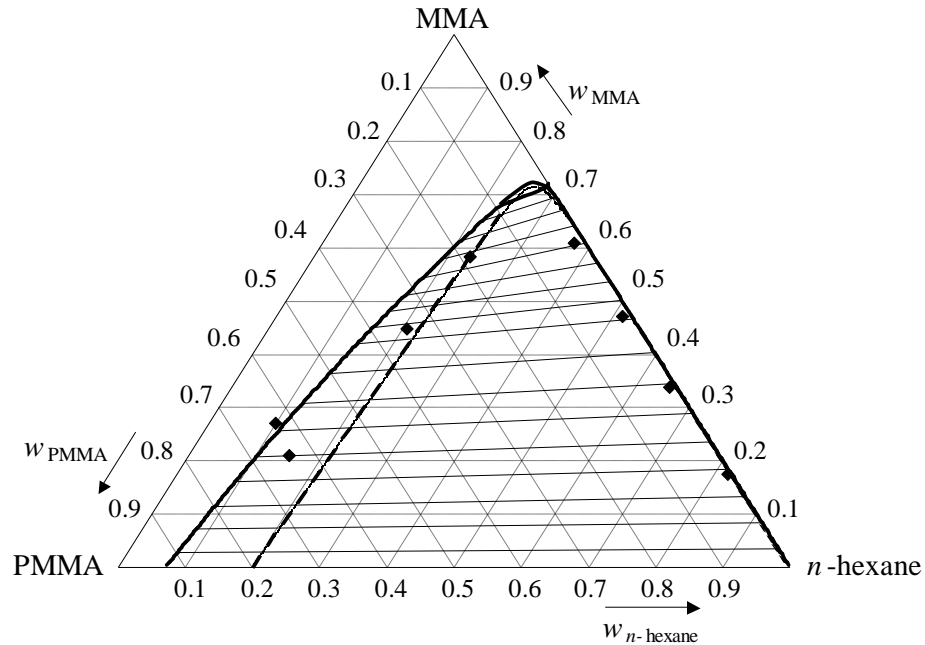
Figure 2-8. Theoretical ternary diagram. (—) Binodal curve; (--) spinodal curve; (—) tie lines; (♦) cloud points measured by LLS technique [63].

2.2.4. Conversion curve along a dispersion polymerization of MMA in n-hexane

To investigate the behavior of the polymerization system at higher conversions, a dispersion polymerization was carried out until complete depletion of the monomer. Several mixtures were prepared containing the same initial compositions as LS4 (Table 2-1) and monomer and LPO were mixed together in 4 mL vials, and a solution of n-hexane containing 0.0027 mol/L-MMA of PDMS was added into the mixtures. Vials were sealed and immersed in the water bath at 70°C. At prespecified reaction times, they were taken from the bath, and hydroquinone was added to stop the polymerization.

For each sample, the monomer conversion was gravimetrically determined, and the results are presented in Figure 2-9. The conversion curve shows the typical S-shape produced by an early gel effect. The process auto-acceleration is observed at monomer conversions close to the system phase separation point. This is due to the appearance of the second (polymer-rich) phase. In this phase, the mobility of the growing macro-radicals is highly limited even at low conversion, thus promoting an early and strong gel effect.
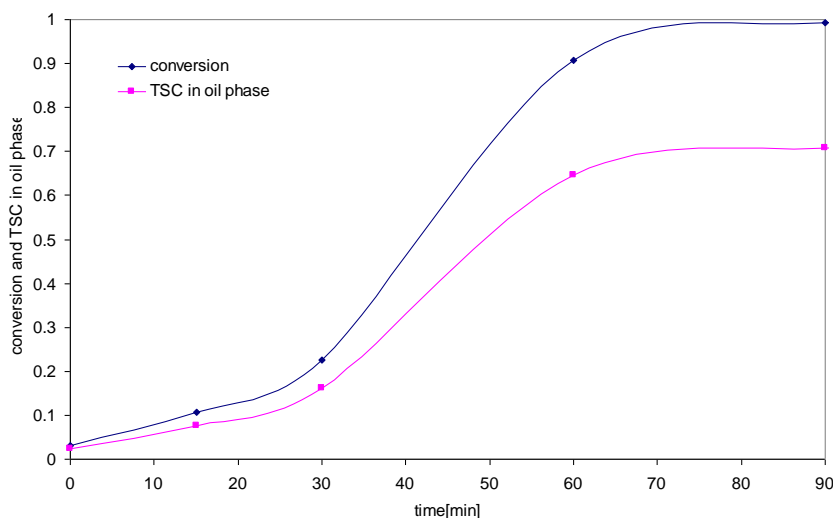
Figure 2-9. Evolution of the monomer conversion for the dispersion polymerizations of MMA in n-hexane at 70°C.

2.3. Conclusion

In this chapter, the *in situ* polymerization of MMA in the presence of a non-polar nonsolvent *n*-hexane was investigated through experimental work for the construction of a ternary phase diagram for the MMA/PMMA/*n*-hexane system. Both visual examination and LLS techniques were used to determine the onset of the turbidity. In the case of visual titration, at high n-hexane contents, the transition from a clear solution to a turbid solution occurred very fast, and the visual examination of the polymerizing monomer/n-hexane mixtures was quite accurate and reproducible. However, when using low nonsolvent contents, a significant amount of polymer was produced before reaching the cloud point and the technique reproducibility was very poor. Specially, the reaction mixtures in the vials exhibited partial turbidity because of high viscosity and it was difficult to pinpoint the exact cloud point. To improve the accuracy in determining the cloud points along the *in situ* polymerizations, and to overcome the experimental difficulties of the visual examination technique in the region of high polymer contents, LLS was used to detect the nascent polymer precipitation even at high polymer contents. And the ternary phase diagram of MMA/PMMA/n-hexane which can cover all the region was investigated. Also, the binodal curve was theoretically calculated in our lab. We also drew the conversion curve from experimental data, and an auto-acceleration process was observed at low conversion.

Chapter 3 Control of Various Morphological Changes of Poly Methyl Methacrylate by Micro-Dispersive Suspension Polymerization

3.1. Introduction

3.1.1. Suspension polymerization

Suspension polymerization is a heterogeneous polymerization process that uses mechanical agitation to mix a monomer or mixture of monomers in an oil phase while the monomers polymerize, forming spheres of polymer. The suspension polymerization process is typically carried out in well- stirred batch reactors. Suspension polymerization employs a diluent (organic) in which neither monomer nor polymer is soluble [59,60]. In suspension polymerization process, micron-size droplets of aqueous monomer solution are dispersed into an organic phase before polymerization. Free radical polymerization then proceeds in each small droplet like bulk polymerization.

3.1.2. Dispersion polymerization

In dispersion polymerization the monomer and the initiator are both soluble in the polymerization medium, but the medium is a poor solvent for the resulting polymer. Therefore,

the reaction mixture is homogeneous at the beginning of polymerization but the polymer precipitates out from the solvent as monomer conversion increases. The resulting particles are generally monodisperse and in the range of about 0.1 ~ 10 μm [61].
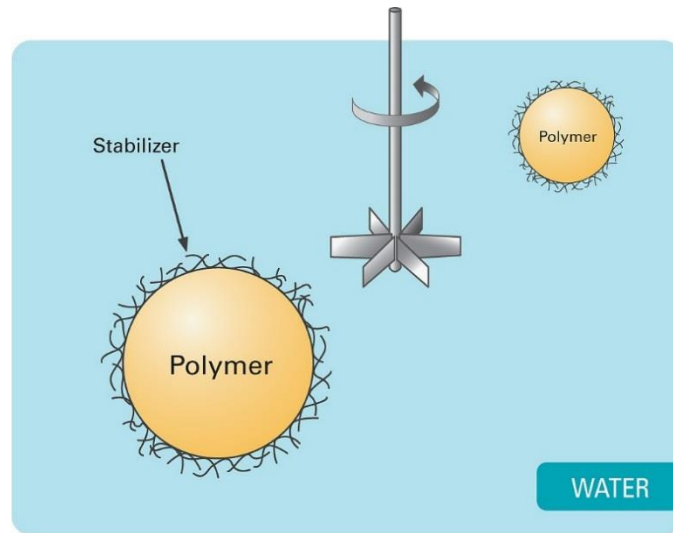
(a)
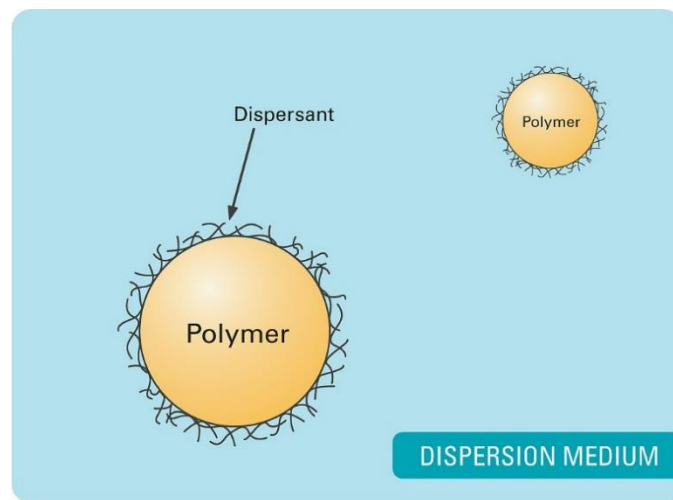
(b)

Figure 3-1. Schematic of (a) regular suspension polymerization and (b) regular dispersion polymerization.

3.2. Experimental

3.2.1. Materials

Methyl methacrylate (MMA) (from Sigma-Aldrich) was used as a monomer and cyclohexane (from J.T.Baker) and hexane (from Fisher) were used as solvents. 2, 2'-Azobisisobutyronitrile (AIBN) (from Aldrich) and Lauroyl peroxide (LPO) (from Atochem) were initiators. Poly vinyl alcohol (PVA), Poly vinyl pyrrolidone (PVP), and hydroxyl propyl cellulose (MW=~80000) were used as stabilizers in a water medium. Four types of PVA (87-89% hydrolyzed, MW = 85000-124000), (87~89% hydrolyzed, MW=124000~186000), (96% hydrolyzed, MW=95000), (80% hydrolyzed, MW=9000~10000) (from Aldrich) were tried. Two types of PVP (MW=40000 and 360000) (from Aldrich) were tried. Polydimethylsiloxane (PDMS) (MW=4000~6000, 5000~20000, and 20000~30000) (from Gelest) were used as stabilizers in oil phase. Deionized water was used as a continuous phase.

2, 2'-Azobisisobutyronitrile (AIBN)   Poly (vinyl pyrrolidone)

Fully hydrolyzed grade

Partially hydrolyzed grade

Poly vinyl alcohol
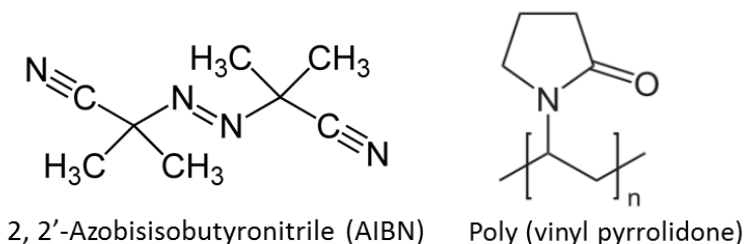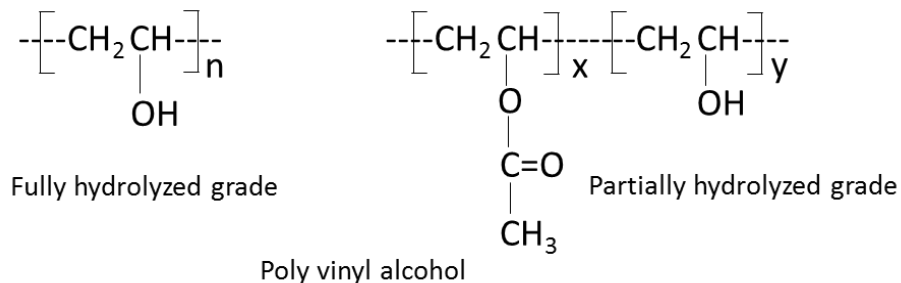
Figure 3-2. Chemical structures used in the micro dispersive suspension polymerization of MMA [111].

3.2.2. Micro dispersive suspension polymerization

The investigated method is micro dispersion suspension polymerization (MDSP). It is a hybrid of suspension and dispersion polymerization. The micron-sized polymer particles are polymerized by suspension polymerization, and internal morphology of particle is polymerized by dispersion polymerization inside the polymer particles. Figure 3-3 illustrates the schematics of micro dispersive suspension polymerization.

The experiments were carried out using a 500ml jacketed glass reactor (internal diameter 10 cm) with a five-bladed impeller. The working volume was 250ml in this system (Fig. 3-4). PVA (PVP or hydroxypropyl cellulose) was dissolved in the deionized water. The oil mixture of MMA, solvent, initiator, and PDMS was prepared and added to the PVA solution. (In some experiments the oil mixture was homogenized at 3000, 8000, or 9500 rpm in advance.) The mixture was moved to a glass reactor, purged with N_2 for 30 min in the ice bath and then polymerized at 70°C. The stirring speed was maintained at 500 rpm. Samples were taken from the reactor during the

polymerization for conversion and morphology. After 1 hr 30min, the polymerization was stopped and particles were washed several times with methanol, filtered off, and dried overnight in vacuum.
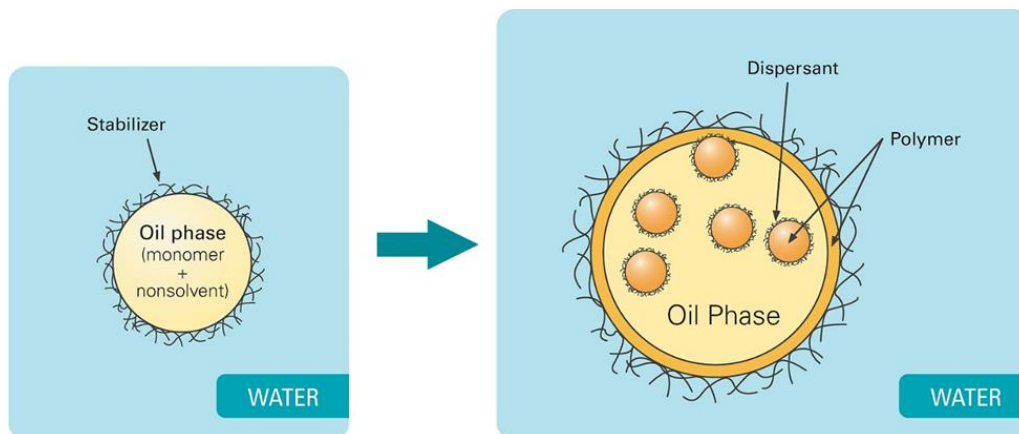
Figure 3-3. The schematic illustration of micro dispersive suspension polymerization.
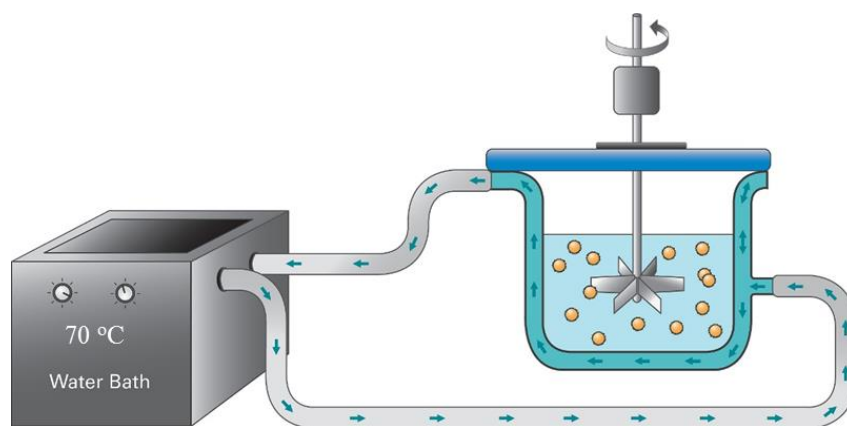
Figure 3-4. Polymerization apparatus for micro dispersive suspension polymerization.

3.2.3. Characterization of polymer particle morphology and molecular weight distribution

The polymer particle morphologies were examined using a scanning electron microscope (Hitachi SU-70 and AMRAY). To analyze the cross-section of polymer particles, polymer

31

particles were embedded with epoxy resin. The cured epoxy embedded particle samples were microtomed using a Leica RM2235 Microtome or mechanically fractured. The polymer molecular weight was measured by gel permeation chromatography (GPC, Waters) with chloroform as a mobile phase.

3.3. Results and discussion

3.3.1. Effect of initial monomer/nonsolvent ratio

The initial monomer/nonsolvent ratio is one of the key reaction variables that govern the evolution of particle morphology. We varied the initial ratios (in vol.) of monomer/nonsolvent from 1 to 9. In these experiments, all other reaction conditions (temperature, initiator concentration, stabilizer concentration, etc.) were kept constant. The most important observation from the experiments is that polymer particles of different morphologies have been produced (Fig. 3-6 ~ 3-9). To our knowledge, there is no literature on the polymerization that yields all the particle morphologies as shown in Figure 1-1 by a single-stage polymerization process. Figure 3-5 shows different morphologies of PMMA particles varying the initial ratio of MMA/n-hexane and the ternary phase diagram where each reaction path was plotted.

On the basis of experimental results, we first provided our interpretation of the morphological development of the polymer particles from thermodynamic view point using the ternary phase diagram for the monomer/PMMA/*n*-hexane system as shown in Figure 3-5.
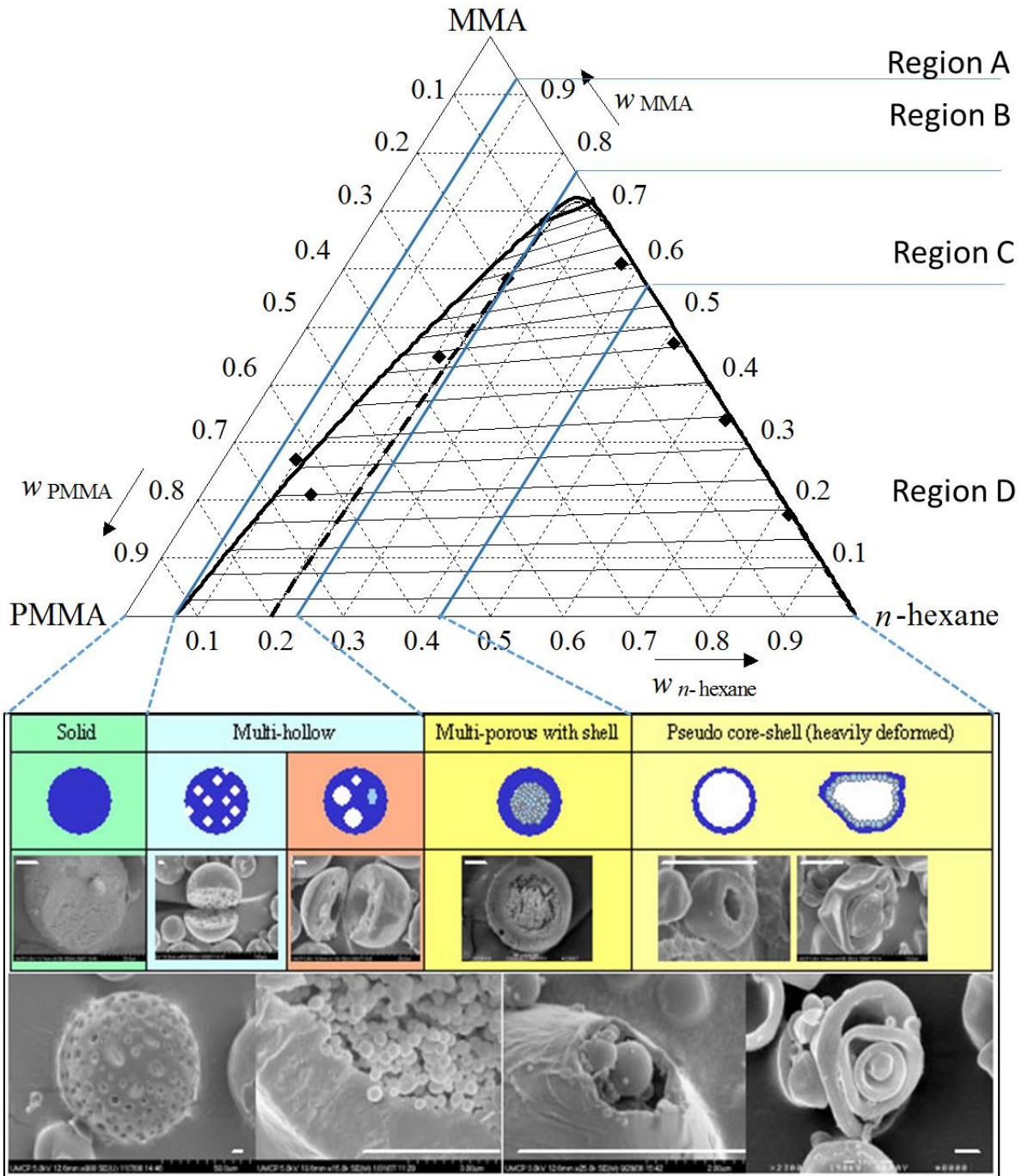
Figure 3-5. Morphological development of the polymer particles from thermodynamic view point using the ternary phase diagram for the monomer/PMMA/n-hexane system.

At very high MMA/hexane ratios, the monomer-nonsolvent mixture was incapable of inducing the system phase separation and the solid particles were produced. Therefore, in the water medium solid PMMA particles without pores or hollows were formed (Fig. 3-6).

<center>(a)   (b)</center>
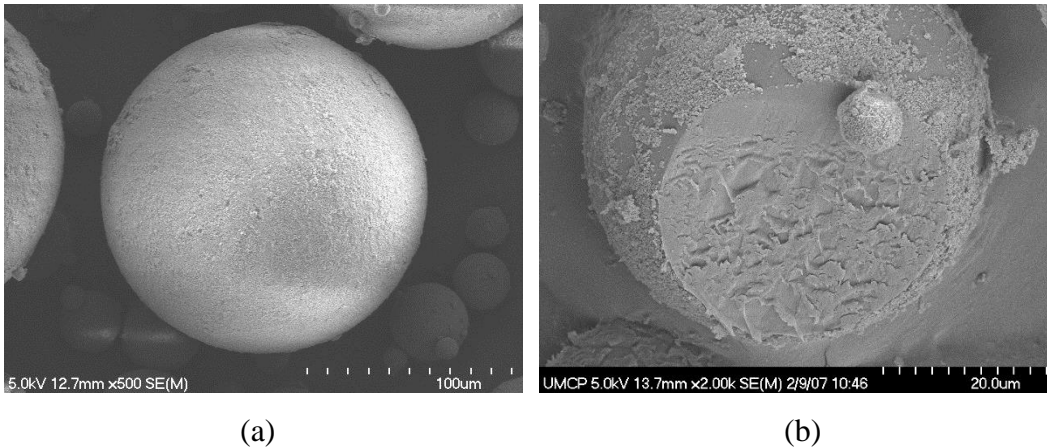
Figure 3-6. SEM images of the solid particle by suspension polymerization (95 wt % of MMA). (b) is the image of a cross section of (a).

Region B

With a slight increase in the *n*-hexane content, the system phase separates (after an initial homogenous stage) with polymerization. Since the amount of nonsolvent is still relatively low, the polymer-rich phase is continuous along the complete polymerization. At early stages of the polymerization, the solvent-rich phase is the continuous phase, and the system behaves as explained for Region D. As the polymerization proceeds, the volume of the solvent-rich phase becomes smaller because of the monomer consumption and the continuous migration of polymer chains toward the polymer-rich phase. However, the system undergoes a phase inversion process.

After a thermodynamically unstable period of phase co-continuity, the voluminous polymer-rich phase formed by discrete primary particles experiences a rapid coagulation to eventually produce a continuous phase.

(a) (b)

(c) (d)
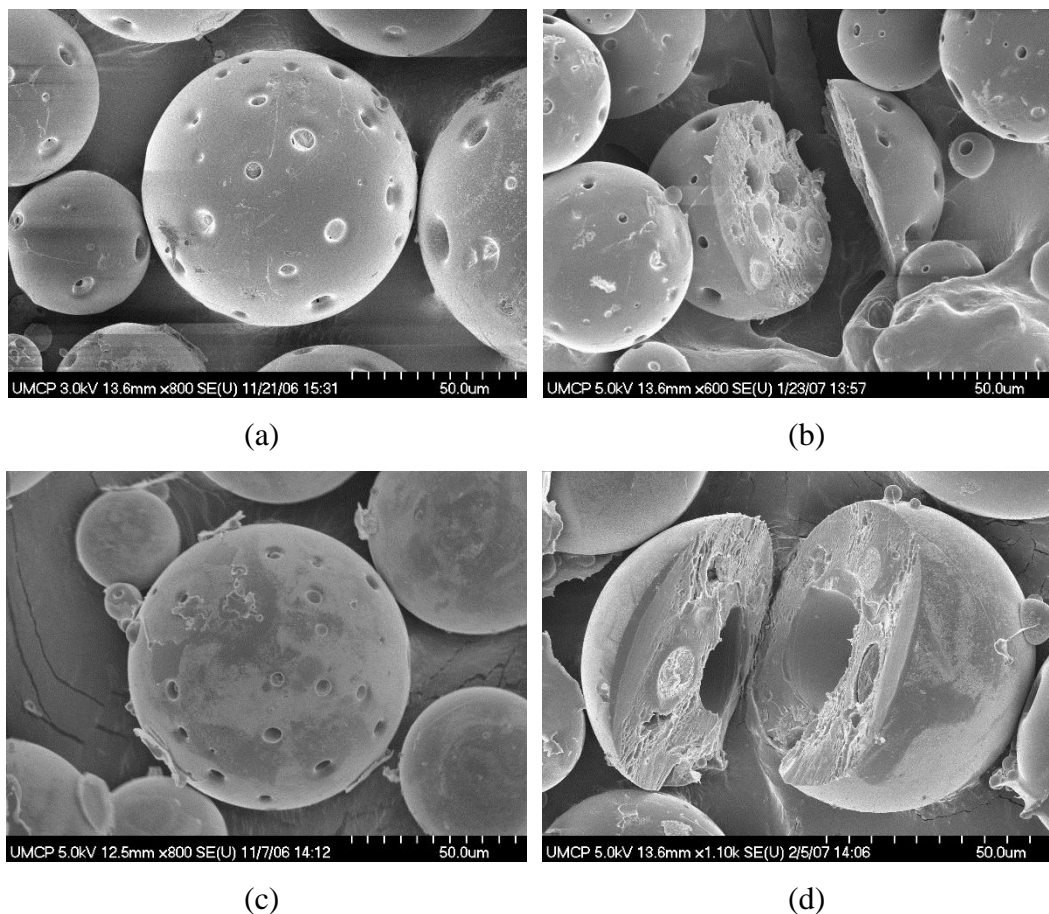
Figure 3-7. SEM images of the multi hollow particle by micro dispersive suspension polymerization (85 wt % of MMA).

Region C

A further increment in the initial nonsolvent content can yield two different kinds of morphologies. If the initial solvent fraction is high enough, the solvent-rich phase is the continuous phase along the complete polymerization. Polymer chains produced in that phase continuously

precipitate as primary particles that grow because of the aggregation with other primary particles and because of the polymerization of the monomer that is swelling them.

(a)   (b)
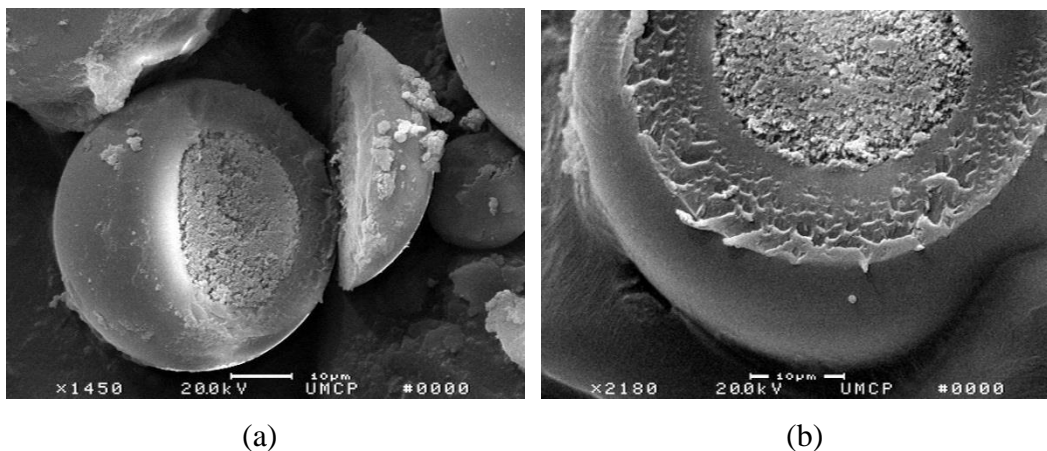
Figure 3-8. SEM images of a pomegranate-like internal structured particle by micro dispersive suspension polymerization (77 wt % of MMA).

Region D

If the initial nonsolvent content is too high, the amount of polymer is too low even at the end of the polymerization, and the particles cannot preserve their spherical shape. As a result, heavily deformed particles with nearly empty interior are produced.

(a)   (b)
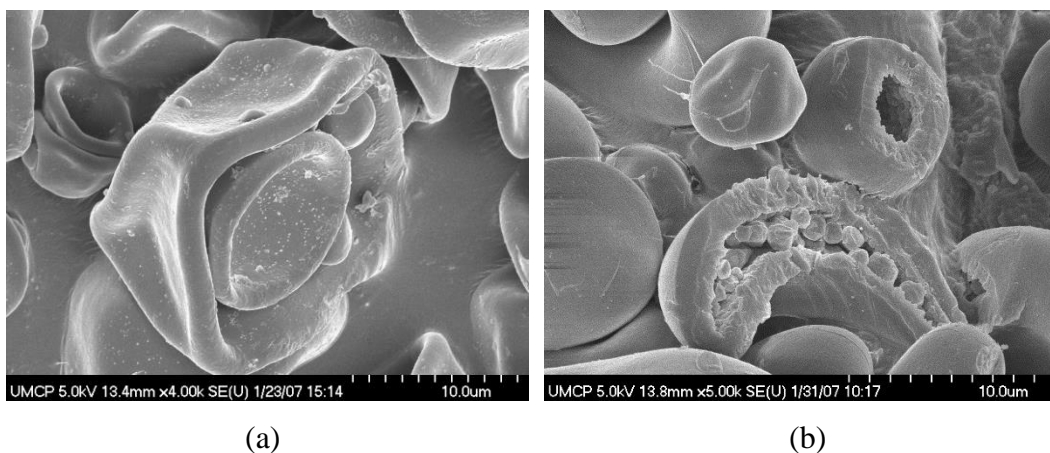
Figure 3-9. SEM images of the pseudo core-shell (heavily deformed) particle by micro dispersive suspension polymerization (59 wt % of MMA).

36

Luciani et al. [62] explained the morphological evolution of these particles using the ternary phase diagram (Fig. 3-10). Point A denotes the initial composition of the reaction mixture used in our experiment. Since no polymerization takes place in the aqueous phase because PVA does not form micelles in the water phase and because the LPO initiator is only soluble in the suspended oil phase, the suspended monomer droplets can be adopted as isolated micro-batch reactors. Therefore, as the first approximation in Fig. 2-2, the reaction path inside the suspended monomer micro-droplets can be represented by a straight line parallel to the monomer/polymer axis, as indicated by reaction path A-B-C in Fig. 3-10. It can be seen that the investigated MMA/PMMA/n-hexane ternary system phase separates at relatively low monomer conversions, when the reaction path intercepts the binodal curve. However, the reaction path does not stay on that straight line because of complex physical and chemical phenomena coexisting in the monomer microdroplet. As soon as the reaction path intersects the binodal curve, polymer chains start precipitating in a continuous solvent-rich medium in the form of primary sub-particles. These sub-particles should undergo agglomeration until the amount of PDMS (i.e., secondary steric stabilizer) is able to prevent it. Interestingly, the binodal and spinodal curves are overlapped in the region where the reaction path intersects the binodal curve, suggesting that the morphology evolution is ruled by spinodal decomposition rather than nucleation and growth mechanism [62].
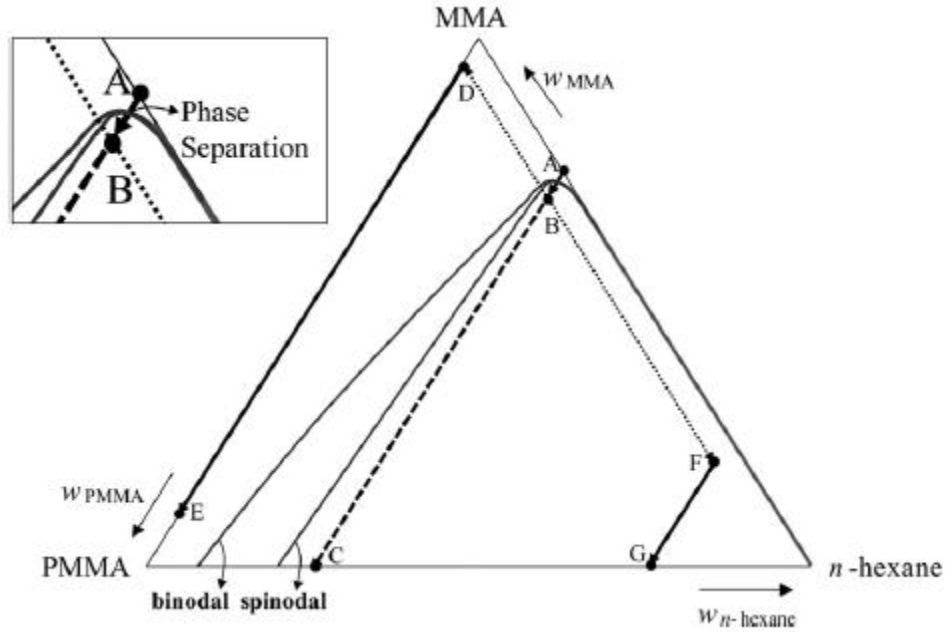
Figure 3-10. Ternary phase diagram of MMA/PMMA/n-hexane system at 70 ºC [62] with possible reaction paths that resulted in different morphologies of PMMA particles [62].

One more interpretation is required to describe formation of the pericelluar membrane (shell). Here, we note the significant differences in the water solubility of the MMA (~ 1.5 g/L of water) and the n-hexane (~ 0.013 g/L of water). When an organic droplet containing MMA and n-hexane is suspended in water, the droplet-water interface becomes the region where MMA, primary suspension stabilizer, and water coexist. However, this region should be very unfavorable for n-hexane because it is strongly hydrophobic. Hence, the formation of an intra-droplet compositional profile should be promoted (Fig. 3-11 (a)). Since the outer region of the suspended monomer droplets is better for the monomer rather than for the hydrophobic solvent, a faster pseudo-homogeneous polymerization should be induced, leading to the early formation of a dense polymeric structure at the particle surface (Fig. 3-11 (b)). Conversely, the inner region of the droplet should be for the hydrophobic solvent, thus promoting the precipitation of polymer sub-

particles (Fig. 3-11 (c)). The rate of this second mechanism (Fig. 3-11 (c)) should be much slower due to the dilution effect caused by the high concentration of the nonpolar solvent. Moreover, due to the low concentration of monomer at the inner region of the droplet, the dispersion polymerization can be considered to take place under "starved" conditions.

(a) (b) (c) (d)
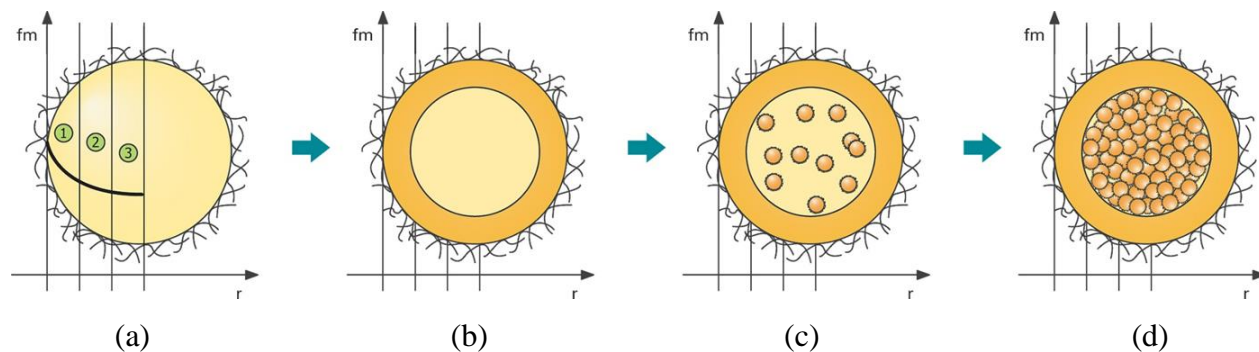
Figure 3-11. Morphological interpretation of the evolution of the core-shell pomegranate-like structure.

3.3.2. Effect of polymeric stabilizer type

The type and properties of polymeric stabilizer also play an important role in preventing the droplet coalescence by providing a protective coating for each droplet dispersed in the aqueous phase. PVA (partially hydrolyzed) and PVP used in our preliminary experiments are soluble in water and other polar solvents. PVP binds to polar molecules such as water exceptionally well. The molecular weight and the degree of hydrolysis of the stabilizer molecules are known to affect the effectiveness of the stabilizer in producing stable droplets of controlled size distribution. We found that when PVP is used, the outer shell of a hollow polymer particle is quite porous, apparently left by a small amount of water absorbed into the polymer layer (Figure 3-12). These

results indicate that understanding the chemical and physical phenomena at the particle-water interface, especially in the early stage of polymerization is needed. Such understanding can also be utilized to design new particle structures and morphologies.

(a1)   (b1)

(a2)   (b2)

(a3)   (b3)
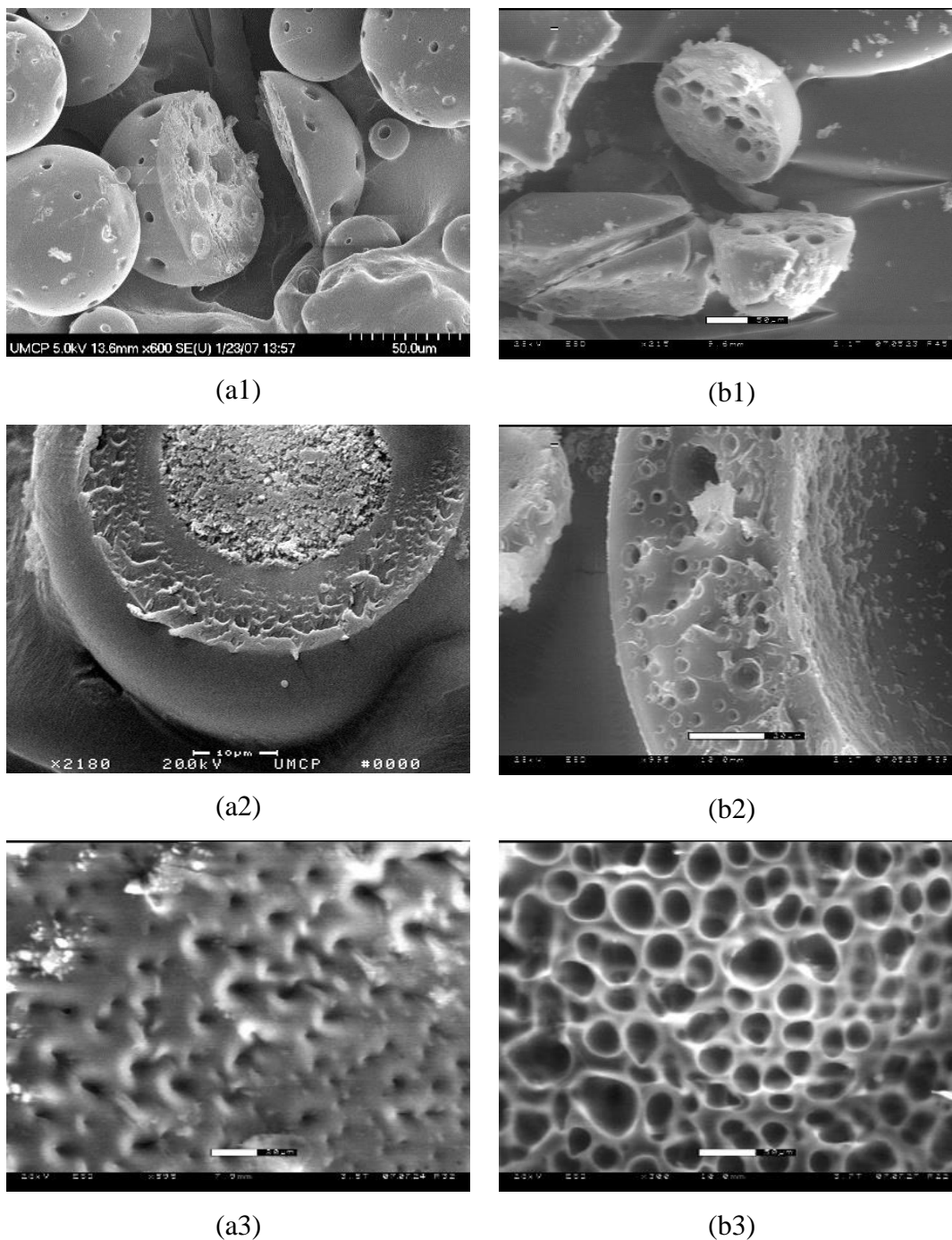
Figure 3-12. Comparison of internal morphologies of using (a) PVA with (b) PVP as stabilizers.

3.3.3. Molecular weight distribution (MWD) of polymer particles

Because of extreme heterogeneity in the polymerization environment inside and outside the polymer particles, the molecular weight distributions of the PMMA particles obtained in our experiments were found to deviate quite significantly from other MMA polymerization processes. The most notable difference is the broad or often bimodal MWD and thus, very high polydispersity ($PD > 10$). Figure 3-13 shows the MWD curves for the micro dispersive suspension polymerization with conversion. At low conversion, almost all of polymers formed are in the lower MW region. As reaction progressed, higher MW polymers start to appear at the expense of low MW chains. At high conversion, there is no more regeneration of new particles, instead the polymeric chains grew steadily until a high MW is attained.
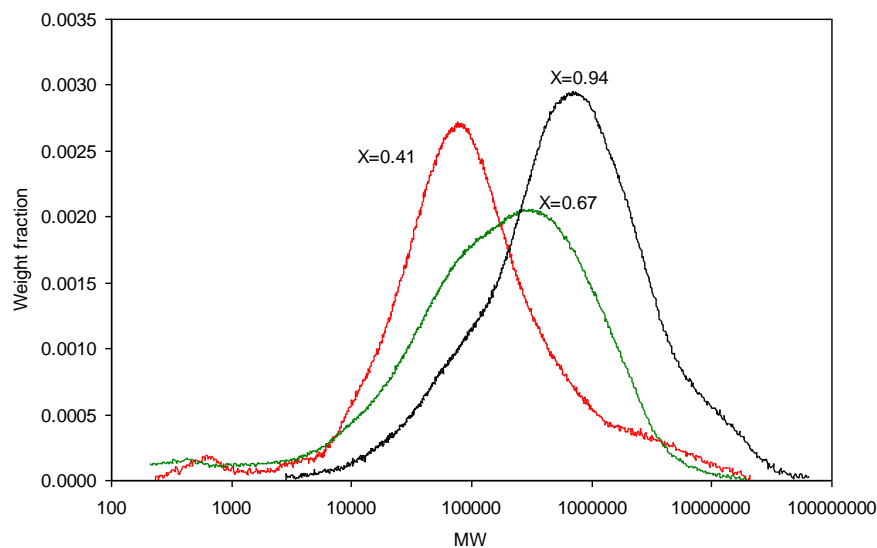
x	Mn	Mw
0.41	24187	312240
0.67	21793	391691
0.94	124014	1268786

Figure 3-13. MWD curves of macroscopic and intraparticle dispersion polymerization of MMA.

Compared to regular suspension and dispersion polymerizations, the micro-dispersive suspension polymerization (in case of core-shell structured PMMA particles) has a bimodal curve. (Fig. 3-14)
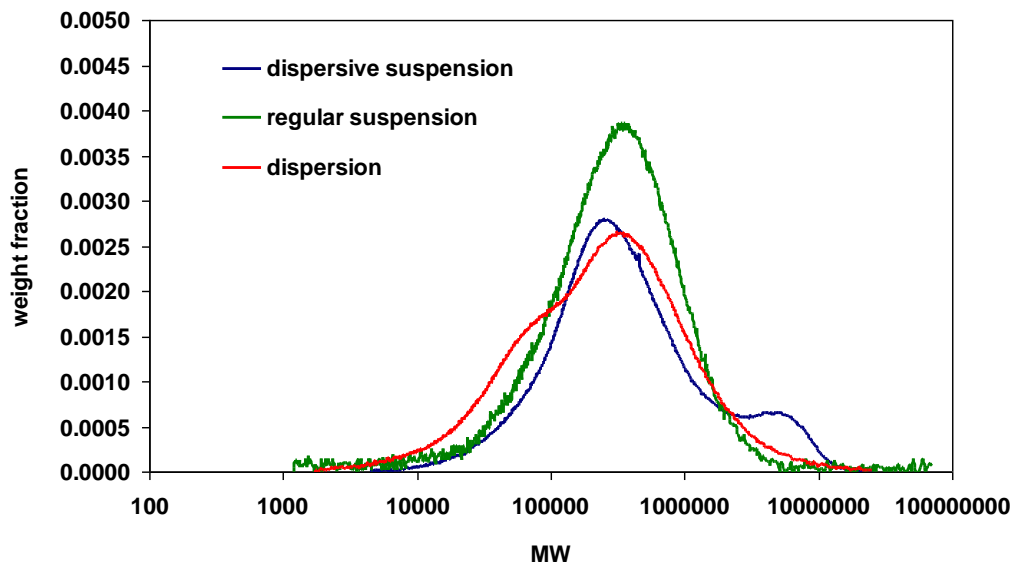
polymerization	Mn	Mw
suspension	7.9×10^4	5.6×10^5
dispersion	7.8×10^4	4.3×10^5
micro dispersive suspension	1.5×10^5	6.5×10^5

Figure 3-14. Comparison of MWDs of regular suspension/dispersion/micro dispersive suspension polymerization

The first peak of MWD for dispersive suspension polymerization could be presumed to be the core dispersion particles. However, the peak for suspension was placed in the similar MW. To demonstrate what the two peaks mean, macroscopic dispersion polymerization of MMA (in the 500 ml-reactor) and intraparticle dispersion polymerization under same reaction conditions (in a 4 ml-vial) were employed. In Fig. 3-14, it was also interesting to observe that the polymer molecular

weight was very high for the intraparticle dispersion polymerization. If the same condition is applied to the core part of core-shell PMMA particles, the second peak placed in higher MW can be demonstrated to be from the core part.
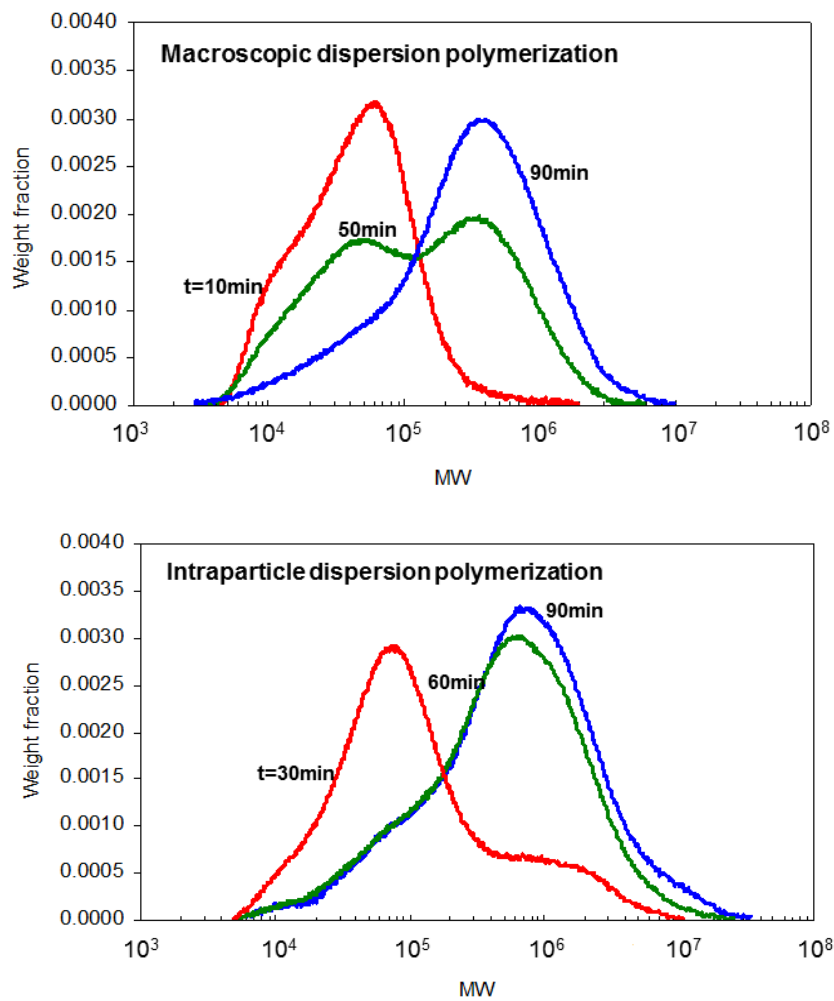
Figure 3-15. MWD curves of macroscopic and intraparticle dispersion polymerization of MMA.

Table 3-1. Reaction conditions of macroscopic and intraparticle dispersion polymerization. (LPO and PDMS concentration and reaction temperature were same.)

	MMA	n-hexane	Mixing
Macroscopic	175 ml	75 ml	500 rpm
Intraparticle	1.4 ml	0.6 ml	sonication

MWDs of different morphologies of PMMA particles by micro dispersive suspension polymerization were compared in Figure 3-16. Multihollow PMMA particles had one peak in the MWD whereas the core-shell particles had two peaks. It could be explained by the monomer concentration being relatively even over the droplet.
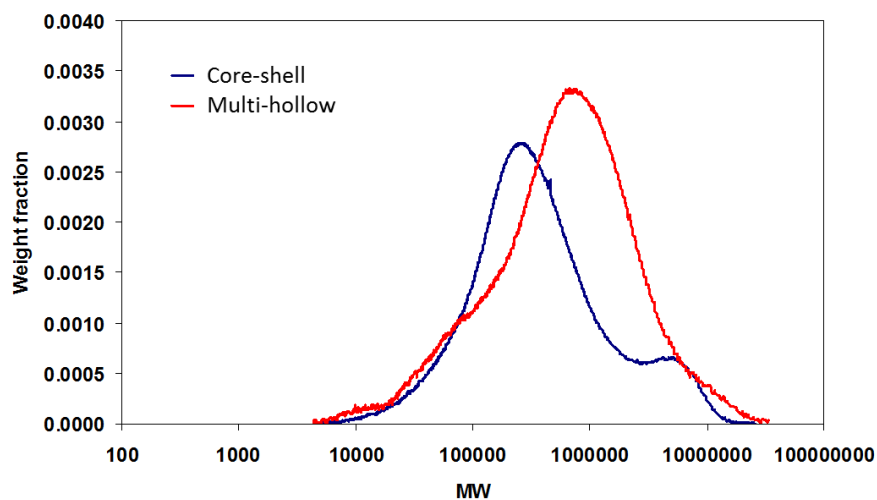
Structure	Mn	Mw
multi-hollow	1.5×10^5	6.5×10^5
porous core-shell	1.4×10^5	1.0×10^6

Figure 3-16. Comparison of MWDs of core-shell structured PMMAs and multi-hollow PMMAs.

3.4. Conclusion

The proposed polymerization technique offers several unique advantages. Firstly, it can be applied to many other polymer systems where the polymer dissolves in its own monomer. Another

important advantage of the proposed technique is that it is a single-stage process and existing suspension polymerization process can be easily modified to institute the proposed polymerization technique, making the mass production of polymer particles economically realizable at a low manufacturing cost. Finally, it also offers a variety of polymer particle morphologies including single hollow morphology with controlled shell thickness, multihollow morphology with controlled hollow sizes and numbers, and other variations of these morphologies for many interesting potential applications.

Chapter 4 Introduction to the Synthesis of Partially Neutralized Sodium Polyacrylate Micro-Particles by Inverse Suspension Polymerization

4.1. Background and Motivations

4.1.1. Super Absorbent Polymer

Certain free radical polymers such as sodium polyacrylate are called superabsorbent polymers (SAP) because they can absorb and retain extremely large amounts of water or aqueous solutions relative to their own mass. For example, SAP can absorb 15 to 500 times of deionized water per gram of polymer [64-66,60,67]. Figure 4-1. Illustrates the swelling of sodium polyacrylate polymer particles after absorbing water.

Figure 4-1. Swollen Na-polyacrylate; the right sample has swelling capacity of water 243.1 g/g.

Applications of superabsorbent polymers

The properties of superabsorbent polymers can be employed in many different applications. The largest use of superabsorbent polymers is in personal hygiene products. These consumer products include disposable infant diapers, children's training pants, adult incontinence articles, and feminine sanitary napkins. According to a report from 'Transparency Market Research' [68], the global superabsorbent polymer (SAP) market size is 1,861.8 kilo tons or 6.06 billion in 2013. Also, it is anticipated to reach USD 8.78 billion by 2020. The demand for feminine hygiene as well as baby diaper keeps increasing and the rising aging population brings the need of adult incontinence products.
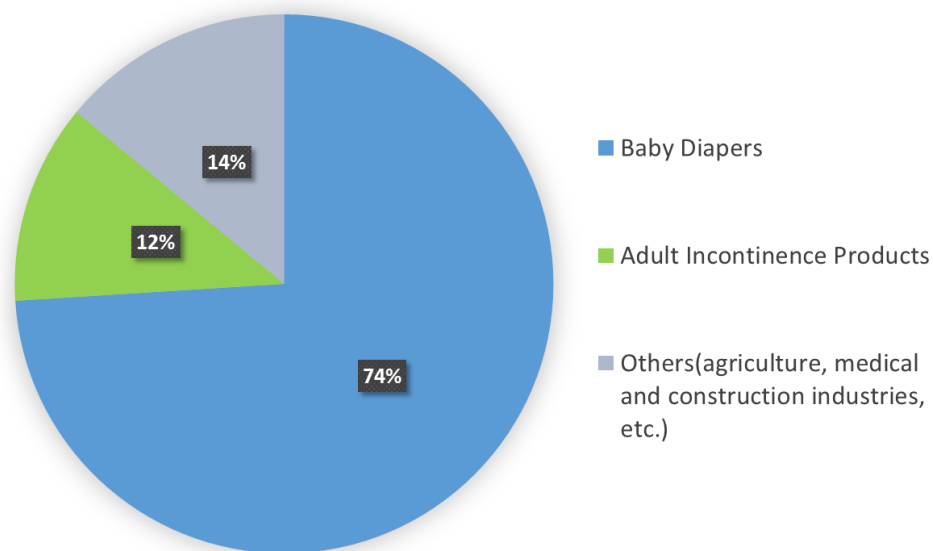
Figure 4-2. Global superabsorbent polymers market volume share, by application in 2013 [68].

The global superabsorbent market is highly dominated by several companies constituting more than 90 % of the market share in 2013. Key manufacturers of superabsorbent polymers

include Nippon Shokubai Co. Ltd, BASF, Bayer AG, Formosa Plastics Group, and Mitsubishi Chemical Holdings Corporation. Commercial SAP products are made via bulk or suspension polymerization and the bulk polymer product is ground or pulverized to small particles [59,60,69-75].

In the agricultural area, acrylic copolymers are used as water reserving materials that store over 100 times its weight in tap water, releasing a steady supply of water as the plants need it. And, coated polyacrylamide with the fertilizers can prevent the nutrients from dispersing too quickly as the fertilizer dissolves and minimize the leaching of fertilizer salts. Superabsorbent polymer helps waste treatment easy by flocculating solids in a liquid. Also, industrial cables, food, and medicines can be prevented from absorbing water by packaging with superabsorbent polymers [67].

In medicine, SAP is used as a wound dressing core covered with a non-adherent knitted polypropylene fabric, which absorbs blood and infections from wounded tissue and diffuses the antimicrobial agents such as chlorhexidine [66]. Also, it is used to remove body fluids during surgery [76]. Biocompatible sodium salt of carboxy methyl cellulose sodium salt (CMC), hydroxyl ethyl cellulose (HEC), and poly ethylene glycol (PEG) with various molecular weights were used to prepare oral hydrogels with the ability to absorb large amount of water [67].

In the field of pharmaceuticals, SAPs are used in drug delivery for gastric retention applications using the very fast swelling property, which is due to an increased capillary of the interconnected pore structure [77].

In the construction industry, water leakage is a problem. A sealing composite that swells slightly in water can be prepared by blending superabsorbent powder with rubber. The sealing composite is used between the concrete blocks that make up the walls of the structures. When water contacts the composite, the sealant swells slightly and makes an impermeable barrier to

further penetration of water [65]. In the same manner, water-blocking tape prepared by applying a dispersion of superabsorbent polymer in a polymeric binder can prevent water intrusion in fiber-optic communication cables and power transmission cables [65].

Superabsorbent polymers can also be used as a material for energy conservation in buildings. Wang et al. developed a "smart window" made of thermally sensitive poly(N-isopropyl acrylamide) (PNIPAAm) microgel colloids. Those which are sensitive to heat are particularly useful for saving energy. When it gets hot outside, the windows become opaque (polymers swell) to block unwanted heat from entering a building and they become transparent again as temperature drops. But current methods for making these windows use jelly-like hydrogels that swell in the heat, which hurts performance [78].

Swelling mechanisms of SAP

Let us consider how sodium polyacrylate polymers absorb so much water. Partially crosslinked sodium polyacrylate is one of the most well-known superabsorbent polymers and it has the chemical structure as shown in Fig. 4-3.
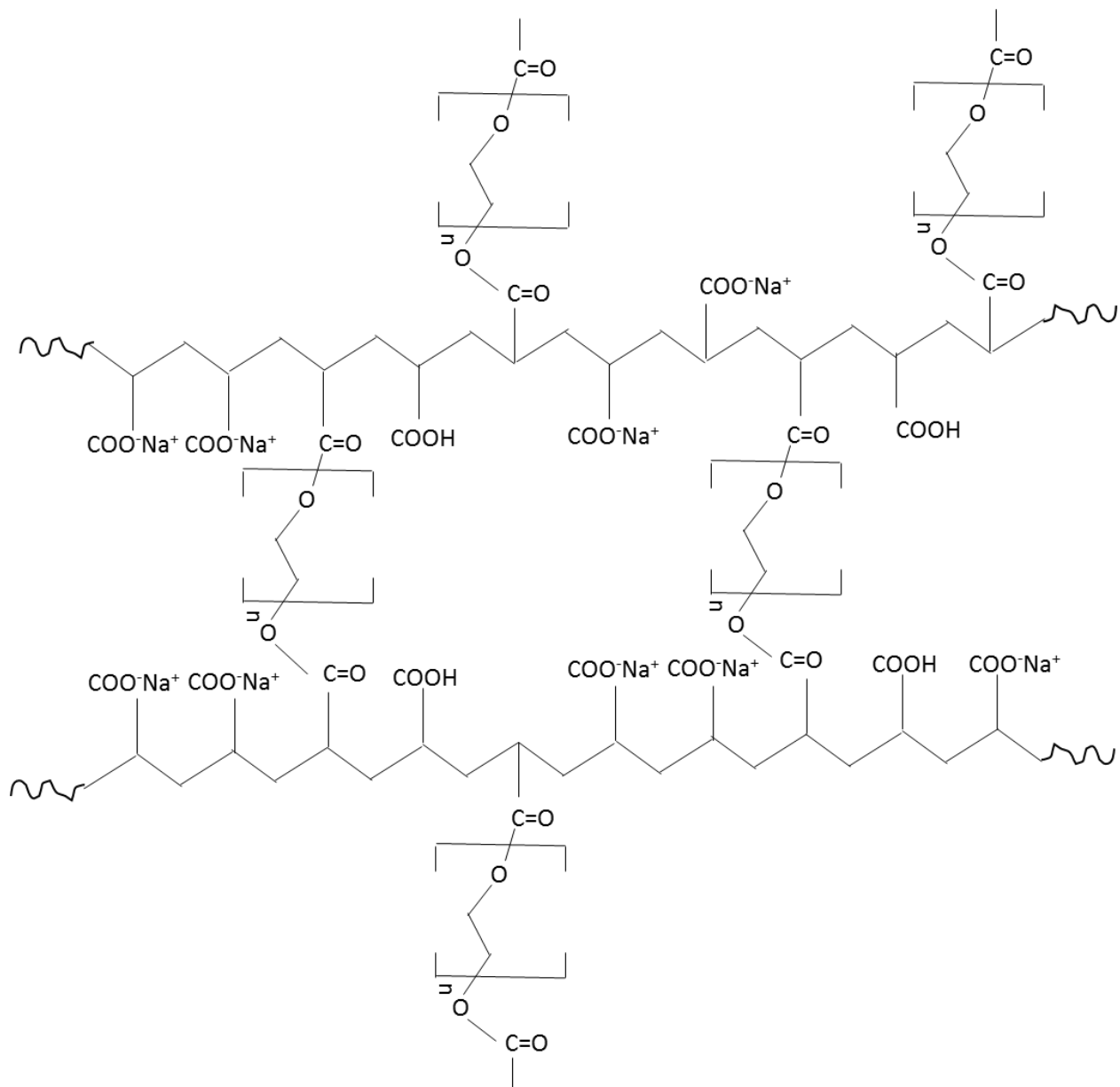
Figure 4-3. Superabsorbent sodium polyacrylate polymer with partial crosslinking [79].

The polymer derived from acrylic acid is hydrophilic in nature because of pendant carboxylic acid groups (-COOH). Some of these acid groups are partially neutralized by sodium hydroxide (NaOH) and hence as water is added to the polymer, a strong polymer-water interaction, hydration, occurs via the ions of the polymer (COO- and Na+) to attract a large amount of water

molecules [64]. Also, the hydrogen atoms are attracted to non-bonding electron pairs (lone pairs) on the oxygen atoms of other water molecules, which forms hydrogen bonds. Figure 4-4 shows the linked water molecules inside a polyacrylate network with ions and other water molecules.
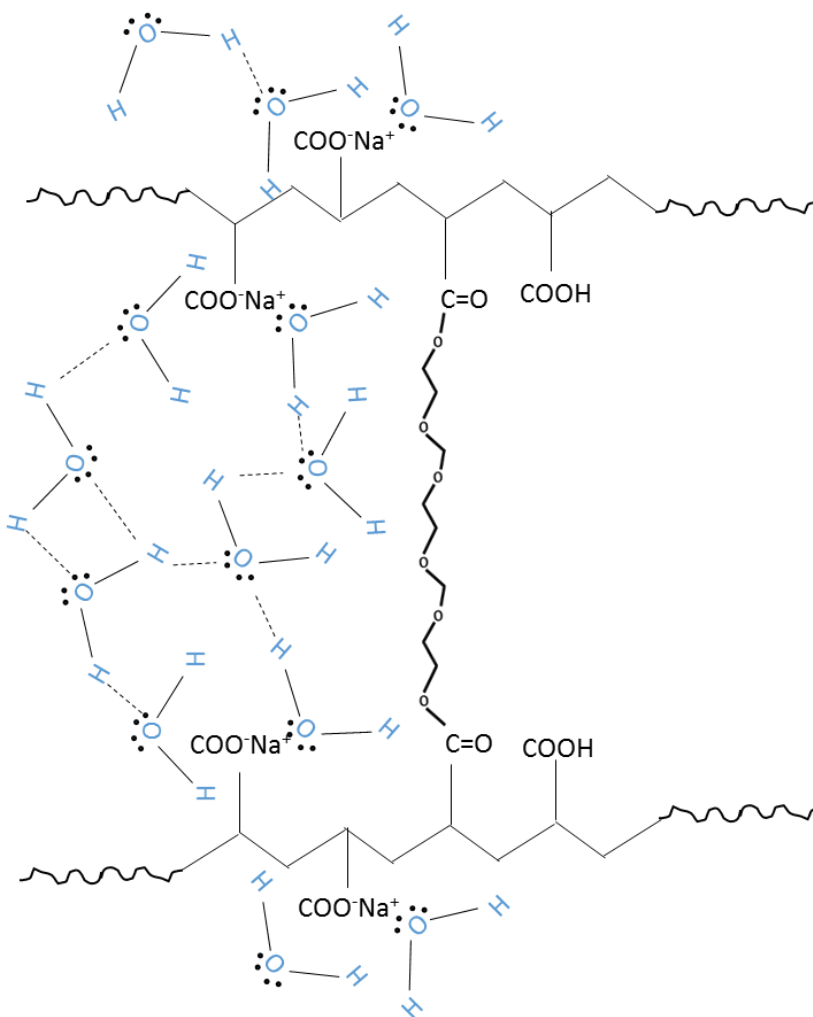
Figure 4-4. The schematic diagram of the swollen SAP structure where water molecules are linked to the ions and water each other.

The most important mechanism to make SAP swell in water is osmosis. Osmosis is the spontaneous net movement of solvent molecules through a semipermeable membrane into a region of higher solute concentration [64]. Osmosis is in the direction to equalize the solute concentrations on both sides. In SAP crosslinking between polymer chains makes a three dimensional network and this net plays a semipermeable membrane role. The ions (COO^- and NA^+) are solute in the net. So the driving force for swelling is the difference between the osmotic pressure inside and outside SAP. When the sodium increases outside of a superabsorbent polymer, the osmotic pressure will decrease, and so SAPs absorb urine or NaCl (aq) less than deionized water [64].

The extent of swelling represents a competition between two forces. The free energy of mixing causes water to penetrate and try to dilute the polymer network (osmosis). As the polymer chains in the crosslinked polymer network begin to elongate under the swelling action of the water, they generate an elastic retractive force in opposition to this deformation. The volumetric swelling reaches steady state when the two forces balance each other [72,94].

4.1.2. Synthesis techniques for polyacrylate

Superabsorbent acrylate polymers can be synthesized by several different techniques, such as bulk, solution, suspension, emulsion, and dispersion polymerizations.

Bulk polymerization

Bulk processing is the oldest industrial SAP process technology. In a bulk polymerization process, acrylic acid is partially neutralized by NaOH and directly polymerized using water-

soluble initiators in presence of a crosslinking agent. The partially crosslinked polymer is made in a kneader reactor that can handle highly viscous polymers (figure 4-5). Because of the high concentration of monomer, the rate of polymerization and the degree of polymerization is very high. However, the viscosity of reaction increases remarkably with the conversion and so the heat is generated during polymerization. Therefore, it is hard to control the temperature. The advantage of bulk polymerization is that high molecular weight polymer with high purity can be produced since no other material is involved [80].

Figure 4-5. The commercial kneader reactor [81].

Solution polymerization

Solution polymerization is a method of industrial polymerization. In this procedure, the acrylic acid and a crosslinker are dissolved in water at a desired concentration, usually from about 10% ~ 70%. The polymerization is initiated thermally, by UV irradiation, or by a redox initiator system. The major advantage of solution polymerization is that the solvent acts as a heatsink over the bulk polymerization. However, due to the nature of polyacrylate swelling in water, the product

obtained is still a rubbery gel. The prepared superabsorbent polymers need to be washed with methanol or solvent to remove the unreacted monomers, oligomers, crosslinking agent, the initiator, and extractable (soluble) polymer [80]. The representative example is porous poly(2-hydroxy ethyl methacrylate) hydrogel, which is a biomedicine material [64, 82].

Inverse emulsion polymerization

In emulsion polymerization, the monomer is insoluble in the polymerization medium, but it is emulsified by a surfactant. Unlike in suspension polymerization, the initiator is soluble in the medium and not in the monomer. Under these conditions, relatively large droplets of monomer (about $1 \sim 10$ μm or larger) are formed in the medium and excess surfactant creates micelles with a relatively small quantity of monomer (about $50 \sim 100$ Å) in the medium. Monomer in the micelle polymerizes quickly, and then more monomer from the droplets diffuses into the growing particle and reacts with initiator [61]. GE et al. synthesized polyacrylic acid particles in a rage of $5 \sim 30$ nm using an inverse (W/O) emulsion polymerization method [83].

Kriwet et al. investigated polyacrlic acid nano and micro particles by inverse emulsion polymerization. They were stabilized by a co-emulsifier system consisting of Span 80 and Tween 80 in a liquid paraffin. The particle size is dependent on the type of radical initiator used. When lipophilic radical initiators, such as azobis-isobutyronitrile (AIBN), are used, almost all nanoparticles are generated with diameters in the range of 80 to 150 nm dispersed in oil. Whereas, with water-soluble initiators, such as ammonium persulfate (APS), micro particles were obtained in the size range of 1 to 10 μm [84]. Wang et al. produced sodium polyacrylate by inverse suspension polymerization, using Span 60 as the dispersant, cyclohexane as the organic phase, *N,N'*-methylene bisacrylamide as the crosslinking agent, and potassium persulfate as the initiator.

Sodium polyacrylate particles in range of 10 ~ 50 μm were shown only in the polarizing microscope images and thus dried samples couldn't be seen at this article [85].

Dispersion polymerization

In dispersion polymerization the monomer and the initiator are both soluble in the polymerization medium, but the medium is a poor solvent for the resulting polymer. Therefore, the reaction mixture is homogeneous at the beginning, and the polymer is precipitated in a solvent. As a result, spherical polymer particles are monodisperse and in the range of about 0.1 ~ 10 μm [61].

In the academic area, monodisperse polyacrylamide microparticles were prepared by dispersion polymerization in an aqueous alcoholic media (tert-butanol/water mixture) initiated by 2,2'-azobisisobutlronitrile using poly(*N*-vinylpyrrolidone) as a steric stabilizer [86]. Minami et al. prepared Poly(acrylic acid) (PAA) particles by dispersion polymerization of acrylic acid in ionic liquid without a crosslinker. The particles were so small in range from 90 nm to 5 μm. They extracted polymer particles with water but not dried particles [87].

Inverse suspension polymerization

Inverse suspension polymerization is a heterogeneous radical polymerization process that uses mechanical agitation to mix a monomer or mixture of monomers in an oil phase while the monomers polymerize, forming spheres of polymer. An inverse suspension polymerization process is typically carried out in well- stirred batch reactors. Inverse suspension polymerization employs a diluent (organic) in which neither the monomer nor polymer is soluble [67,70]. In the

inverse suspension polymerization process, micron-size droplets of aqueous monomer solution are dispersed into an organic phase before polymerization. Free radical polymerization then proceeds in each small droplet in the same way as solution polymerization.
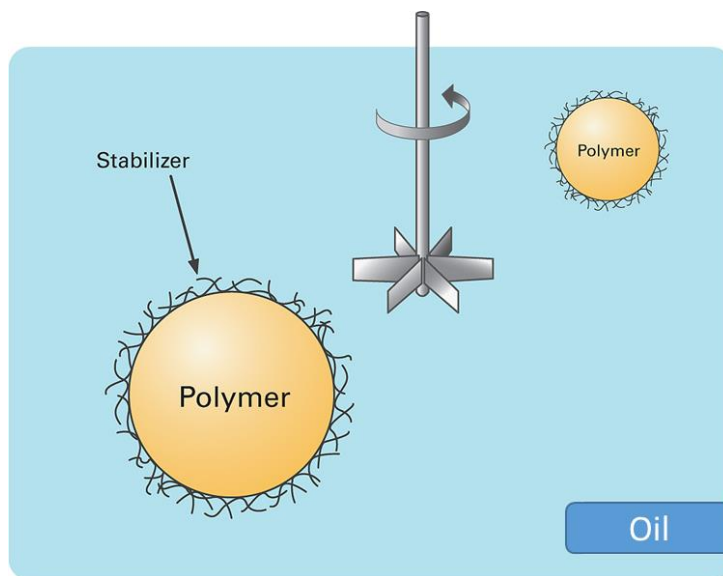
Figure 4-6. Description of inverse suspension polymerization.

A reason to use this technique is to simplify the handling of the rubbery gel polymerization product. The low viscosity suspension of the monomer and polymer droplets is easy to agitate well and more efficient removal of reaction heat is possible. In addition, the particle size of the product is more easily defined since it depends on agitation speed and amount of dispersant or suspending agent (surfactant or stabilizer) [69].

Mayoux et al. synthesized crosslinked poly(acrylic acid) by inverse suspension polymerization using potassium persulfate ($K_2S_2O_8$) as the initiator, *N, N'-*methylenebisacrylamide (MBAC) as the crosslinker and sorbitan monooleate as the surfactant. Particle diameters ranged from 10 to 130 μm, but particles aggregated and the shape was not

spherical in SEM images. Also, they only showed the optical microscopy images of wet spherical particles but not dried particles after all the post treatments [59].

Liu et al. polymerized acrylic acid initiated by a water soluble redox pair in the inverse suspension system. A few microns of polymer particles were produced, but they were aggregated [70-72].

Benda et al. investigated a new polymerization technique for the synthesis of the high molecular weight hydrophilic polymers. In this technique the initiated water solution monomer droplets were polymerized slowly by falling through an unstirred oil phase which fills in a long vertical reactor. The size of swollen beads was around 1~2 cm and beads were monodisperse. However, it took a long time to get a considerable amount of polymer particles [73].

Kiatkamjornwong et al. synthesized neutralized poly(acrylic acid-*co*-acrylamide) using inverse suspension polymerization. They investigated the size and size distribution of polymer particles by varying the concentration and type of suspending agent, which lead to different HLB (hydrophile-lipophile balance) numbers. The hydrophile-lipophile balance (HLB) number is the degree to which it is hydrophilic or lipophilic. The surfactant with an HLB number below 10 tends to be oil-soluble and the surfactant with an HLB number above 10 tends to be water-soluble. Smooth surfaced polymer particles in range of 50~140 µm were synthesized [74,75].

This chapter is concerned with the study of inverse suspension polymerization of partially neutralized acrylic acid. As will be discussed in detail in this chapter, we have observed many interesting polymer particle morphologies. Figure 4-7 illustrates the SEM images of a few examples of sodium polyacrylate SAP microparticles. The analysis of morphologies of sodium polyacrylate microparticles synthesized by inverse suspension polymerization, as shown in figure 4-7, have not been reported in the literature.

(a)

(b)

(c)

(d)
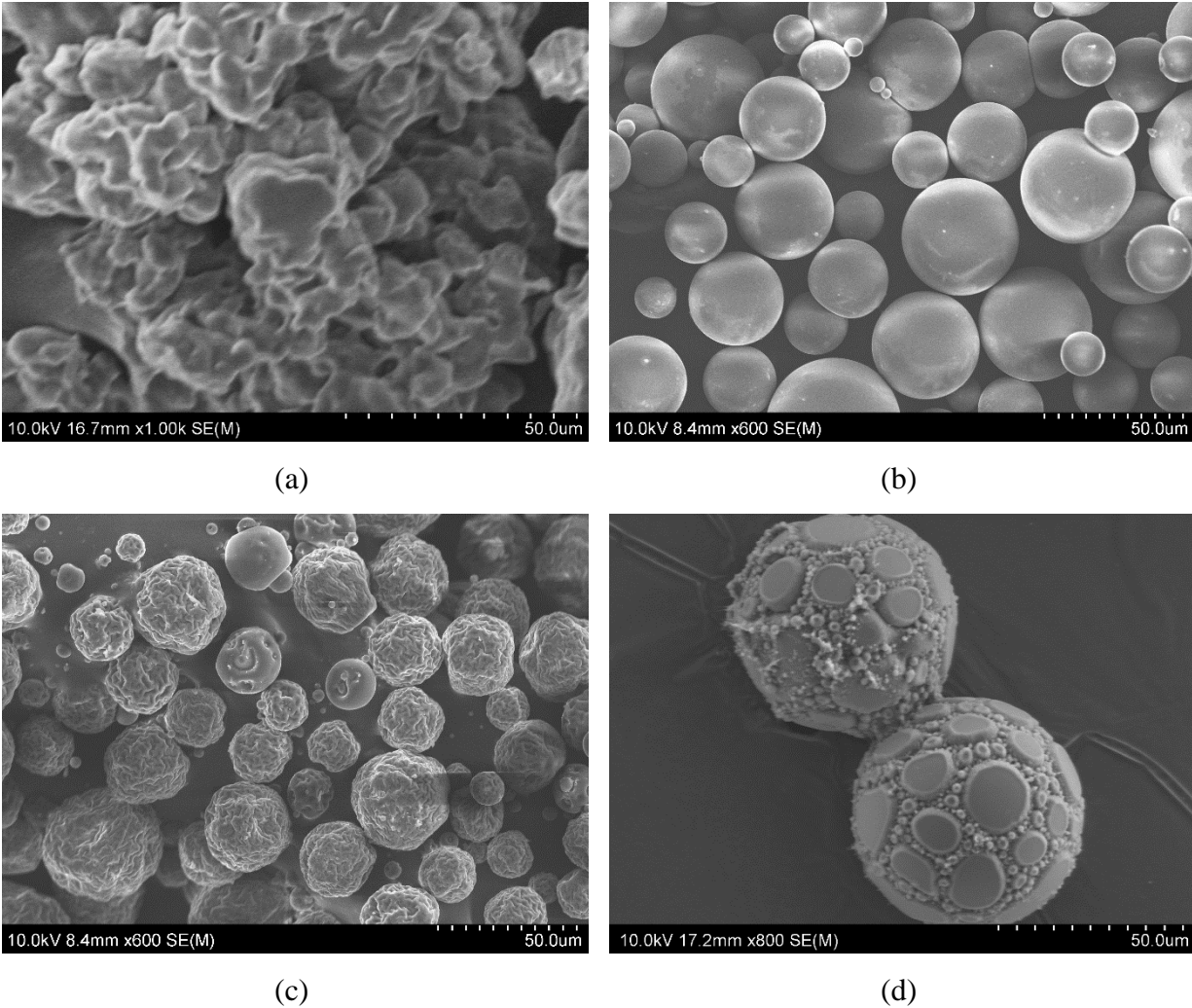
Figure 4-7. SEM images of PAA particles. (a) Commercial product, (b)~(d) PAA particles obtained in this study.

Crosslinking process during/after polymerization

Crosslinking can be conducted during polymerization or after polymerization. The synthesis methods introduced above mostly accompany crosslinking process during polymerization. In case of crosslinking after polymerization, the polyacrylate is formed in a first step, as a soluble polymer, which is then reacted in a second step with a suitable crosslinking agent.

A benefit of this technology is that the absorbent polymer can be formed in to a desired shape by mixing the suitable polymer and crosslinker and curing in place, for example into fibers or onto the surface of a sheet tissue. Drawbacks to this technology are the complex steps, the handling of the viscous solutions of polymer and their thorough mixing with the crosslinker and any catalysts required [80].

4.2. Research Objectives

As mentioned above, sodium polyacrylate is an industrially very important polymer for many applications. However, in industry sodium polyacrylate is mostly manufactured by bulk polymerization and the polymer is pulverized the bulk using a kneader to obtain small discrete polymer particles. It is an environment-unfriendly process and the produced granules from bulk have irregular shapes, not spheres.

Discrete spherical polyacrylate particles have many advantages over bulk or granular products from bulk polymerization. This study is aimed at investigating the inverse suspension polymerization of acrylic acid to make spherical polymer particles. In particular, the study is focused on how the resulting polymer morphology and characteristics are affected by the polymerization conditions.

In chapter 5, we present the experimental results of an inverse suspension polymerization where a high shear homogenizer was used to generate submicron size droplets of monomer-containing the aqueous phase. Chapter 6 is focused on the synthesis of polymer microparticles with wrinkled or cracked external surfaces. Finally, in chapter 7, we report the experimental study

of the particle synthesis where each spherical microparticle has a smooth external surface with high conversion of polymerization, and the kinetic calculations of it.

Chapter 5 Inverse Suspension Polymerization of Acrylic Acid Using a High Shear Mixing Device

5.1. High shear mixing before polymerization

In suspension polymerization, the size evolution of droplets/particles of the dispersed phase is composed of three stages [88]. In the first stage, the droplet size distribution results from the breakup-coalescence equilibrium when the viscosity of dispersed phase is low. In this stage, stabilizers adsorbed at the monomer droplet surface decrease the interfacial tension to make the monomer disperse in the medium, and build the thin layer to prevent the coalescence of the monomer droplets. In the second stage, the viscosity in the droplets/particles increases with conversion and so the size of particles increases due to the coalescence. In the final stage, the coalescence stops due to the elastic nature of particle collisions. This point is called the particle identity point. Once that the particle identity point has been passed, the particle size and its distribution cannot be changed and remain constant within 10 ~ 1000 μm [88].

Agitation affects the particle size and its distribution [89]. An increase of agitation speed promotes breakup of droplets, but more increasing agitation increases the frequency of coalescence. However, if the monomer droplets are made and the size is set using a high shear mixing device prior to the polymerization, it is feasible to obtain dispersed particles with sizes of ~ 10 μm using mild stirring rates during the polymerization [90]. This part is aimed at producing the sub-micron size polyacrylic acid particles with the simple steps of the inverse suspension polymerization using high shear mixing technique to generate aqueous droplets. A high shear rotor-stator mixer (Fig. 5-

1) operates by pumping the suspension through the narrow gap between a perforated cylinder (the stator) and the blades of a rapidly rotating stirrer inside it (the rotor) where the forces are sufficient to make droplets below 10 μm [91].

<div align="center">(a)</div>

<div align="center">(b)</div>
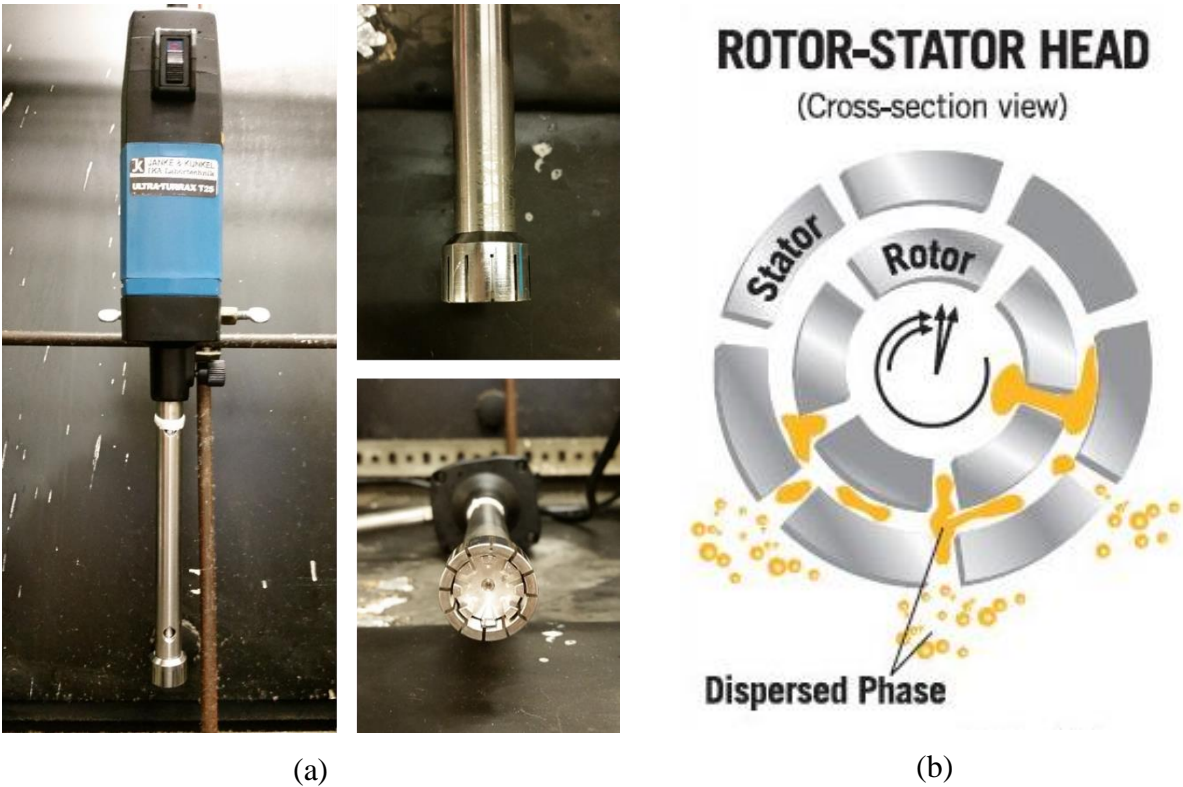
Figure 5-1. (a) The T25 ultra-turrax from IKA laboratory technology and (b) the principle of homogenization [91].

The important factor in this process is the usage of a highly efficient stabilizer that is capable of maintaining sub-micrometer particle size. Kriwet et al. [84,92] suggested that a "co-surfactant system", which contains Span 80 (sorbitan monooleate) with a low HLB (4.3) and Tween 80 (polyethyleneglycol sorbitan monooleate) with a higher HLB (15), can be used to optimize the stability. The HLB, hydrophilic-lipophilic balance, value of a surfactant is a measure

of the degree to which it is hydrophilic or lipophilic [75]. This value is determined by calculating the molecular mass of the hydrophilic portion of the molecule over the molecular mass of the whole molecule. When the HLB value is between 3 to 7, the surfactant is proper in the W/O system.

$$CH_2O - \overset{\overset{\displaystyle O}{\|}}{C} - CH_2(CH_2)_5CH_2CH = CH\ CH_2(CH_2)_6CH_3$$
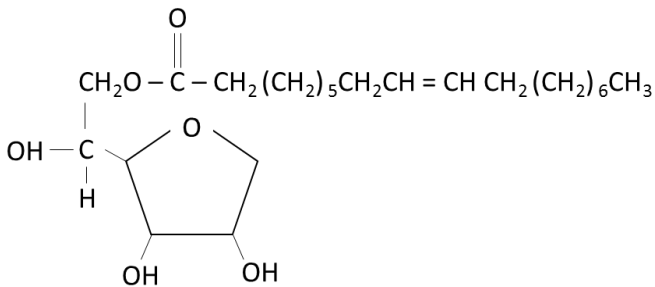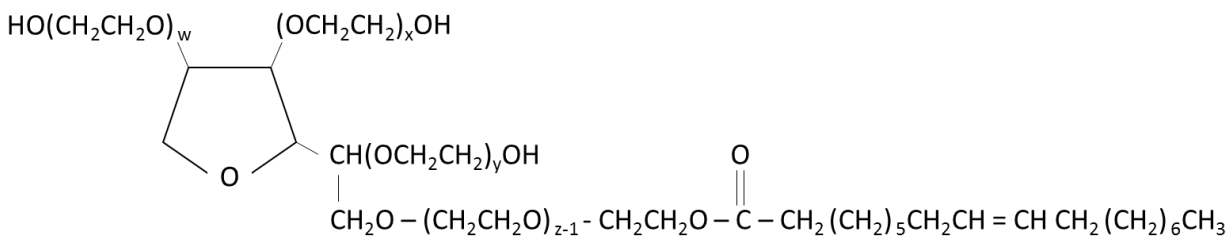
(a) Span 80

$$w + x + y + z = 20$$

(b) Tween 80

Figure 5-2. The structures of Span 80 and Tween 80 [111].

In figure 5-3, the hydrophilic portions of Span 80 and Tween 80 were adsorbed on the surface of water droplet in the oil medium.
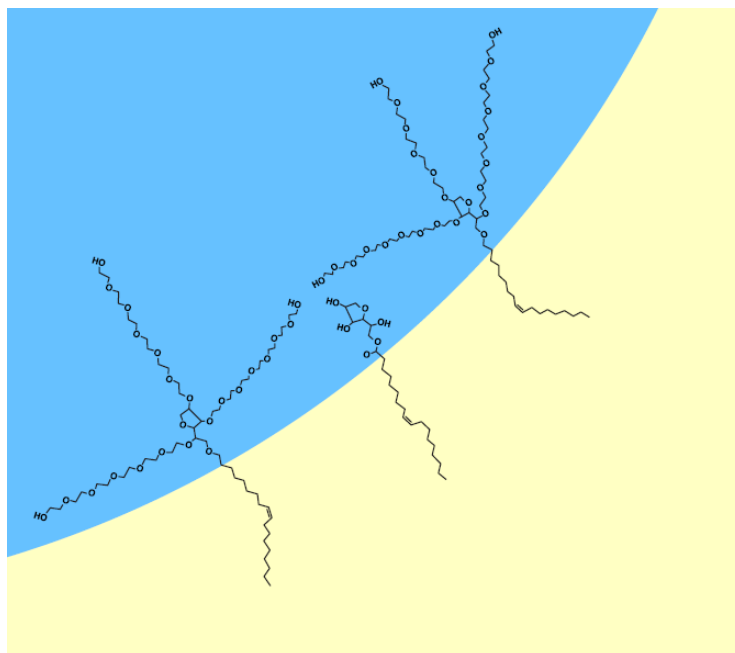
Figure 5-3. The Schematic representation of the geometrical packing of the surfactants at the water-oil interface in dispersed water droplets [93].

In order to prove the effect of co-surfactant system as a result of varying the ratio of two surfactants, the simple test was performed. (Figure 5-4)

Five vials of the 4 ml of deionized water and 10 ml of heptane mixture were prepared. Five different ratio of Span 80/Tween 80 (0 : 10, 2.5 : 7.5, 5 : 5, 7.5 : 2.5, and 10 : 0, total volume is 2 ml each) were dissolved in each vial. The 2 g of sodium polyacrylate particles (Sigma-Aldrich) was added in each vial and stirred using a magnet bar for 1 hr. In each vial, HLB values of co surfactant are 15, 12.3, 9.7, 7.0, and 4.3 from a simple calculation using the fraction.
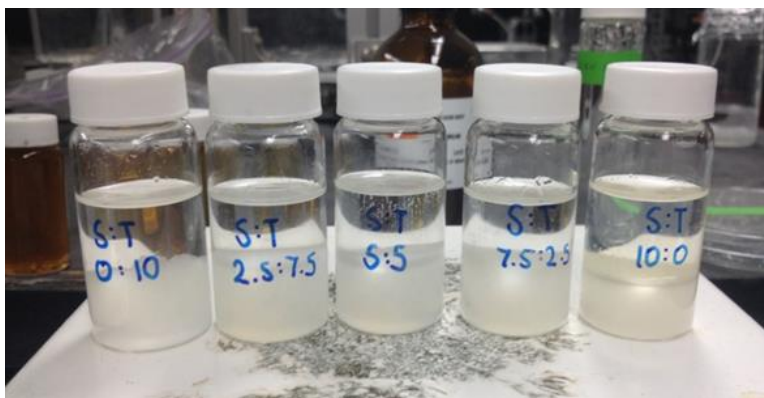
t = 0
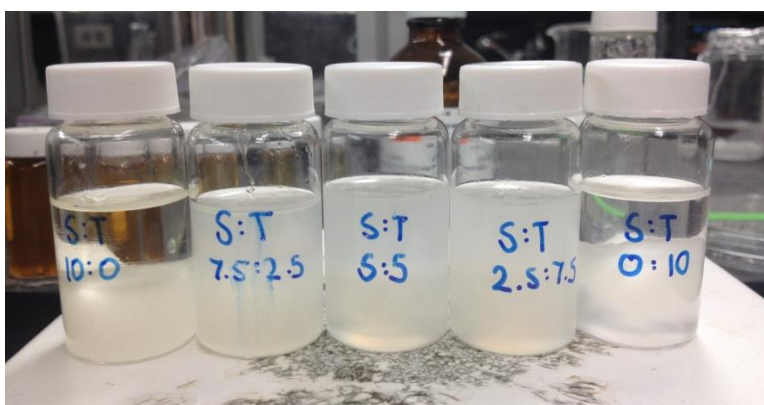
t = 1 hr

Figure 5-4. The vial test for the effect of co-surfactant system as varying the ratio of two surfactants.

In figure 5-4, the solutions in three vials (ratios of Span 80/Tween 80 are 2.5 : 7.5, 5 : 5, and 7.5 : 2.5) were well dispersed after 1 hr and thus experiments in this chapter were based off this result. As mentioned above, a 3~7 HLB value is proper in this W/O system. Thus, we chose the 2.5 : 7.5 ratio of Span 80 to Tween 80. An HLB value between 8 to 16 is known to be proper O/W emulsifier [75]. Therefore, in the other two vials, oil droplets may be emulsified in water.

5.2. Kinetics of partially neutralized sodium polyacrylate by free radical polymerization

5.2.1. Partial neutralization of acrylic acid

As mentioned earlier in this chapter, neutralizing the polymer chains increased the osmotic pressure of the superabsorbent polymer and the swelling capacity. Therefore, acrylic acid needs to be neutralized by a sodium hydroxide solution. Also, the solubility of some types of crosslinkers is affected by the pH of the monomer solution [94].
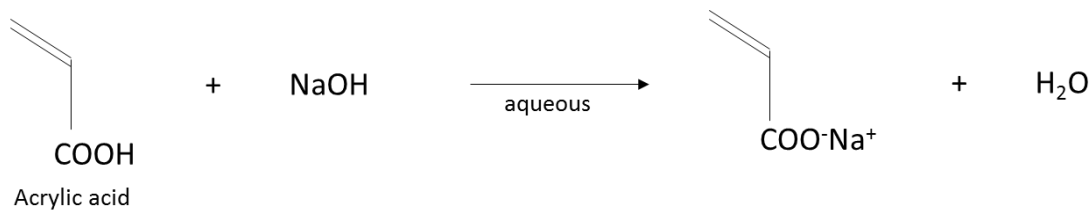
Fundamentals of neutralization of a weak acid and base

Consider the equilibrium reaction for the ionization of an acrylic acid [95].

$$CH_2CHCOOH(aq) + H_2O(l) \rightleftharpoons CH_2CHCOO^-(aq) + H_3O^+(l)$$
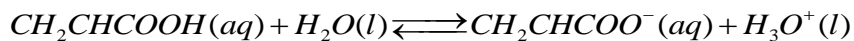
The acidity constant is

$$K_a = \frac{[CH_2CHCOO^-][H_3O^+]}{[CH_2CHCOOH]}$$

This can be shown by re-arranging the expression for K_a

$$[H_3O^+] = K_a \frac{[CH_2CHCOOH]}{[CH_2CHCOO^-]}$$

$$pH = pK_a - \log \frac{[CH_2CHCOOH]}{[CH_2CHCOO^-]}$$

As pK_a of acrylic acid is known to be 4.25 at 25°C from the reference [96], pH can be calculated as each neutralization ratio.

Table 5-1. The values of pH as varying different neutralization ratio.

Neutralization ratio (α)	$\dfrac{[CH_2CHCOOH]}{[CH_2CHCOO^-]}$	$pH = pK_a - \log \dfrac{[CH_2CHCOOH]}{[CH_2CHCOO^-]}$
0.5	1	4.25
0.6	$\dfrac{4}{6} = 0.67$	4.43
0.7	$\dfrac{3}{7} = 0.43$	4.62
0.8	$\dfrac{2}{8} = 0.25$	4.85
0.9	$\dfrac{1}{9} = 0.11$	5.20
0.99	$\dfrac{0.01}{0.99} = 0.01$	6.25

Crosslinking is the joining of molecules with a smaller molecule. In the case of superabsorbent polymers, the most common type is the covalent crosslink - an organic molecule that contains two or more double bonds. These molecules are incorporated into the backbone of the polymer chains as they grow during the polymerization reaction. The crosslinkers typically used in superabsorbent polymers are di- and tri-acrylate esters [69,94]. Crosslinkers play a major role in modifying the properties of superabsorbent polymers as well as the swelling and mechanical properties. The swelling capacity has as inverse relationship with the crosslinking density [69,94].

In this work poly (ethylene glycol diacrylate) (PEGDA) (Fig. 5-5) was used in the acrylic acid polymerization using the high shear mixing device as a crosslinking agent in variable concentrations.
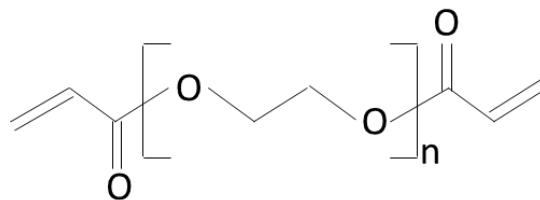
Figure 5-5. Poly (ethylene glycol diacrylate) (PEGDA) [111].

Initiation
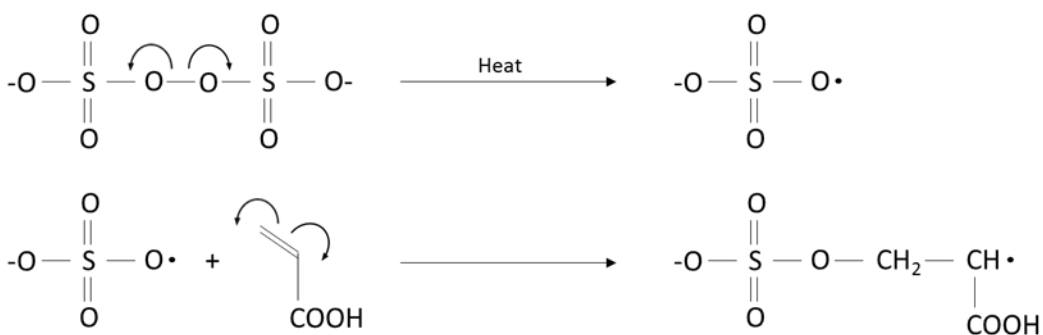
Propagation
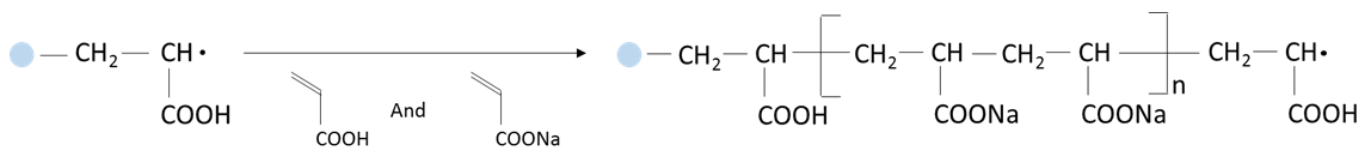
Termination

Figure 5-6. Schematic description of chain initiation and propagation of partially neutralized acrylic acid [79].
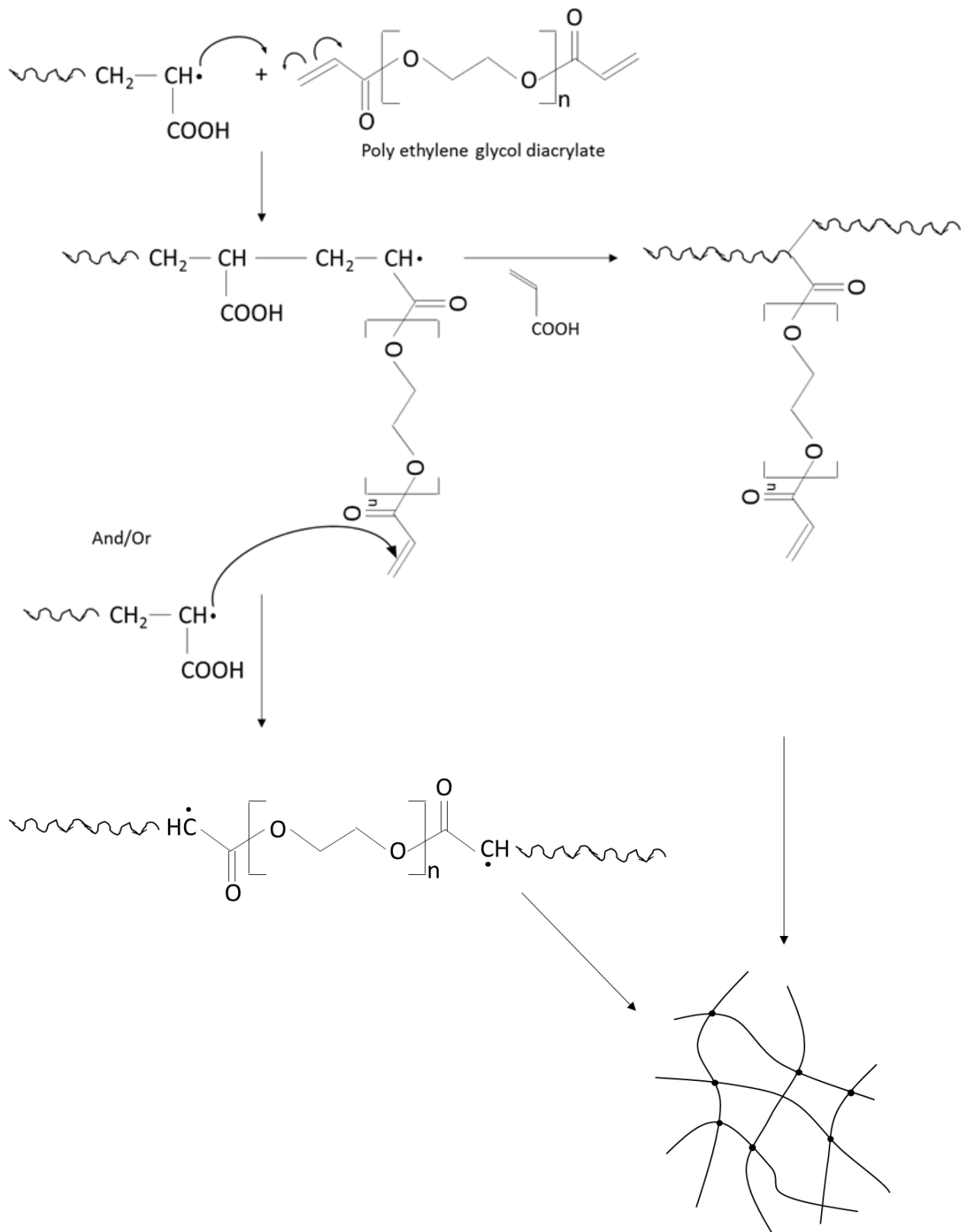
Figure 5-7. Schematic description of crosslinking reaction of acrylic acid [79].

5.2.2. Kinetics of Free Radical Polymerization of Acrylic Acid

The structure of a polymeric network is ultimately determined by the method of synthesis. The monomer and crosslinker concentrations, the initiator type and concentrations, the relative reactivities of the monomers, the solvent used, and reaction temperature are all important factors that affect the rate of the polymerization [97].

In this section, we investigate the effects of the concentrations of monomer and initiator, temperature, and reaction time on the rate of polymerization and the morphology of Na-polyacrylate particles.

In free radical polymerization, very small concentrations of free radicals are generated by chemical reactions, and the chain growth occurs very fast following the addition polymerization mechanism. The polymerization consists of initiation, chain propagation, chain transfer and chain termination reactions. The free radical polymerization is represented by the following stoichiometric equations. [98].

$$I \rightarrow 2R^{\bullet} \qquad\qquad k_d$$

$$R^{\bullet} + M \rightarrow RM^{\bullet} \qquad\qquad k_p$$

$$RM^{\bullet} + M \rightarrow RM^{\bullet} \qquad\qquad k_p$$

$$RM^{\bullet} + RM^{\bullet} \rightarrow polymer \qquad\qquad k_t$$
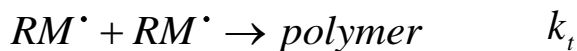
In most of free radical polymerizations, the polymerization is linearly dependent on the monomer concentration, but for acrylic acid polymerization, Manickam [99], Kabanov [100], and Cutie at al. [98] suggested that the rate of acrylic acid polymerization rate is 3/2th order with respect to acrylic acid concentration and 1/2th order with initiator concentration.

$$R_p = k_p \left(\frac{fk_d}{k_t} \right)^{1/2} [M]^{3/2} [I]^{1/2} \qquad \text{(eq. 5.1)}$$

Cutie et al. reported the estimated the polymerization parameters for acrylic acid at 55°C. (Table 5-2) In this study, the polymerization was carried out at 60°C and 65°C. Since the rate constant $\ln k$ is proportional to $\dfrac{1}{T(K)}$, the parameters at 60°C and 65°C can be calculated.

Table 5-2. Estimated parameters.

Parameters	at 55°C [99]	at 60°C	at 65°C
k_d	9.15×10^{-4} min^{-1}	1.02×10^{-3} min^{-1}	1.13×10^{-3} min^{-1}
k_p	2.32×10^{6} $L/mol \cdot$ min	1.86×10^{6} $L/mol \cdot$ min	1.50×10^{6} $L/mol \cdot$ min
k_t	1.94×10^{10} $L/mol \cdot$ min	1.36×10^{10} $L/mol \cdot$ min	9.63×10^{9} $L/mol \cdot$ min

From eq. 5.1 monomer concentration at time = t can be induced as following.

$$\frac{1}{[M]^{1/2}} - \frac{1}{[M]_0^{1/2}} = k_p \left(\frac{f_i I_0}{k_d k_t} \right)^{1/2} \left(1 - e^{-\frac{k_d t}{2}} \right) \qquad \text{(eq. 5.2)}$$

Assume that $f_i = 0.5$.

Then conversion, x , at time $= t$ is

$$x = 1 - \frac{[M]}{[M]_0} \qquad \text{(eq. 5.3)}$$

Using the estimated data (table 5-2), eq. 5.2 and eq. 5.3, the polymerization rate and the conversion

in this system were plotted.
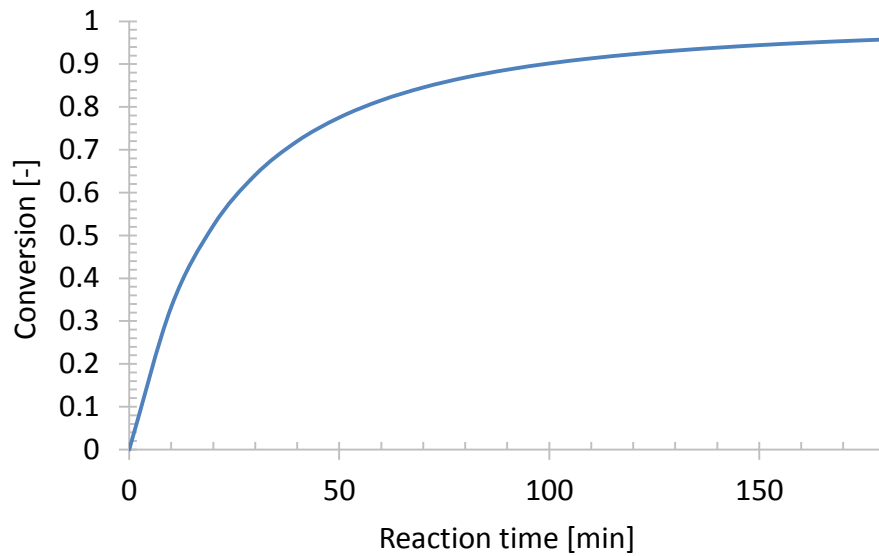
Figure 5-8. Calculate conversion curve using reaction parameters [98].

5.3. Experimental

5.3.1. Materials

Acrylic acid (AA, CH2=CHCOOH, anhydrous, 99%, contains 180~200 ppm MEHQ (monomethyl ether hydroquinone) as an inhibitor, Aldrich) was used as a monomer. The monomer was added dropwise into the prepacked column charged with aluminum oxide (Aldrich Chem. Co.). Sodium hydroxide (NaOH, Sigma Aldrich) was used to neutralize the acrylic acid. Toluene, mineral oil, hexane, and heptane (Fisher scientific) were used as polymerization mediums and non-solvents. Potassium persulfate ($K_2S_2O_8$), ammonium persulfate (($NH_4)_2S_2O_8$), and sodium persulfate ($Na_2S_2O_8$) (Sigma Aldrich) were used as initiators. Span 80 (sorbitane monooleate, Fluka) and Tween 80 (Polyethylene glycol sorbitan monooleate, Sigma-Aldrich) were used as suspension stabilizers and poly (ethylene glycol diacrylate) (PEGDA, Aldrich) was used as a crosslinking agent.

Titration of acrylic acid by an aqueous solution of sodium hydroxide

The acrylic acid was partially neutralized drop by drop by an aqueous solution of sodium hydroxide (17.5% w/w). During the neutralization, the beaker was kept cool in the ice bath to prevent excessive heat release and *pH* was measured using the *pH* meter (Oakton *pH* 11 meter with "All-in-One" electrode) (Figure 5-9). Before measuring the *pH* of the titrated solution, the *pH* meter was calibrated using the acrylic acid (*pH* = 2.5 [101]) as well as the buffer solutions of

pH 4, *pH* 7, and *pH* 11. Titration proceeded until the *pH* value matched with above calculated

value at each neutralization ratio (Table 5-1).
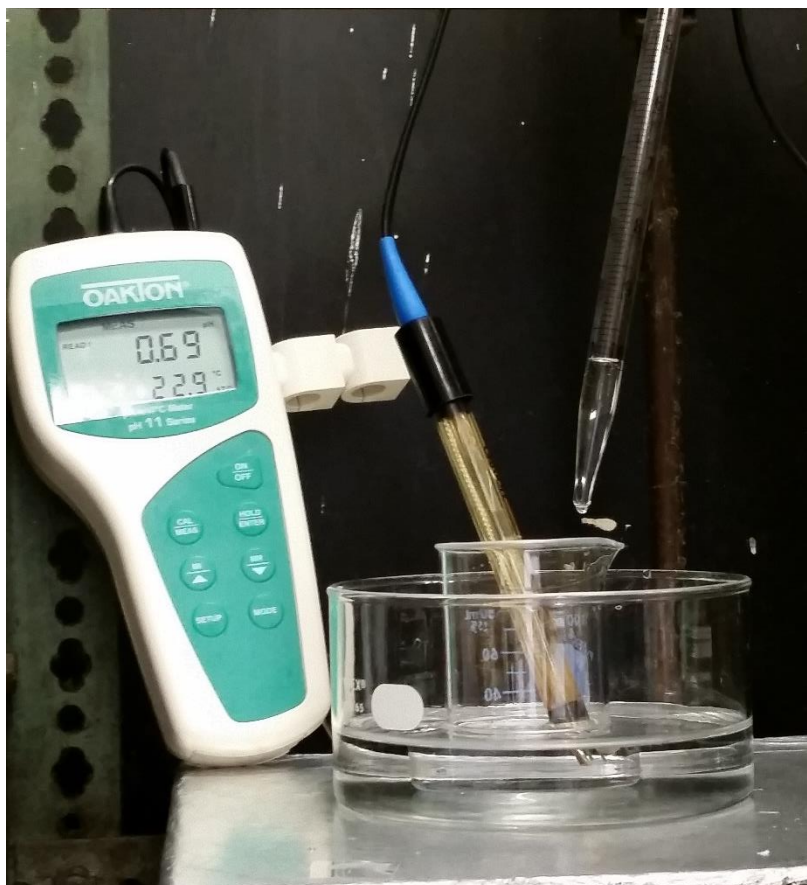
Figure 5-9. Titration of acrylic acid by an aqueous solution of sodium hydroxide measuring the

pH .

5.3.2. Inverse Suspension Polymerization of acrylic acid using the high shear mixing device

In a 25 ml-beaker the 2.83 mol % PEGDA was dissolved in a partially neutralized sodium-

acrylate solution and the clear mixture obtained was degassed by nitrogen bubbling for about 30

min. The 19.6 mole % in the oil phase of stabilized mixtures of Span 80 and Tween 80 were dissolved in heptane or hexane in a 125 ml- glass flask. 0.898 ~ 0.977 mole % of potassium persulfate ($K_2S_2O_8$ (KPS), Aldrich) in monomer was dissolved in the aqueous monomer solution after degassing and it was added to the oil phase (stabilizer/solvent) in the flask. The high shear mixing was applied at 1000 ~ 8000 rpm for 30 ~ 180 sec using the T25 Ultra-Turrax (IKA) homogenizer. And then the homogenized mixture was transferred to a 100ml-jaketted reactor, heated to 65°C and stirred at 500 ~ 600 rpm. The polymerization was conducted for 2 hr. After polymerization, 100 ml of methanol was poured into the reactor for 30 min while the reaction mixture was agitated, and the polymer particles were recovered. After drying the polymer particles under a vacuum at 40°C, sodium polyacrylate particles were obtained.
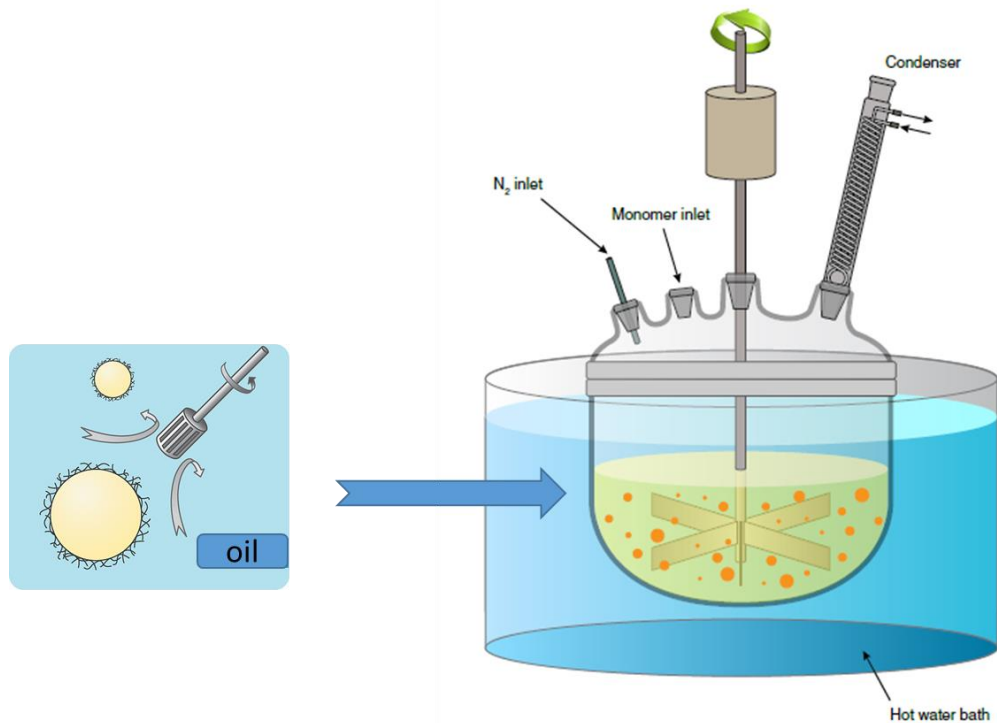
Figure 5-10. Schematic illustration of inverse suspension polymerization after high shear mixing.

5.3.3. Characterization

The size and the surface morphology of polymer particles

The size and the surface morphology of spherical Na-polyacrylate particles was analyzed by scanning electron microscopy (SEM). Also, the particle surface was analyzed by energy-dispersive X-ray spectroscopy (EDX).

Swelling capacity

The swelling capacity was determined by teabag method [102-104]. 0.2 g of poly acrylic acid was placed in a sealed teabag (7X9 cm) and put in a deionized water for 5 hrs and allowed to swell. The soaked teabag was removed from the deionized water and hung up to remove excess water for 30 minutes and then weighted.

Figure 5-11. Illustration of tea bag method and an image of measuring swelling capacity by the tea bag method.

Conversion

The conversion of Na-polyacrylate particles was measured by the gravimetric method. At the end of the reaction, the polymer solution in the reactor was poured slowly into the ten times amount of methanol and agitated with a magnetic bar for 30 min. After filtering, particles were dried at 40°C for three days and then weighed. As the polymerization time was varied, obtained polymers were weighed and conversion data were obtained.

5.4. Results and Discussion

5.4.1. Effect of homogenization

When the high shear mixing was not performed before the inverse suspension polymerization, the size of particles increased to as large as 140 μm (mostly within 20 ~ 100 μm). In contrast, with the high shear homogenization, the polymer particle size was below 5 μm and it was observed that inner morphology of the particles was different from those particles obtained without using homogenizer (Fig. 5-12). The solubility of heptane in water is 0.0003 % at 25°C, which is very small. However, the solubility of water in heptane is 0.01 % at 25°C. A hollow in the particle could be explained that some amount of water transfers to heptane during homogenization due to the large surface area of droplets and the high shear energy. Thus, the place of water was turned into a hollow in the center of the droplet.
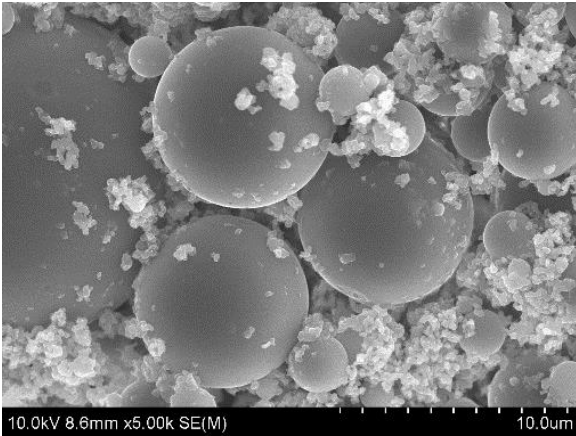
<div align="center">(a1)</div>
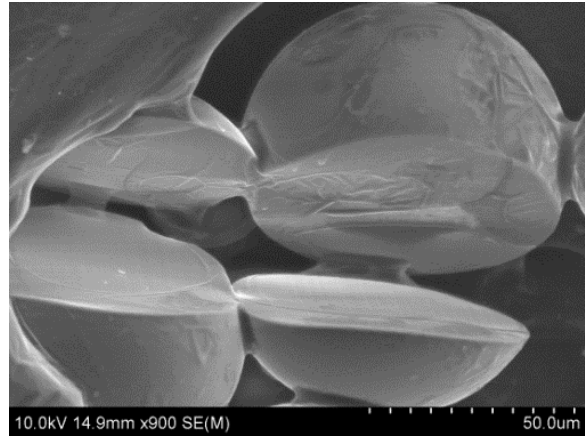
<div align="center">(a2)</div>
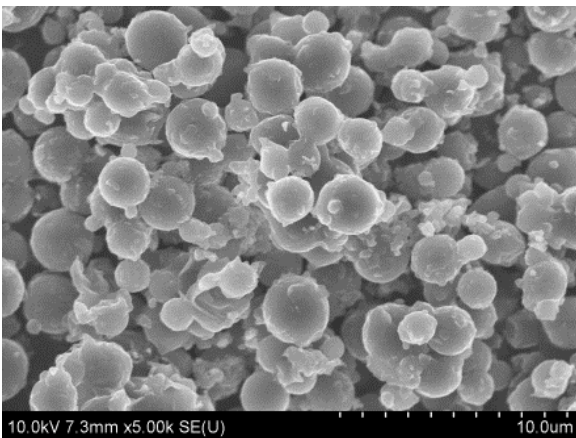
<div align="center">(b1)</div>
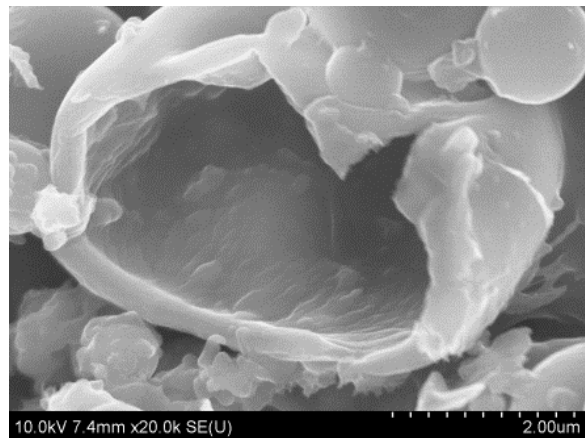
<div align="center">(b2)</div>

Figure 5-12. Effect of the high shear mixing before polymerization on the morphology of partially neutralized sodium polyacrylate. (a) no high shear mixing and (b) high shear mixing at 8000 rpm for 3min. The concentrations are the same (30 vol.% in aqueous phase).

5.4.2. Effect of homogenization speed and time before inverse suspension polymerization

When the aqueous/oil mixture was homogenized at 8000 rpm for 3 min, the size of polymerized particles were even and in range below 5 microns. Although a few attempts were

<div align="center">79</div>

made to use shorter homogenization time (less than 3 minutes) to increase the size of particles,
little change in the particle size was observed. Instead, nano-sized particles (around 500 nm) were
observed. Figure 5-13 shows different morphologies with varying the homogenization speed and
duration. When the speed of homogenization was lowered from 3000rpm to 1000rpm, particles
over 10 microns were obtained but more nano-sized particles were present outside the particles.
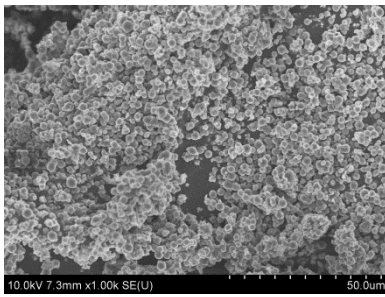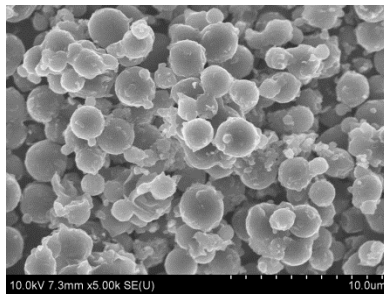
(a1)	(a2)	(a3)
(b1)	(b2)	(b3)
(c1)	(c2)	(c3)
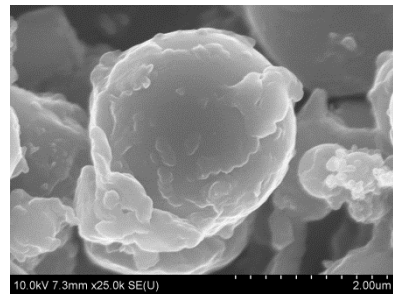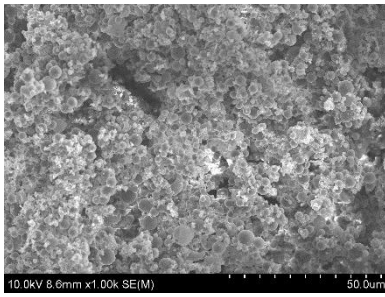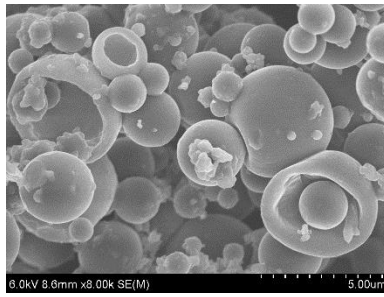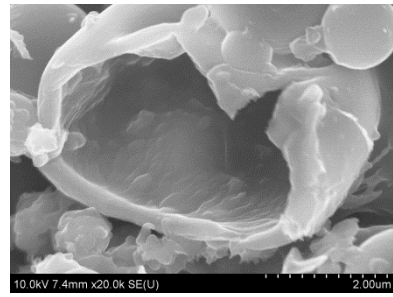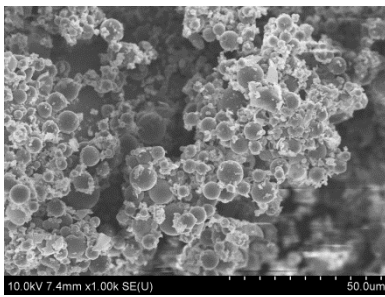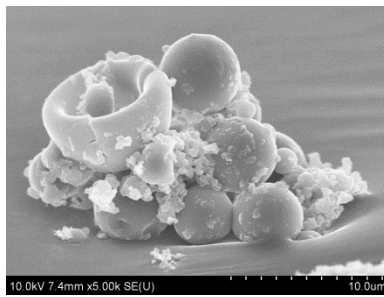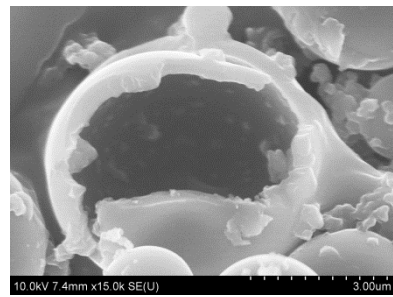
| (d1) | (d2) | (d3) |

| (e1) | (e2) | (e3) |
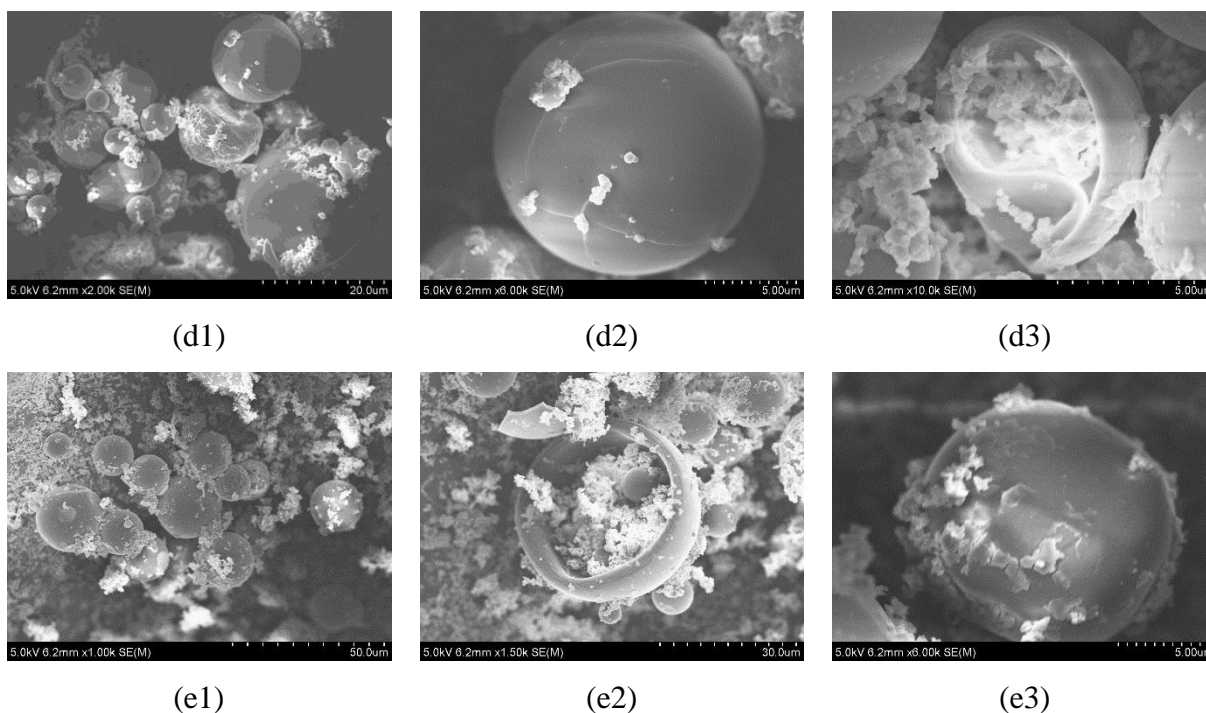
Figure 5-13. SEM images of poly acrylic acid particles via high shear homogenization before polymerization; 69% of Neutralization, water/AA ratio = 30 vol. % of AA, KPS = 0.94 mole% of AA, PEGDA = 2.8 mole% of AA, reaction for 2hrs; (a) Homogenization at 8000 rpm for 3min, (b) Homogenization at 8000 rpm for 30sec, (c) Homogenization at 8000 rpm for 5sec, (d) Homogenization at 8000 rpm for 2sec, (e) Homogenization at 1000 rpm for 30sec.

5.4.3. Effect of neutralization after homogenization (α = degree of neutralization)

The neutralization of the poly (acrylic acid) plays an important role in the swelling of superabsorbent polymers. First of all, we needed to check if the acrylic acid was neutralized. For that purpose, the fully neutralized sodium polyacrylate polymer particles were analyzed using EDX. In figure 5-14, blue dots were spread all over the polymer particles, which indicates that Na ions are well-linked to the polyacrylate.
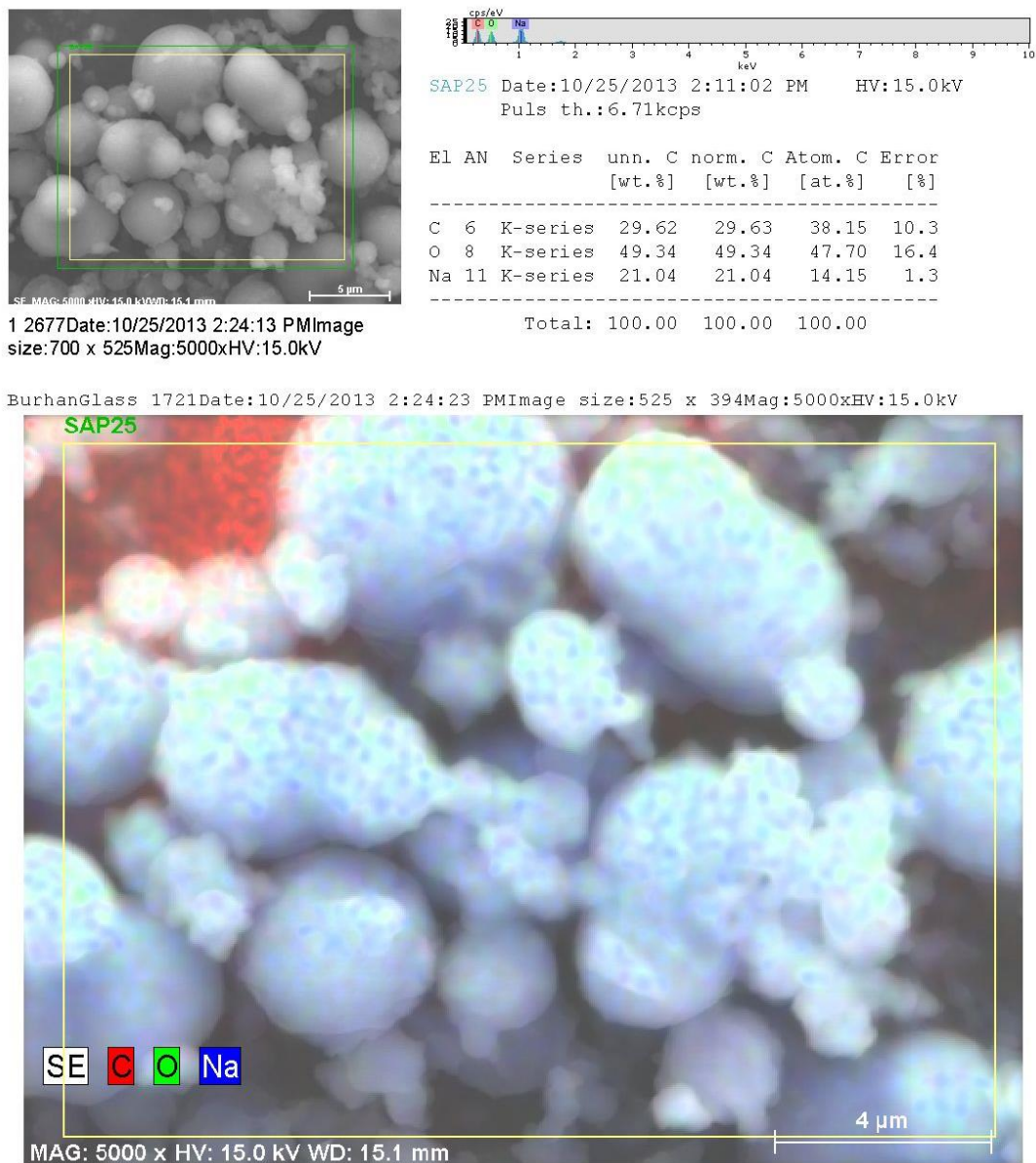
Figure 5-14. EDX analysis of partially neutralized polyacrylate.

Higher degree of neutralization gives rise to lower initial rate of polymerization [99]. Commercially AA is neutralized as much as 70% of acids in monomer. In this investigation, when below 50 % of AA was neutralized ($\alpha < 0.5$), polymer particles were easily aggregated. When α values were 0.7, 0.9, and 1.0, very fine polymer particles were obtained. When the α value was

0.7, the average shell thickness (δ) was 0.47 μm and polymer particles were more deformed. In the case of 90 % neutralized polyacrylate, the average shell thickness was 0.63 μm (figure 5-15). It is probably explained by the water affinity. As the neutralization ratio increases, ions in the polymer particles increase, and more water can bind in the network. Thus, less water bound to 90 % neutralized Na-polyacrylate may disperse outside than from a 70 % neutralized polymer.

α	0.7	0.9	1.0
δ	0.47 μm	0.63 μm	
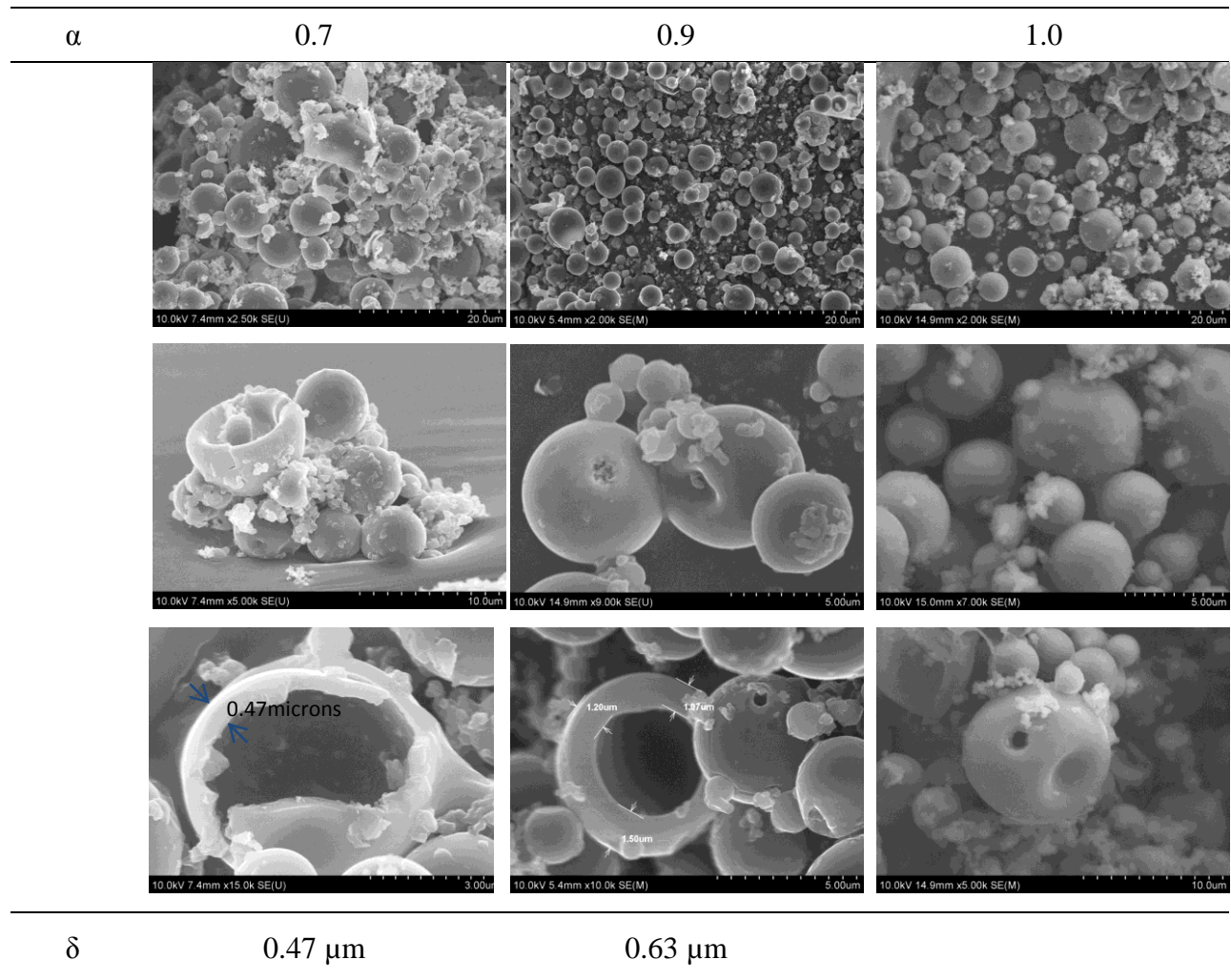
Figure 5-15. Effect of neutralization after homogenization (α = the degree of neutralization) ; SEM images of sodium polyacrylate particles via high shear homogenization at 8000 rpm for 3 min before polymerization; water/AA ratio = 30 vol.% of AA, KPS = 0.94 mole% of AA [0.0027 mol/L], PEGDA = 2.8 mole% of AA, T = 60°C, and time = 2hrs.

83

The swelling capacity is shown in Fig. 5-16. Here, all three samples with different degrees of neutralization have similar values around 330 g/g (water/polymer), although it has been reported in the literature that the increasing neutralization with EGDMA as a crosslinking agent yields higher degree of swelling [72]. It might be because PEGDA makes polyacrylate construct a wider network that is able to absorb larger amount of water than EGDMA. Therefore, when higher than 70 % of acrylic acid was neutralized, swelling capacity may not be much different.
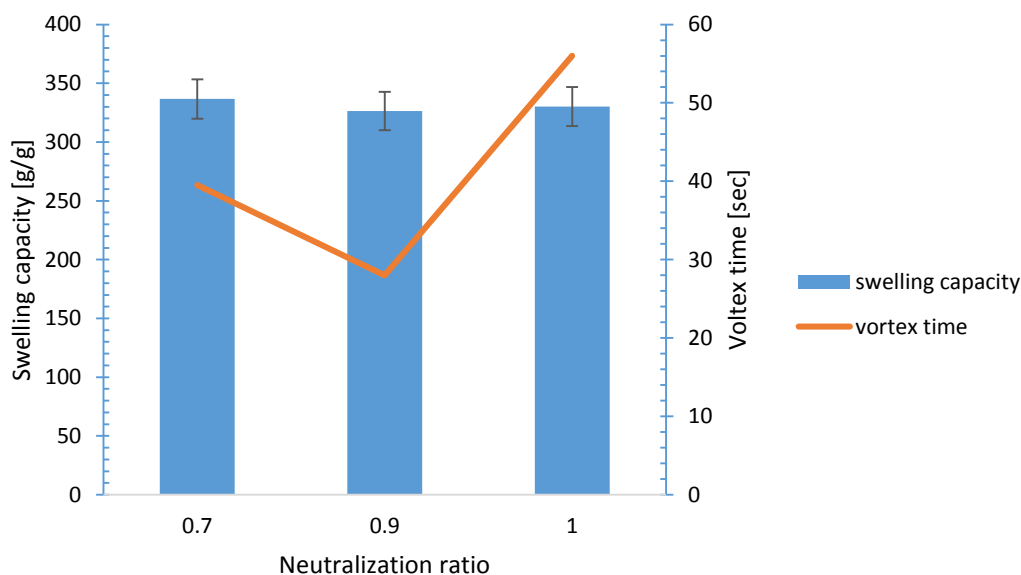
Figure 5-16. Swelling capacity and vortex time varying neutralization ratios; 0.7, 0.9, and 1. Same samples as Fig. 5-15 were characterized.

5.4.4. Effect of the crosslinking agent

The morphology of Na-polyacrylate particles (in Fig. 5-17) had no substantial difference with or without PEGDA. The swelling capacity (Table 5-3) is a little bit higher when PEGDA was

not used. This corresponds with literature [94,109]. As the density of crosslinking is lower, water

uptake increases because there is less network to stop swelling.

(a1)   (a2)   (a3)

(b1)   (b2)   (b3)
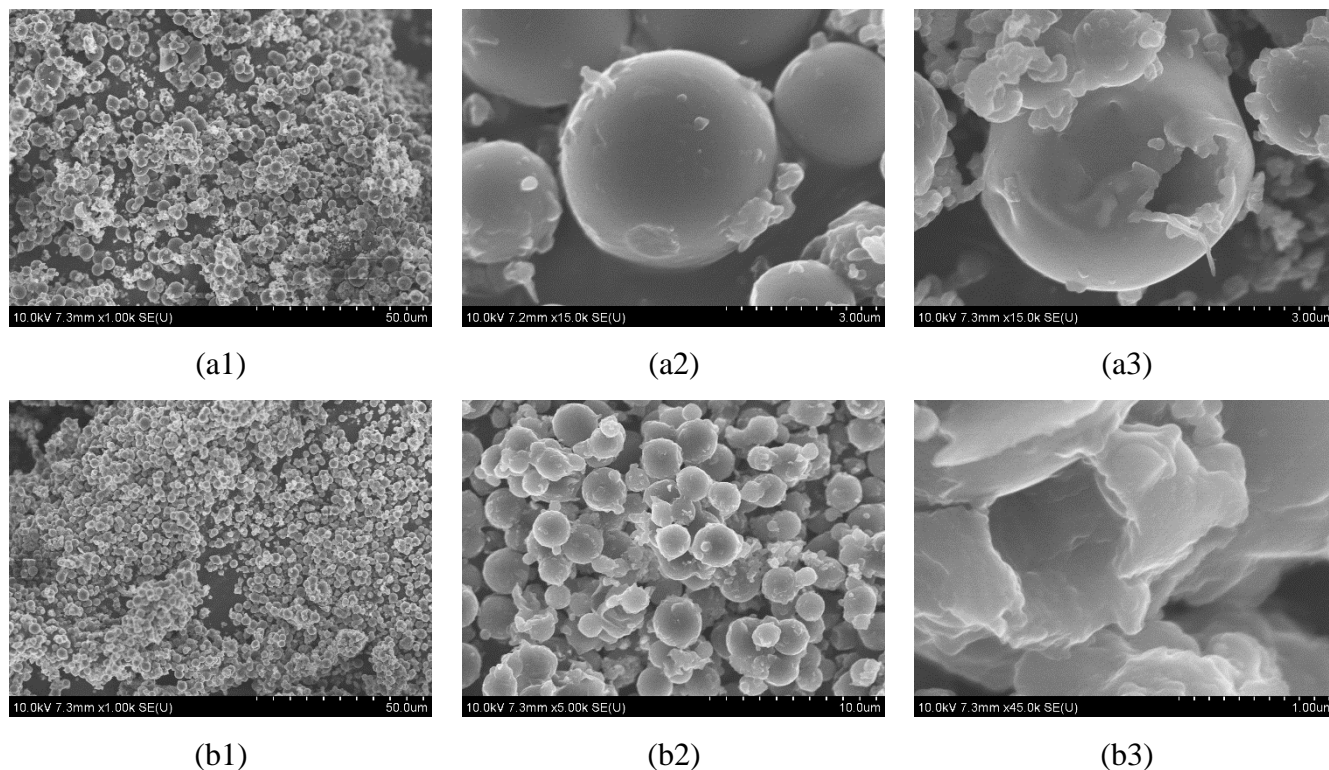
Figure 5-17. The SEM images of sodium polyacrylate particles via high shear homogenization before polymerization; 69% of Neutralization, water/AA ratio = 30 vol.% of AA, KPS = 0.94 mole% of AA [0.0027 mol/L], homogenization at 8000 rpm for 3min, T = 60°C, and time = 2hrs. (a) No PEGDA and (b) 2.83 mole% (in AA) of PEGDA.

Table 5-3. Swelling capacity varying the concentration of PEGDA. Same samples as Fig. 5-17 were characterized.

The Amount of PEGDA	Swelling capacity
0	345 g/g
2.83 mol% of AA	337 g/g

5.4.5. Effect of initiator concentration

0.94 mole %, 0.84 mole %, 0.45 mole %, and 0.21 mole % of KPS in acrylic acid were employed in the inverse suspension polymerization with high shear mixing before polymerization. The morphology of the polymers did not change much. However, when 0.21 mole % of KPS was used, the reaction rate decreased and so the sticky polyacrylic acid particles were found to have been elongated and aggregated into a gel (Figure 5-18).
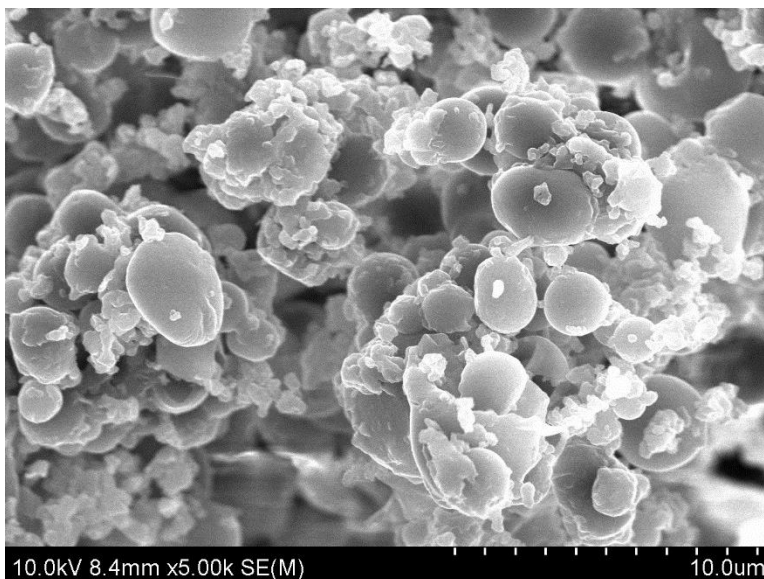
Figure 5-18. The SEM images of sodium polyacrylate particles when 0.21 mole % of KPS was used; 69% of Neutralization, water/AA ratio = 30 vol.% of AA, 2.83 mole% (in AA) of PEGDA, homogenization at 8000 rpm for 3min, T = 60°C, and time = 2hrs.

5. 5. Conclusion

In this chapter, feasible and simple technique to obtain Na-polyacrylate microparticles with sizes below 10 μm was investigated using a high shear mixing device. To maintain the stability of submicron size of aqueous droplets in the oil medium, co-surfactant system containing Span 80 and Tween 80 was used. Neutralization of acrylic acid was proved by EDX analysis. Na-polyacrylate submicron particles were characterized by size, surface morphology, swelling capacity, and conversion. When the speed of homogenization was lowered from 3000 rpm to 1000 rpm, particles over 10 μm were obtained but more nano-sized particles were present outside. When below 50 % of AA was neutralized ($\alpha < 0.5$), polymer particles were easily aggregated and when α values were 0.7, 0.9, and 1.0, very fine polymer particles were obtained. When the α value was 0.9, the average shell thickness (δ) was higher than δ in the case of α is 0.7. And, swelling capacities were around 330 g/g for three α values. When a very low initiator concentration was used, polymer particles were sticky and were heavily deformed.

Chapter 6. Partially Neutralized Sodium Polyacrylate with Wrinkled/Cracked Surfaces

6.1. Inverse Suspension Polymerization of Acrylic Acid without High Shear mixing

In chapter 5, we demonstrated that high shear homogenization of the two phase mixture resulted in sub-micron size polyacrylate particles. In order to increase the size of polyacrylate particles shear speed was decreased to as low as 1000 rpm, but in this rpm range, the polymer particle size was barely affected. Thus, in order to produce large polymer particles (e.g., from 10 to hundreds of microns) with a spherical shape, the inverse suspension polymerization experiments were carried out without high shear mixing.

Method of adding the monomer into the oil phase

In regular suspension polymerization a dispersed phase (oil) was added into the continuous phase (aqueous) before agitation and then they were carried out in the reactor to start the polymerization (e.g., PMMA suspension polymerization in chapter 2~3). However, in this inverse suspension polymerization, the resultant polymers were aggregated and turned into a gel, similar to regular suspension polymerization. In inverse suspension polymerization, a heavier aqueous phase is a dispersed droplet phase in an oil phase. Unless monomer droplets are fully stabilized in a continuous phase, they may not grow to discrete polymer particles. So we chose another way to

add monomer. When the aqueous phase was added drop by drop into the reactor with agitation, discrete polymer particles were obtained; however, there was a dead zone at the bottom of the reactor. To remove the dead zone, a magnetic bar was placed in the reactor and stirred the droplets/polymers stuck on the bottom during the polymerization.
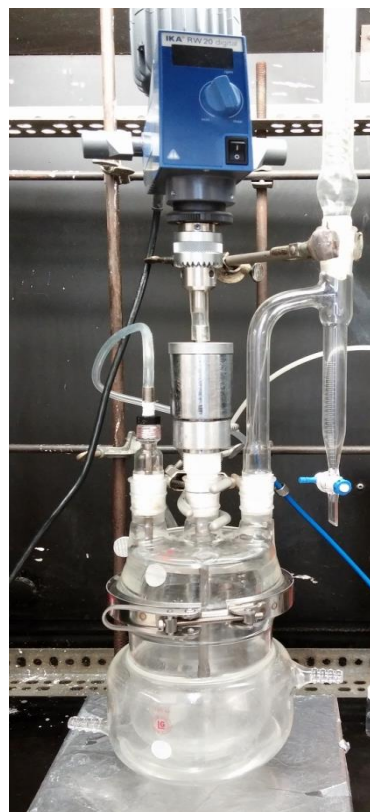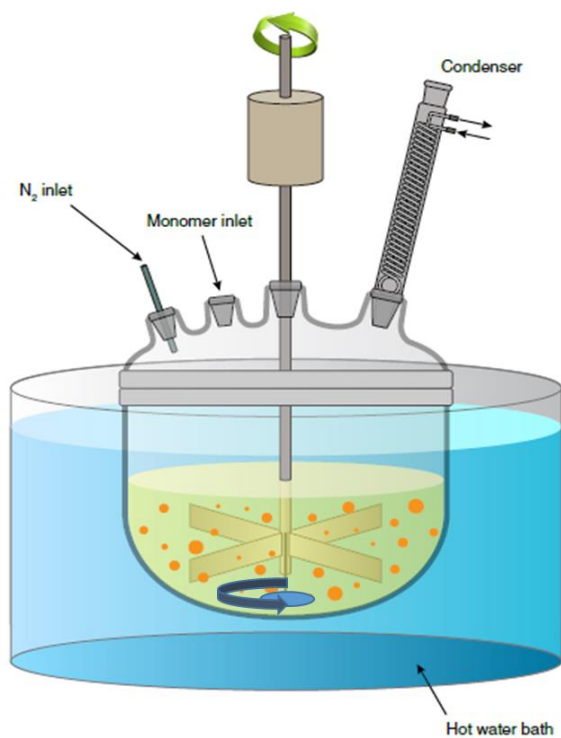
Figure 6-1. Modified polymerization system.

Crosslinking in partially neutralized sodium polyacrylate

In this study ethylene glycol dimethacrylate (EGDMA) and poly (ethylene glycol diacrylate) (PEGDA) were used as crosslinkers in variable concentrations.

Ethylene glycol dimethacrylate   Poly ethylene glycol diacrylate

R = H or CH$_2$CH$_2$OH

Hydroxy ethyl cellulose
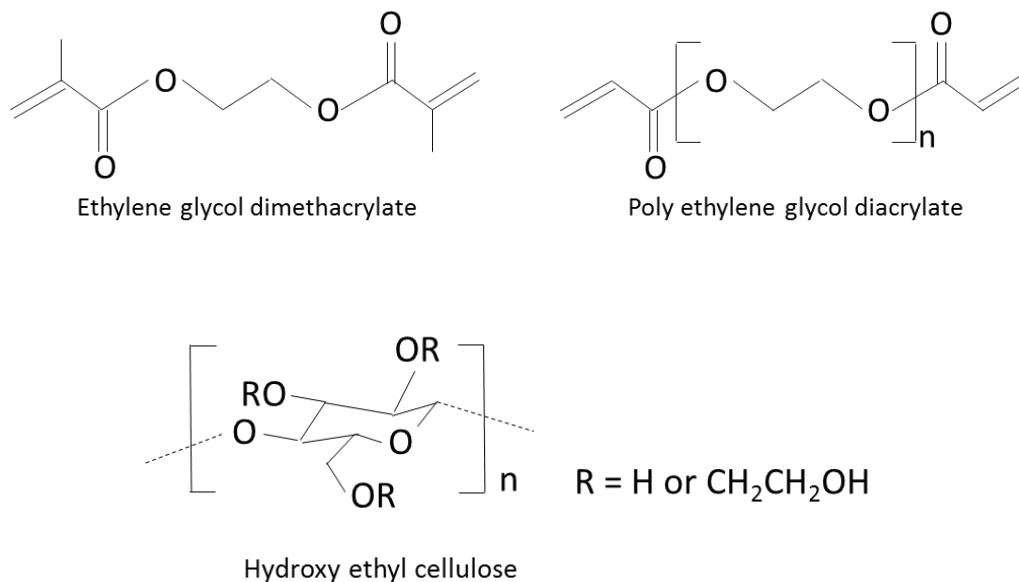
Figure 6-2. Chemical structures of three crosslinking agents [132].

Suspending agents

Compared to the inverse suspension polymerization with the high shear mixing, less amount (3.76 mole % in the oil) of Span 80 or ethyl cellulose was used. The structure of ethyl cellulose is as follows:

R = H or CH$_2$CH$_3$
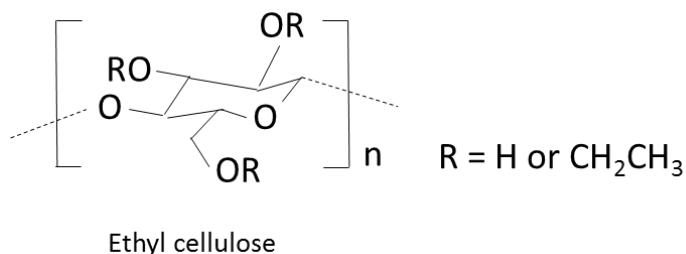
Ethyl cellulose

Figure 6-3. Chemical structure of ethyl cellulose [132].

According to the literature [61, 105], ethyl cellulose has been used to produce polymer particles larger than 100 μm (~ 500 μm or up to 1 mm).

90

6.2. Experimental

6.2.1. Materials

Acrylic acid (AA, $CH_2=CHCOOH$, anhydrous, 99%, contains 180~200 ppm MEHQ (monomethyl ether hydroquinone) as an inhibitor, Aldrich) was used as a monomer. The monomer was added dropwise into a prepacked column with aluminum oxide (Aldrich Chem. Co.). Sodium hydroxide (NaOH, Sigma Aldrich) was used to neutralize the acrylic acid. Cyclohexane, hexane, and heptane (Fisher scientific) were used as polymerization mediums and non-solvents. Sodium persulfate ($Na_2S_2O_8$) (Sigma Aldrich) was used as an initiator. Span 80 (sorbitane monooleate, $C_{24}H_{44}O_6$, Fluka) were used as suspension stabilizers. Ethylene glycol dimethacrylate (EGDMA), poly (ethylene glycol diacrylate) (PEGDA), and hydroxyl ethyl cellulose were used as crosslinking agents.

6.2.2. Inverse suspension polymerization without high shear homogenization

The partially neutralized sodium-acrylate was prepared in the same manner as described in section 5.3.1. 2.83 mol % of poly ethylene glycol diacrylate (PEGDA) of the monomer was dissolved in the partially neutralized sodium-acrylate solution and the clear mixture obtained was degassed by nitrogen bubbling for about 30 min. Span 80 as the suspending stabilizer was dissolved in the non-solvent and this phase was heated to 65°C in a 500 ml-reactor and stirred at 300 rpm by a six bladed agitator (Fig. 6.4). A predetermined amount of sodium persulfate

($Na_2S_2O_8$(SPS), 0.004 mol/L of the aqueous phase, Aldrich) was dissolved in the aqueous solution after N_2 purging, and then the aqueous phase was added dropwise and the agitation of the mixture was kept constant and maintained for 2hr ~ 3hr. At the end of the reaction, the stirring was stopped and two phases were observed: the liquid constituted of cyclohexane was at the top of the reactor and the aqueous suspension of polyacrylate particles was at the bottom. The particles were recovered by methanol precipitation (Three post-treatments with methanol were employed in this work). After drying under a vacuum at 40°C, sodium polyacrylate particles were obtained.

Figure 6-4. The images of the reactor and the agitator used in the experiments; 500 ml-unjacketed reactor with conical flange (I.D.: 108 mm and height: 125 mm), and turbine style agitator (D: 80 mm).

6.2.3. Effect of particle washing on polymer morphology

After polymerization, the polymer particles had been washed using methanol in the previous experiments. Our particles were washed with methanol, but the particle surfaces were found to be wrinkled or cracked. Thus, we applied three different washing methods to examine how the polymer particle morphology is affected by the post-reaction washing procedure.
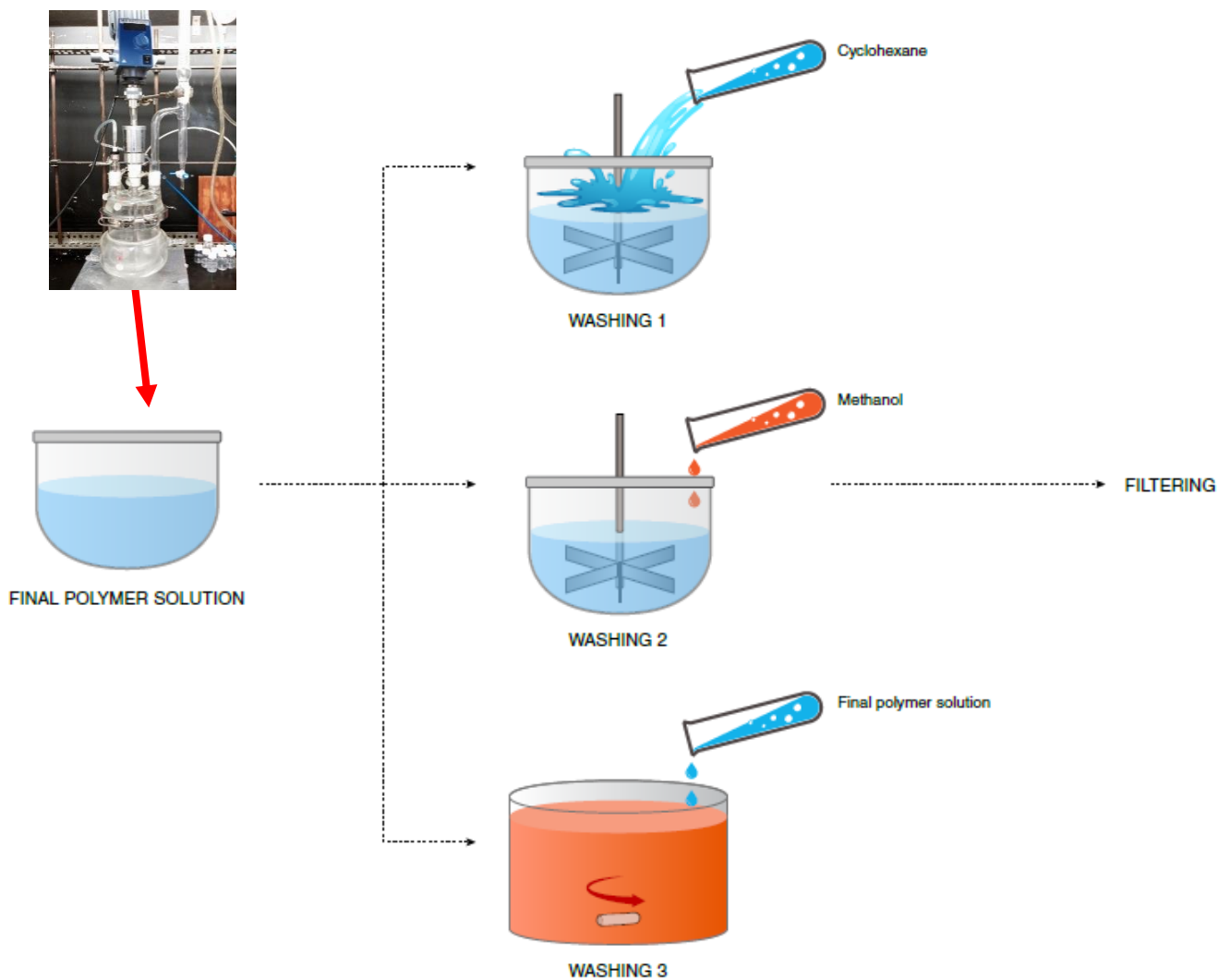
Figure 6-5. Three post treatments after polymerization (washing methods).

Washing 1: Polymer particles were washed using the same organic solvent which was used in the reaction. After polymerization was stopped, 100 ml of cyclohexane was poured into the reactor with agitation for 30 min and then it was filtered and dried.

Washing 2: After polymerization was stopped, 100 ml of methanol was added slowly into the polymer solution in the reactor with agitation for 30 min, and then it was filtered and dried.

Washing 3: Polymer solution was added slowly into an excess amount (more than 10 times of monomer) of methanol and agitated with a magnetic bar for 30 min. Then it was filtered and dried.

6.2.4. Characterization

Speed of absorption

The speed of absorption was measured by the vortex test. 40 ml of deionized water was added to a glass beaker and stirred with a stirring rod at 600 rpm, forming a vortex. 0.18 g of poly acrylic acid particles were carefully introduced into the vortex. At the same time a stop watch was started. When the vortex disappeared, the watch was stopped and the time was recorded [97,102,106]. The time it took for the vortex to disappear is an indication of the free swell absorbing rate of SAP.

Surface area and porosity

To examine how much a wrinkle or crack affected the surface area of polymer particles, Brunauer, Emmett and Teller (BET) method was used to determine of the surface area and porosity

of Na-polyacrylate particles in this study. The BET surface area was measured using a Micrometrics ASAP 2020 apparatus at 77K and the pore size distribution was measured using the Barrett-Joyner-Halenda (BJH) method.

6.3. Result and Discussion

6. 3. 1. Effect of reaction conditions

Effect of post treatments after polymerization (washing methods)

The morphology of poly methyl methacrylate particles (in chapters 2 and 3) was affected by reaction variables (type and concentration of materials and ratios of MMA/solvent, etc.) during polymerization, not by post treatment after polymerization. Because PMMA is a thermoplastic that becomes pliable or moldable above a specific temperature, and thus, the morphology of PMMA cannot be changed after polymerization below the glass transition temperature. However, polyacrylate is hydrogel, which has ions and can be affected by a polar environment. Few pieces of literature have mentioned that their hydrogel turned porous after washing and drying. [107,108]

In our study (Figure 6-6), very different morphologies of Na-polyacrylate particles were obtained when different washing methods were employed as mentioned above. When the first washing method was used, particles were not deformed at all and they had very smooth surface. However, the residual monomer/oligomer and water inside particles couldn't be removed, so the

particles were still swollen and sticky. Thus, it was hard to filter and isolate the polymer particles. When the second washing method was used, polymer particles were hardened since residual monomer and water inside the particles could be removed by methanol and they were easily filtered. However, agglomeration of polymer around the first drop of methanol occurred because the concentration of methanol around the first drop into the polymer solution was relatively high. Washing 3 made very fine polymer particles with no aggregation, and they were easily filtered. However, the particles had wrinkled or cracked surfaces.

(a1)   (b1)   (c1)

(a2)   (b2)   (c2)
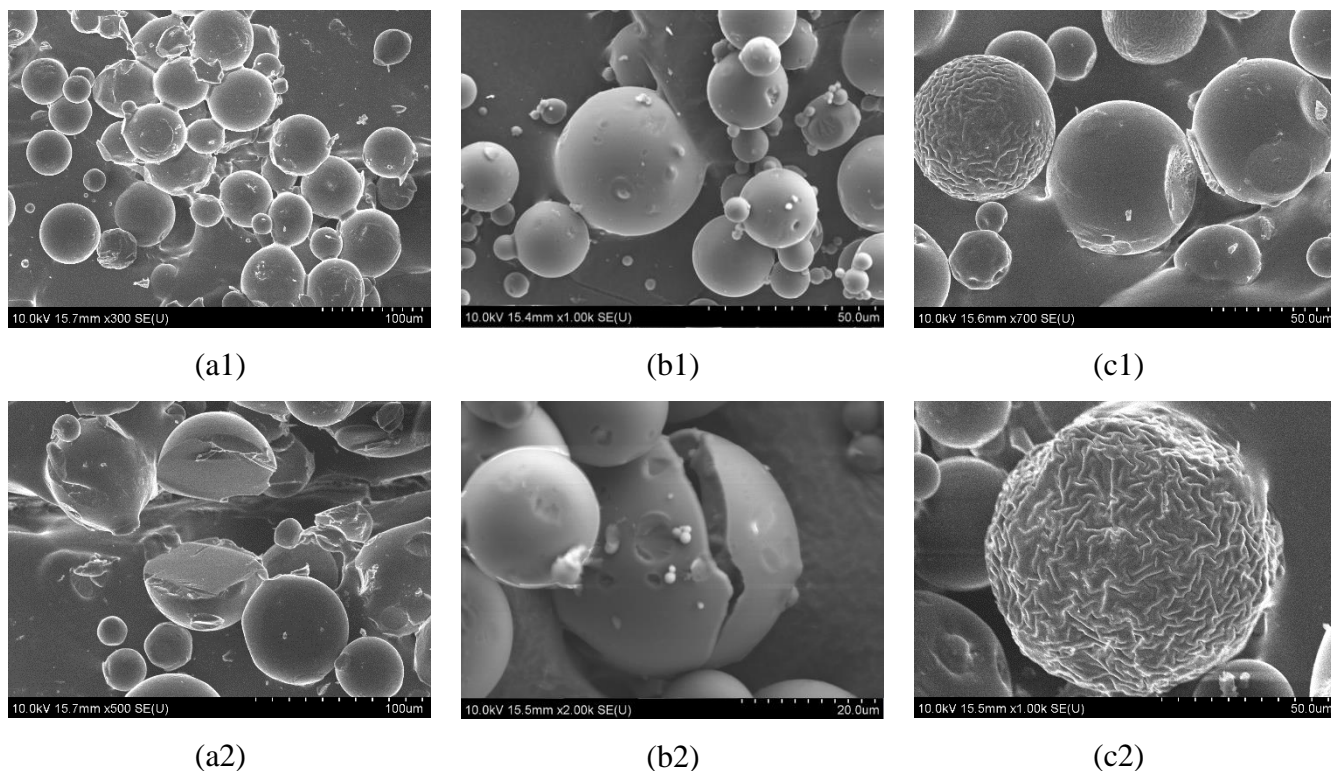
Figure 6-6. The SEM images of sodium polyacrylate particles from the same run (water/AA ratio = 30 vol.% of AA, neutralization ratio = 0.7, KPS = 0.08 mole% of AA, EGDMA = 0.2 mole% of AA, cyclohexane, Span 80 = 0.74 w% in oil, reaction for 2hrs, T = 65°C) which were treated after polymerization by (a) washing method 1, (b) washing method 2, and (c) washing method 3.

The size distribution of polymer particles was practically unaffected by the particle washing method (Fig. 6-7).
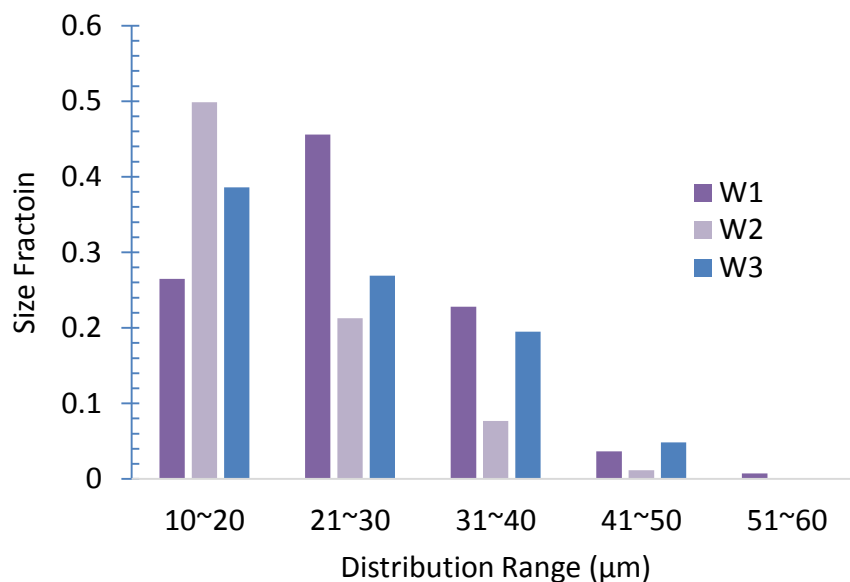
Figure 6-7. Sized distribution of of Na-polyacrylate particles in Fig. 6-6.

From the results of the BET analysis (Fig. 6-8, 6-9), the surface areas were different; 20.372 m²/g (Fig. 6-6 (b) - washing 2) and 41.362 m²/g (Fig. 6-6 (c) - washing 3). It means that wrinkles from washing by a high concentration of MeOH resulted in a larger surface area than the surface area of the smoother particles from other washing method. We will demonstrated in chapter 7 that very smooth Na-polyacrylate particles at highest conversion had much smaller surface area, 4.282 m²/g.

Figure 6-8. The graph of adsorption-desorption isotherm of the polymer sample in Fig. 6-6 (b) (washing 2). Surface Area = 20.372 m²/g and total pore volume = 0.021 cc/g.

Figure 6-9. The graph of adsorption-desorption isotherm of the polymer sample in Fig. 6-6 (c) (washing 3). Surface Area = 41.362 m²/g and total pore volume = 0.031 cc/g.
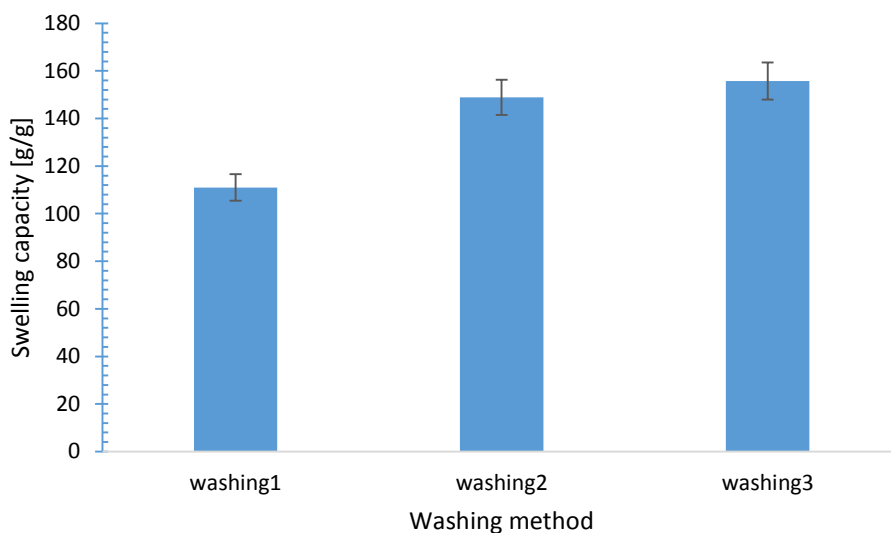
Figure 6-10. Swelling capacity varying the post-treatment to Na-polyacrylate particles in Fig. 6-6.

From the tea bag test applied to three samples in Fig. 6-6, swelling capacity was 111 ~ 156 g/g. The wrinkled polymer particles had a little bit higher swelling capacity than others but these values didn't have a significant difference. The swelling capacity of wrinkled particles is much lower than those obtained in chapter 5 (Fig. 5-16, 5-18). Possible causes can be the type of crosslinking agent and particle size. When the particle size changed from 50 µm to 5 µm using a high shear mixing, the specific surface area increased 10 times, according to a simple calculation. However, it cannot explain this much difference of swelling capacity where it could affect swelling speed. The type of crosslinking agent (EGDMA vs. PEGDA), which we will be discuss in the next part, can affect the swelling capacity because of chemical structure of the SAP network.

Effect of the type of crosslinking agent

All the characterized swelling data from this study regardless of any other reaction conditions showed that the type of crosslinking agent affected the swelling capacity and the

swelling speed the most. Figure 6-11 shows all the swelling data. Most of swelling capacity of Na-polyacrylate crosslinked by PEGDA was much higher than those crosslinked by EGDMA. Also, the swelling speed was faster in case of PEGDA.
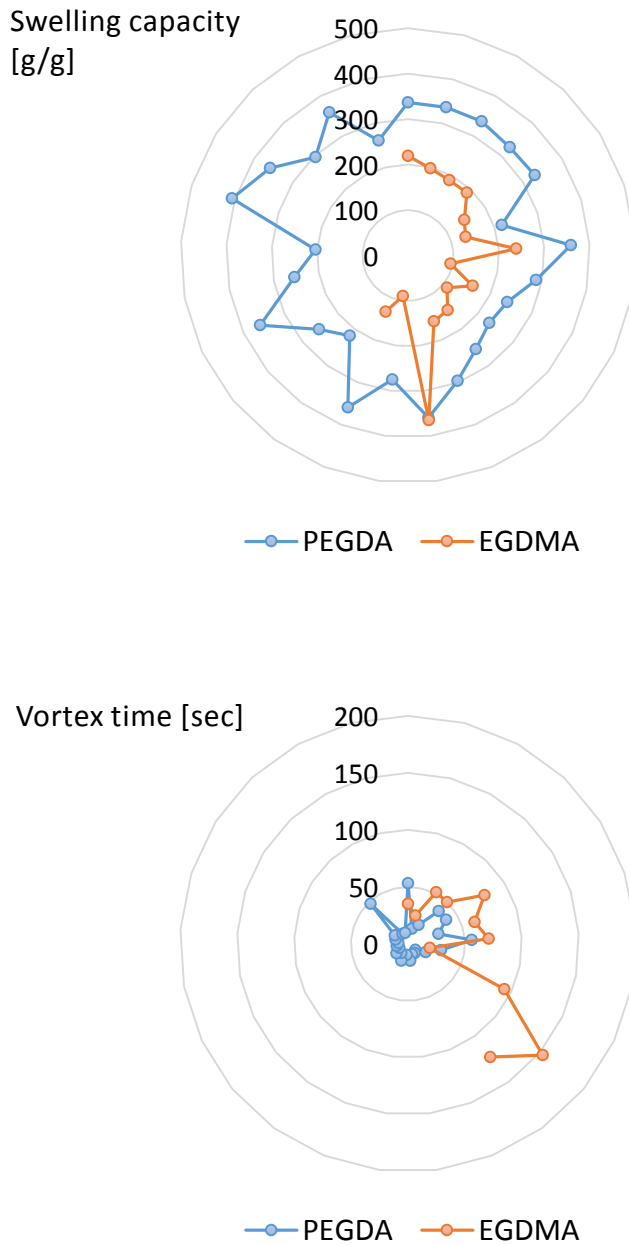
Figure 6-11. Radar map of swelling capacity and vortex speed varying the type of crosslinking agent; PEGDA vs. EGDMA.

Mabilleau et al. [109] demonstrated that the repetition of the --(-C—C—O-)-- unit in EGDMA and PEGDA increase the flexibility of the crosslinking chains (refer to chemical structures in Fig. 5-5 and Fig. 6-2). In their study, they showed that compared to dried linear poly (2-hydroxyethyl methacrylate) (pHEMA), dried EGDMA–pHEMA had much greater hardness and stiffness values. On the other hand, dried PEGDA–pHEMA had a hardness value higher than that of linear pHEMA but lower stiffness. The decrease in stiffness was probably due to the chain length of the crosslink that provided more flexibility to the polymer. Swelling capacity was influenced by crosslinking. Linear pHEMA and PEGDA– pHEMA showed the highest values of swelling capacity, whereas EGDMA–pHEMA showed the lowest value. Also, the swelling speed of PEGDA– pHEMA was faster than that of EGDMA–pHEMA.

Effect of the concentration of crosslinking agent

In Figure 6-12, the concentration of EGDMA was varied with other variables kept constant. When the concentration of EGDMA was low, particles were wrinkled, and when a higher concentration of EGDMA was added, smoother polymer surfaces were obtained.

      (a)   (b)   (c)

(d)   (E)
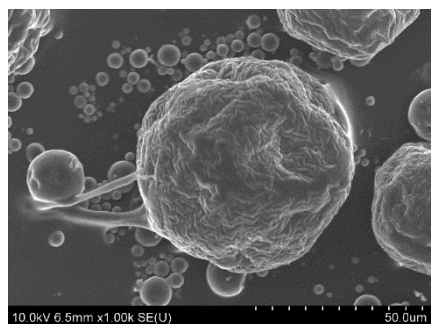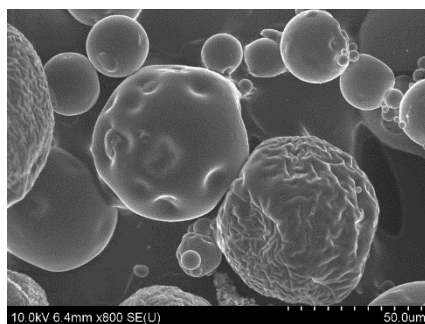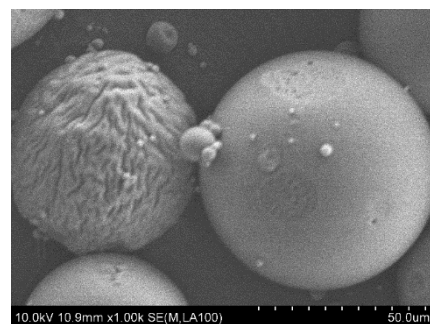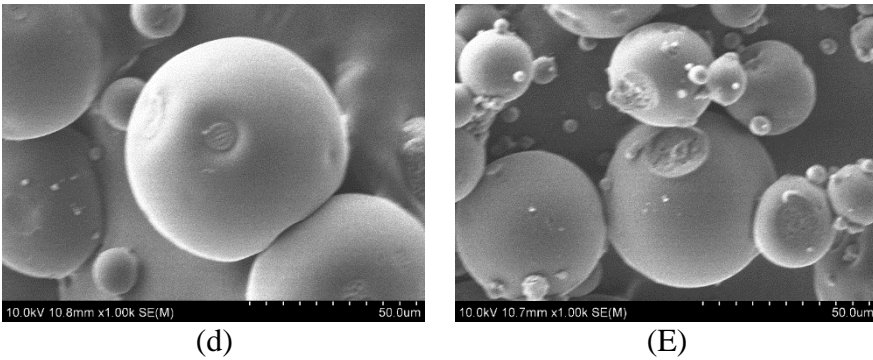
Figure 6-12. The SEM images of sodium polyacrylate particles varying the concentration of crosslinking agent, EGDMA; water/AA ratio = 30 % vol.% of AA, neutralization ratio = 0.7, KPS = 0.08 mole% of AA, reaction for 2hrs, heptane, Span 80 = 0.74 w% in oil, T = 65°C, and washing method 3. EGDMA is (a) 0.2 mole% of AA, (b) 0.4 mole% of AA, (c) 0.6 mole% of AA, (d) 0.8 mole% of AA, and (d) 1.0 mole% of AA.

From the results of BET analysis (Fig. 6-13 ~ 6-15), the surface areas decreased with EGDMA concentrations. It can be explained that a higher density of crosslinking resulted in a stiffer and harder polymer structure. And then the stiffer and harder structure was less affected by outflow of water and less deformed.
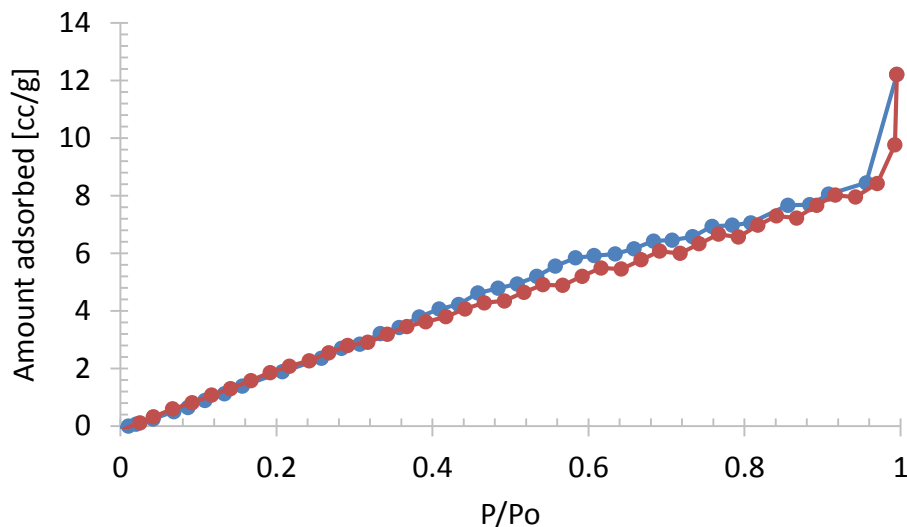
Figure 6-13. The graph of adsorption-desorption isotherm of the polymer sample in Fig. 6-12 (a) (0.2 mol% EGDMA in AA). Surface Area = 68.102 m²/g and total pore volume = 0.018 cc/g.
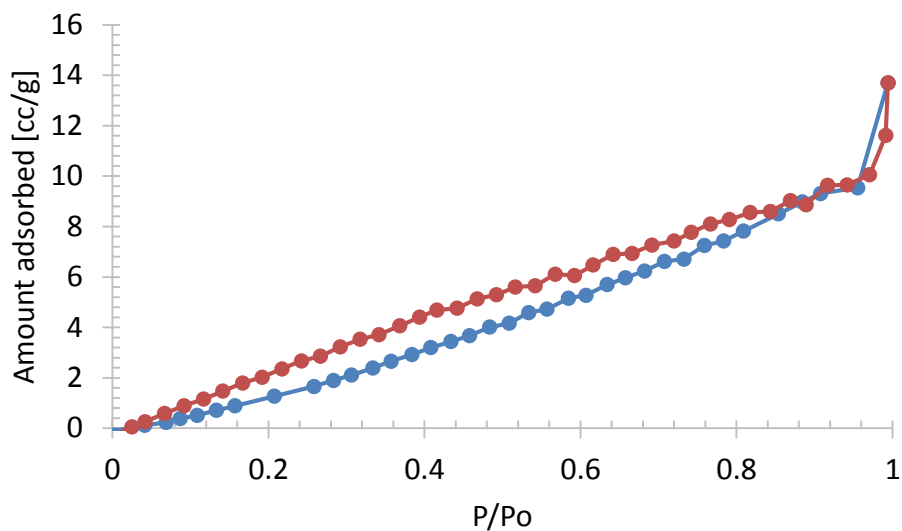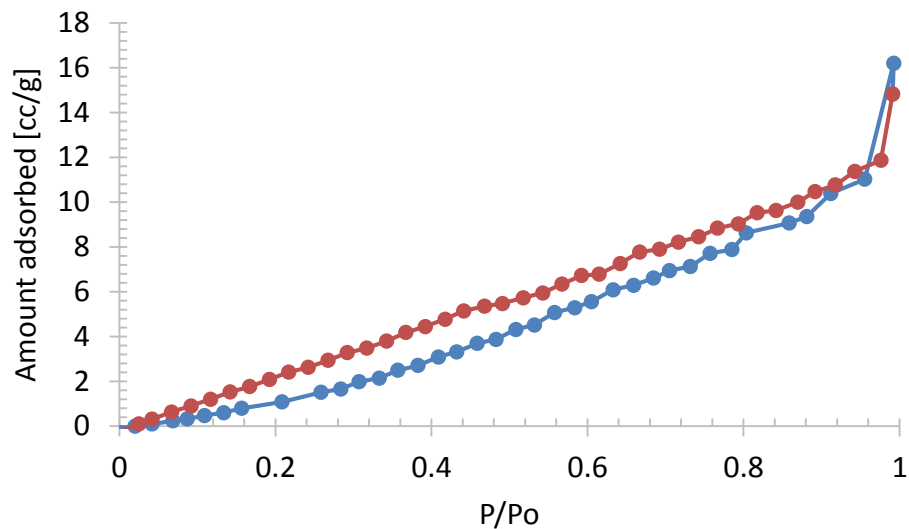
Figure 6-14. The graph of adsorption-desorption isotherm of the polymer sample in Fig. 6-12 (b) (0.4 mol% EGDMA in AA). Surface Area = 30.375 m²/g and total pore volume = 0.025 cc/g.
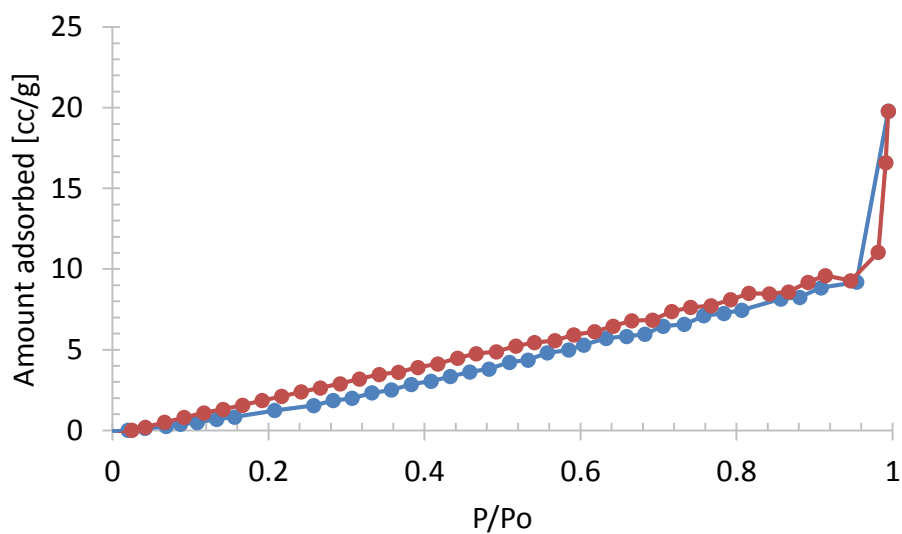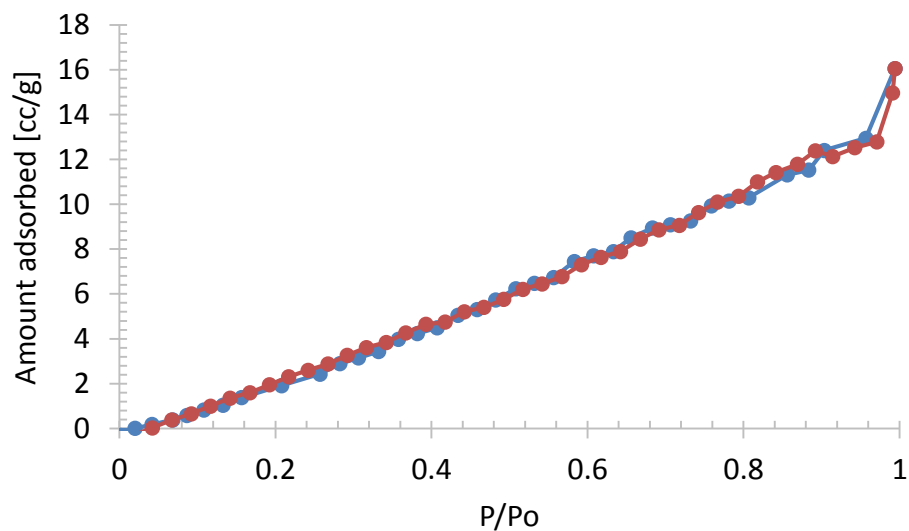

Figure 6-15. The graph of adsorption-desorption isotherm of the polymer sample in Fig. 6-12 (d) (0.8 mol% EGDMA in AA). Surface Area = 21.964 m²/g and total pore volume = 0.025 cc/g.
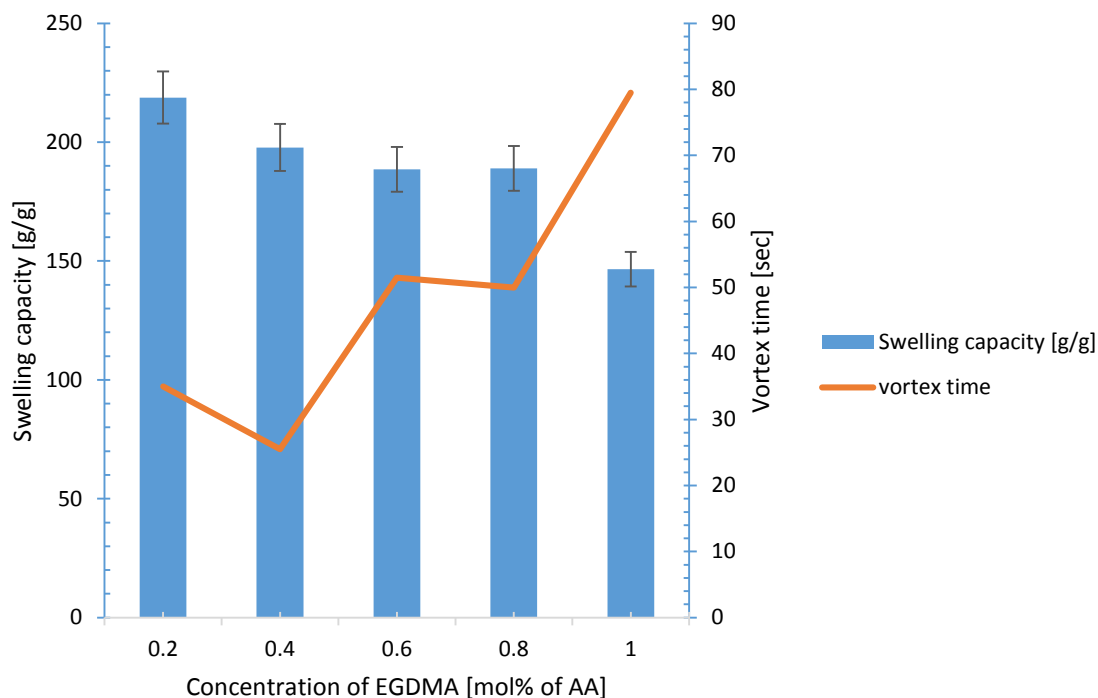
Figure 6-16. Swelling capacity and vortex time varying the concentration of EGDMA in Fig. 6-12.

Figure 6-16 shows that swelling capacity and speed decrease as EGDMA concentration increases. As mentioned in the "swelling mechanism" part, when swelling takes place, water goes in and binds between the dimensional network. At the point of maximum swelling, SAP can no longer retain its three dimensional network structure. If the crosslinking density is high, the maximum point where SAP can retain its 3-D network is low due to low flexibility of structure.

Effect of Neutralization ratio

In view of morphology, there is no huge difference in partially neutralized Na-polyacrylate particles in Fig. 6-17.

(a1)   (b1)   (c1)

(a2)   (b2)   (c2)
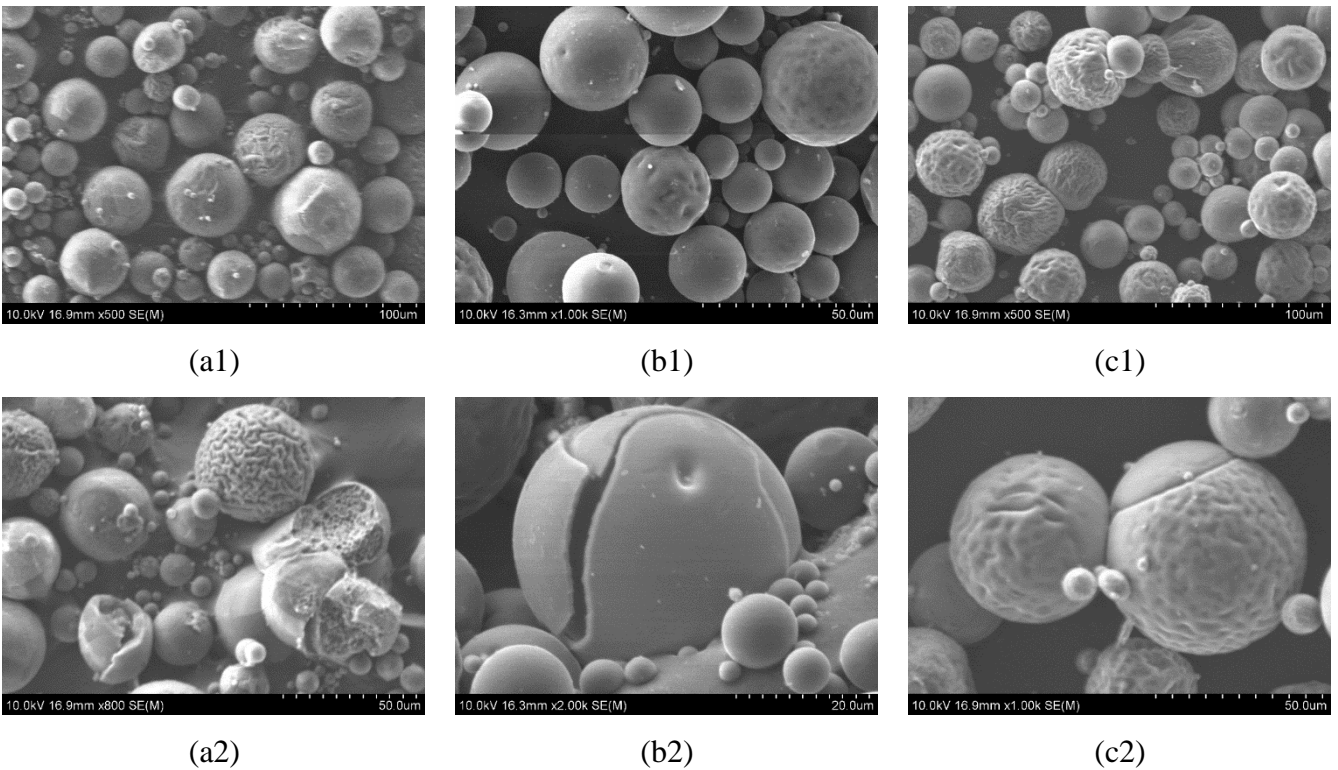
Figure 6-17. The SEM images of sodium polyacrylate particles varying the neutralization ratio; water/AA ratio = 30 vol.% of AA, SPS = 0.09 mole% of AA, PEGDA = 0.06 mol% of AA, cyclohexane, Span 80 = 0.74 w% in oil, reaction for 3hrs, T = 60°C, and washing method 3. Neutralization ratio is (a) 0.6, (b) 0.7, and (c) 0.9.

However, properties of polymer particles were clearly different in three samples (Fig. 6-18). When 70% of the carboxylic group in acrylic acid was neutralized, it had the highest swelling capacity and fastest swelling speed. This can be a reason that 70% of neutralization is applied commercially.
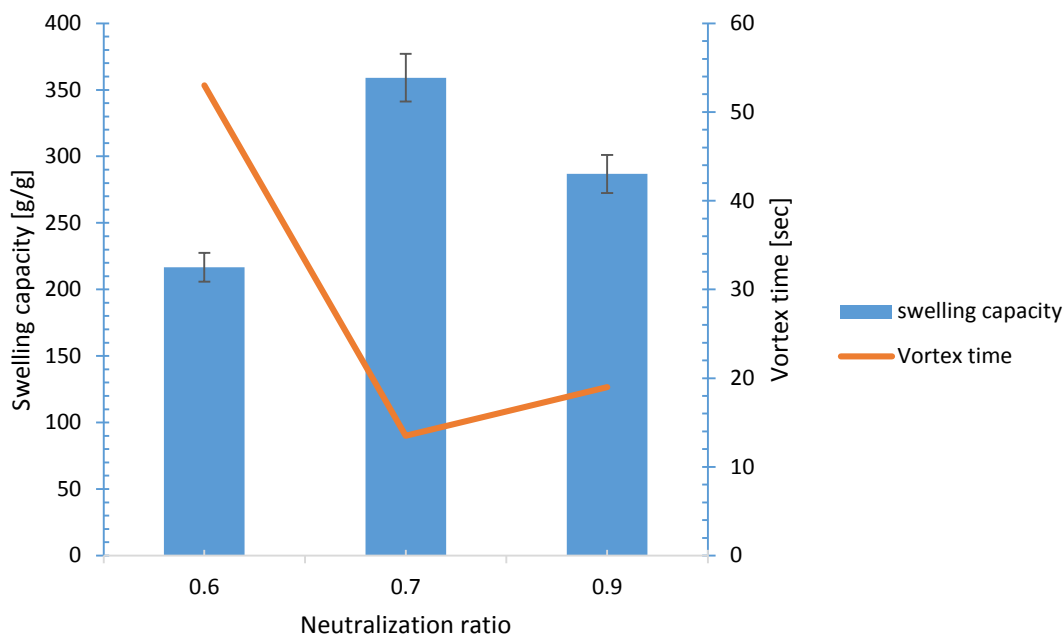
Figure 6-18. Swelling capacity and vortex time varying the neutralization ratio of same polyacrylate in Fig. 6-17.

6.3.2. Change of inner morphology of Na-polyacrylate particles by varying the reaction time

To study the various internal structures of polymer particles obtained through this work in detail, the internal morphology of polymer particles at different reaction times was examined. As shown in Fig 6-19, particles were not fully spherical at low conversion. But as the conversion increases, nano-sized particles were formed inside a droplet and at some point phase inversion occurred and the particles became porous. At very high monomer conversion, the interior particle was solid.
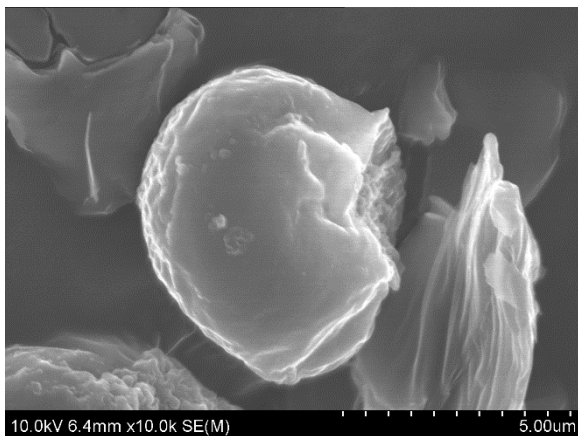
t = 15min
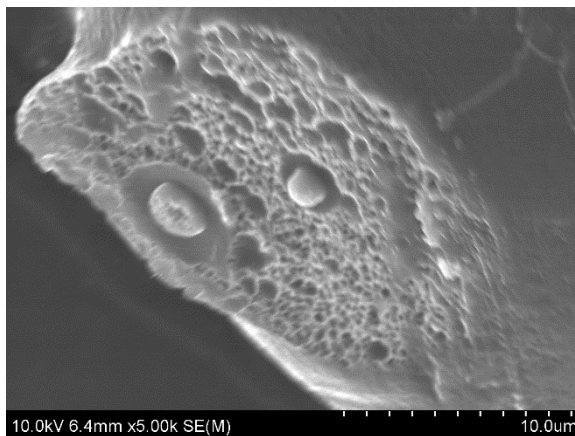
t = 30min
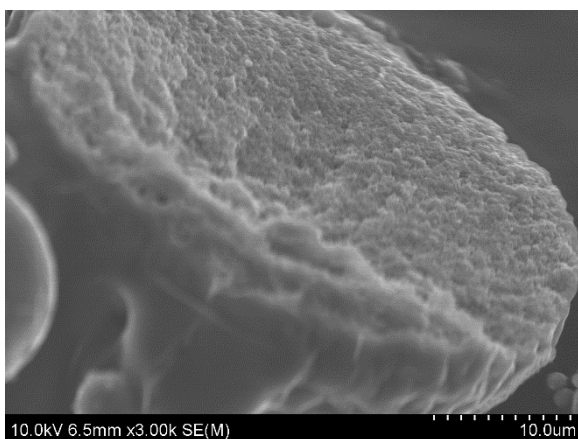
t = 45min
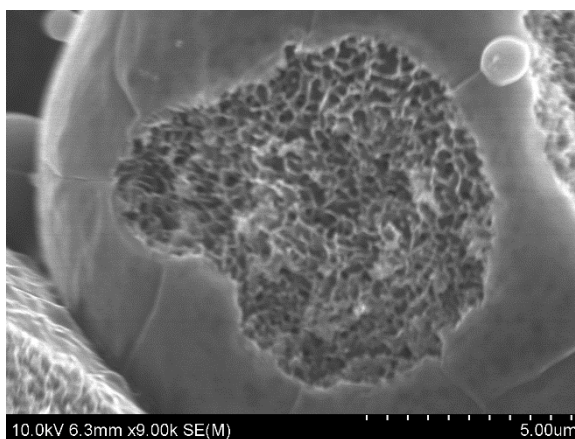
t = 60min
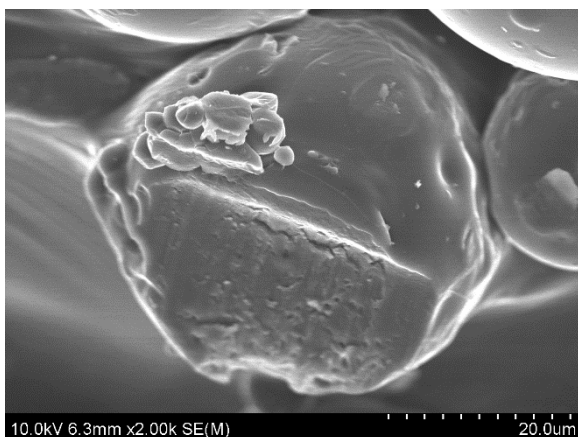
t = 90min
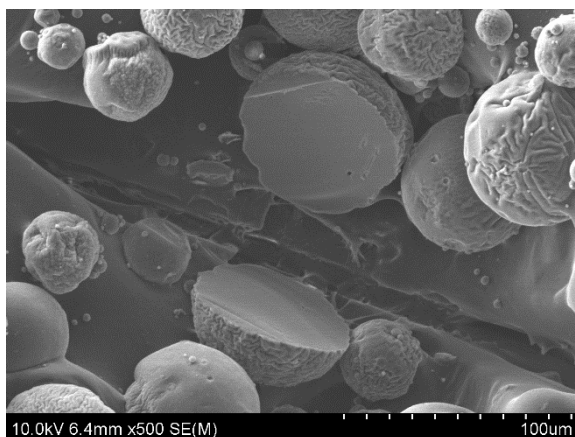
t = 120min

Figure 6-19. Evolution of internal morphology with time. water/AA ratio = 30 vol.% of AA, KPS = 0.08 mole% of AA, Neutralization ratio = 0.7, EGDMA = 0.2 mol% of AA, heptane, Span 80 = 0.74 w% in oil, T = 65°C, and washing method 3.

The evolution of particle inner-morphology can be explained in Fig. 6-20. When an aqueous droplet containing Na-acrylic acid and water is suspended in cyclohexane, the droplet-oil interface becomes the region where AA, Span80, and water coexist. However, this region should be very unfavorable for water because cyclohexane is strongly hydrophobic.($\delta_{AA}=12$, $\delta_{cyclohexane}=8.2$, and $\delta_{water}=23.5$ cla$^{1/2}$cm$^{-3/2}$ [110]) Thus, water tends to go to the center and crosslinked Na-polyacrylate is placed near the surface. When the polymerization is stopped at low conversion, water in the center goes outside and make a hollow in the center of the polymer particle (Fig. 6-20 (a)). As conversion increases, in the center, polymer particles are produced and formed the porous structure particle (Fig. 6-20 (b)). As conversion increases even more, when polymer phase is rich and phase inversion may occur at some point. When the polymerization is stopped after the phase inversion, then polymer particles could have a multihollow inner structure (Fig. 6-20 (c)). When conversion is very high, the inner structure of polymer particles is solid without hollows or pores (Fig. 6-20 (d)).
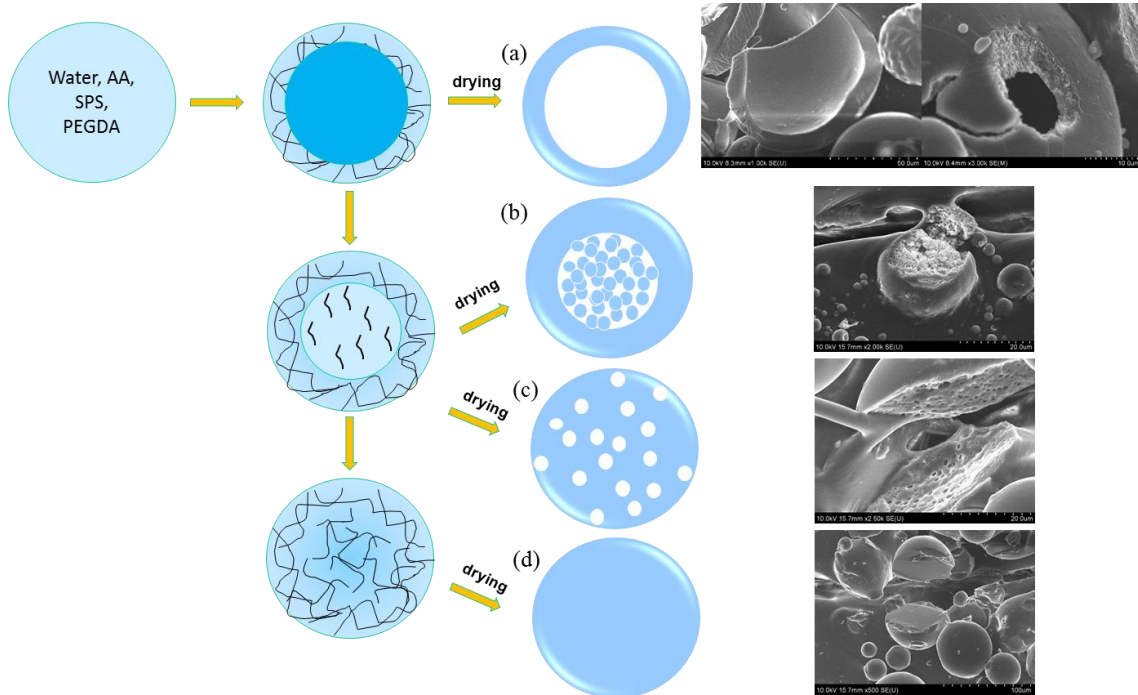
Figure 6-20. Evolution of the internal particle morphology.

6.3.3. Different deformation of partially neutralized sodium polyacrylate with cracked surface

To increase the size of Na-polyacrylate particles up to hundreds of microns, the agitation speed should be reduced, but in that case heavy aqueous droplets settle to the bottom and aggregate. We tried another modified system of the inverse suspension polymerization described in the literature [106] in order to increase the size of Na-polyacrylate particles, and different morphologies of Na-polyacrylate particles were observed.

Materials and experiment

1, 2-dicloroethane (Sigma-Aldrich) (Fig. 6-21) was mixed with cyclohexane as a co-continuous phase to prevent the settling of suspended droplets at the reactor bottom. The concept is that the difference of density between aqueous monomer droplet and continuous oil phase decreases when 1, 2-dicloroethane ($\rho = 1.25$ g/cm^3) is mixed with cyclohexane ($\rho = 0.779$ g/cm^3). Ethyl cellulose (Sigma-Aldrich) was used as a stabilizer.
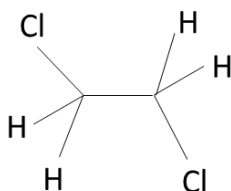
Figure 6-21. Structure of 1, 2-dicloroethane [111].

The partially neutralized Na-polyacrylate was prepared in the same manner as the titration method in section 5.3.1. The 0.06 mol % of PEGDA as a crosslinking agent and 2 mol% of

hydroxyethyl cellulose (Aldrich) as a thickener were dissolved in the partially neutralized sodium-acrylate solution and the clear mixture obtained was degassed by nitrogen bubbling for about 30 min. 0.32 wt% of ethyl cellulose as a suspending stabilizer was dissolved in non-solvent (cyclohexane: 1, 2-dicloroethane = 8:7, density = 1.0) and this phase was heated to 65°C in the reactor stirred at 150 rpm. A predetermined amount of sodium persulfate ($Na_2S_2O_8$(SPS), 0.09 mol/L of the aqueous phase, Aldrich) was dissolved in the aqueous solution after purging by N_2, and then the aqueous phase was added dropwise and the agitation of the mixture was kept constant and maintained for 4 hr. At the end of the reaction stirring was stopped and two phases were observed: the liquid containing cyclohexane was at the top of the reactor and the aqueous suspension of polyacrylate particles was at the bottom. The particles were recovered by methanol precipitation (washing 3). After drying at 40°C, sodium polyacrylate particles were obtained.

As shown below in Fig. 6-22, around 100 μm polymer particles with cracked surfaces were obtained.
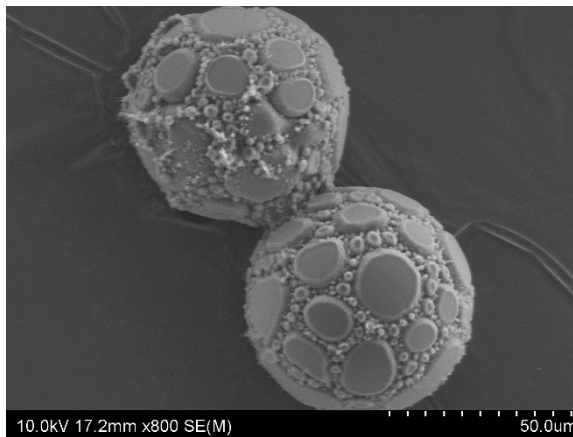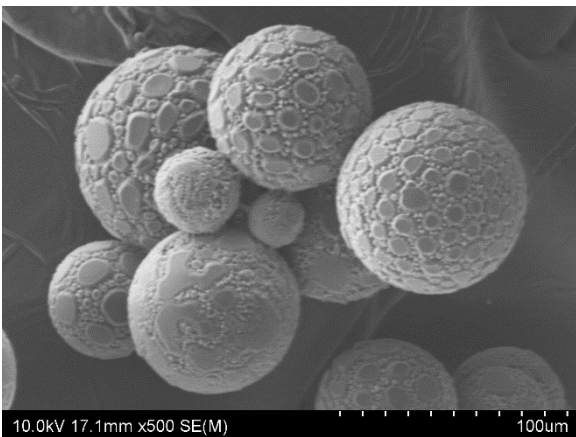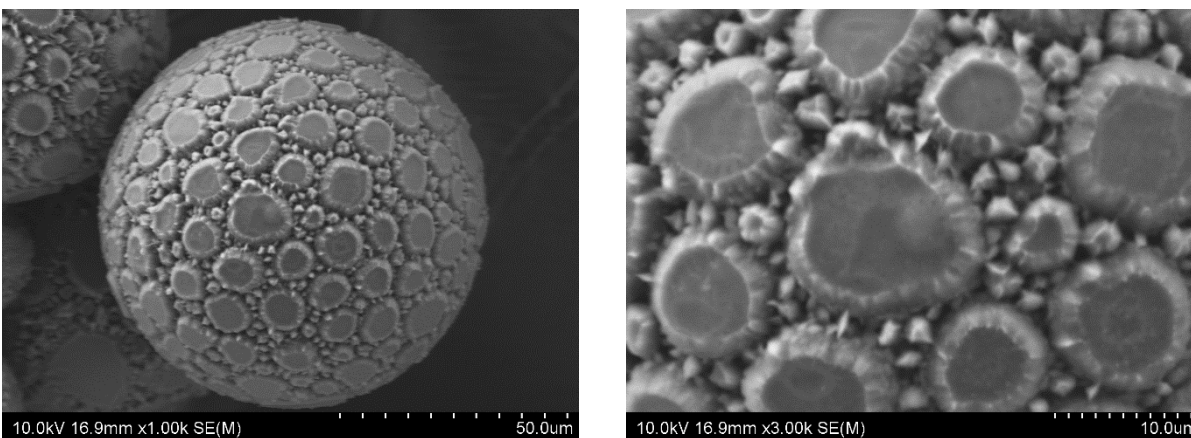
Figure 6-22. The SEM images of sodium polyacrylate particles; water/AA ratio = 30 vol.% of AA, neutralization ratio = 0.7, SPS = 0.09 mole% of AA, PEGDA = 0.06 mol% of AA, cyclohexane and 1,2- dicloroethane, ethyl cellulose = 0.32 w% in oil, T = 65°C, reaction for 4 hrs, and washing method 3.

6.4. Conclusion

In this chapter, we further developed the technique in chapter 5 to increase polymer particle size to tens of microns (up to hundreds of microns). In this process, wrinkled and cracked surfaces of Na-polyacrylate particles were observed in the special environment of post treatment. Surface area, swelling capacity, and swelling speed of different morphologies and sizes were characterized and analyzed. A polymer particle with a wrinkled surface has two times of surface area and this can be use in more applications where a large surface area is needed. When PEGDA was used instead of EGDMA, swelling capacity and speed were much higher because of the more flexible 3D network structure. Due to the same reason, higher concentration of crosslinking decreased swelling capacity and speed. In the case of small size of polymer particles from high shear mixing in Chapter 5, they had higher swelling properties than that of tens of particles without high shear.

Chapter 7 Inverse Suspension Polymerization of Acrylic Acid -Smooth Surface Superabsorbent Polymer Particles

7.1. Increasing the reaction time to improve the maximum conversion of the particles

In chapter 6, we discussed the synthesis of sodium polyacrylate polymer particles with wrinkled or cracked surfaces. It was shown that the post-reaction particle treatment affected the final polymer particle morphology. In Chapter 6, it was also observed that as the reaction time was extended, the polymer particle morphology changed and in particular, after a long reaction time or very high monomer conversion, the resulting polymer particles showed little surface wrinkles. From the model calculation, as shown in Figure 7-1, we found that the monomer conversion reached above 95% conversion after about 3 hr, but afterward, the conversion increases very slowly, yet with quite significant changes are seen in the polymer particle morphology. Thus, in this chapter, we shall present more experimental results on the micro particle synthesis with extra-long reaction times to obtain wrinkle-free sodium polyacrylate micro particles.
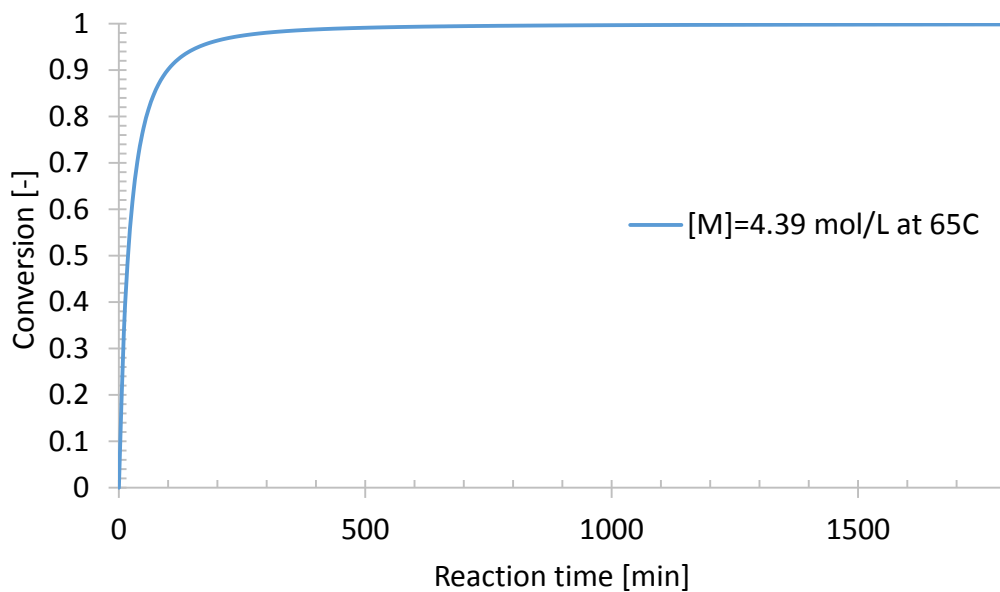
Figure 7-1. Calculated conversion curve up to 20 hrs-polymerization ([M] =4.39 mol/L).

7.2. Result and discussion

7.2.1. Change of particle morphology of Na-polyacrylate particles with reaction time

Polymerization was carried out following the standard procedure as described in Chapter 6 but the reaction time was extended to 20 hr. A small amount of polymer sample was taken from the reactor at each sampling time (1hr intervals) during the course of polymerization. Figure 7-2 shows the summary of SEM images of the polymer particles taken at different reaction times.

time = 2hr   3 hr   4 hr   5 hr

6 hr   7 hr   8 hr   9 hr

10 hr   11 hr   12 hr   13 hr

14 hr   15 hr   16 hr   17 hr

18 hr   19 hr   20 hr
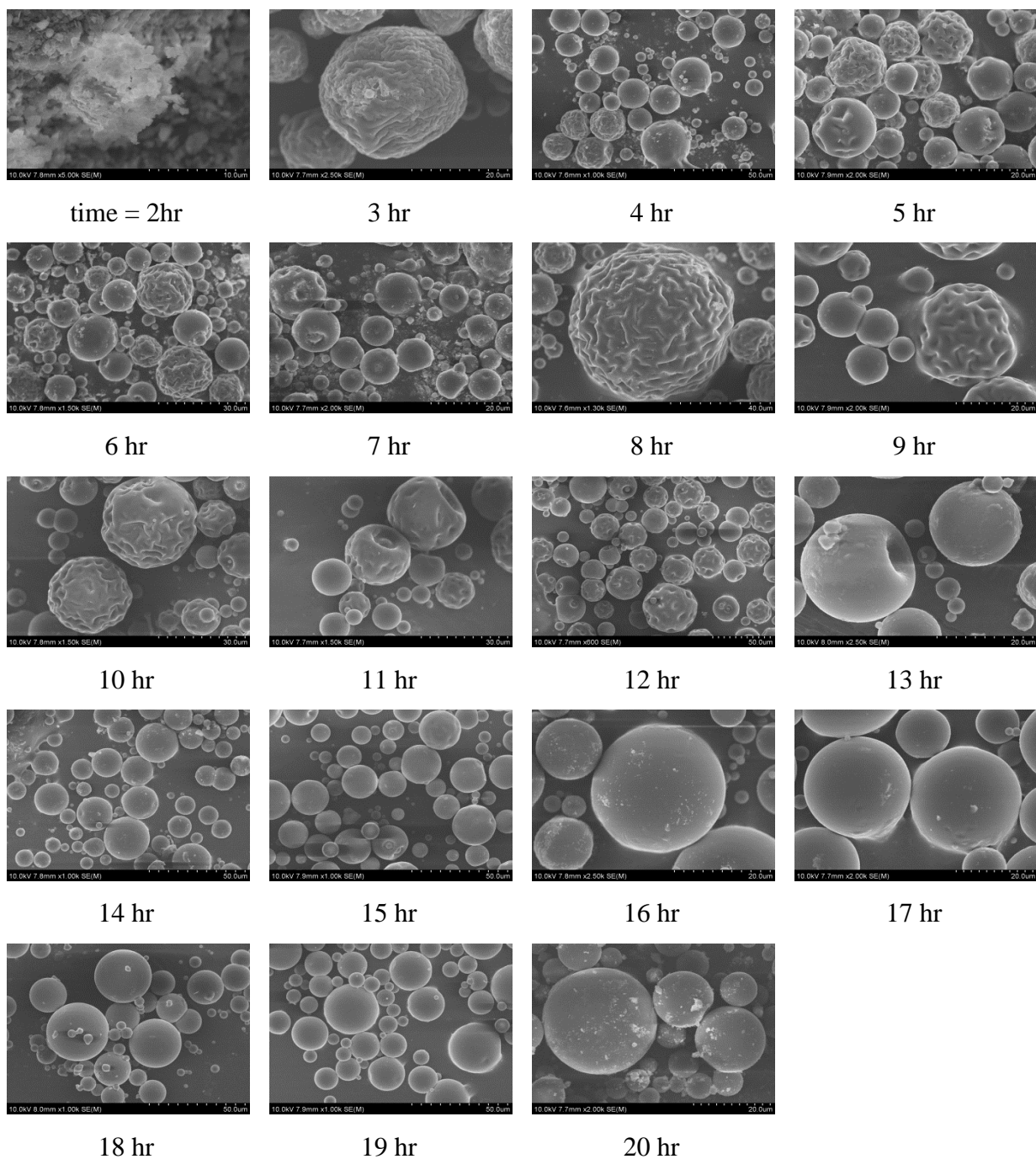
Figure 7-2. The SEM images of sodium polyacrylate particles from the same reactor from time = 2 hr to time = 20 hr (water/AA ratio = 30 vol.% of AA, neutralization ratio = 0.7, SPS = 0.09 mole% of AA, PEGDA= 0.06 mole% of AA, cyclohexane, Span 80 = 0.74 w% in oil, T = 65°C, and washing method 3).

Overall, Figure 7-2 shows that the surface wrinkles disappear after about 13 hr of polymerization. The conversion after 15 hr was 99.6%, which is a large increase from the monomer conversion (95.5%) with particles of wrinkled surfaces (See Table 7-1). It is thought that as the unreacted acrylic acid and water near the wrinkled surface continued to polymerize and crosslink, additional swelling occurred near the surface layer with wrinkles and as a result, eventually the polymer particle surface deformed again to exhibit smooth surfaces.

Table 7-1. Calculated conversions in this system with time.

Reaction time [hr]	Conversion [-]
3	0.955
12	0.995
15	0.996

From the BET analysis of some of these particles (Fig. 7-2), the surface area of polymer particle after 20 hr was only 4.282 m^2/g, indicating that the particle was very close to solid particles with no internal structures. The pore volume (0.00547 cc/g) was also much smaller than 3hr-polymerized particle (0.031 cc/g).
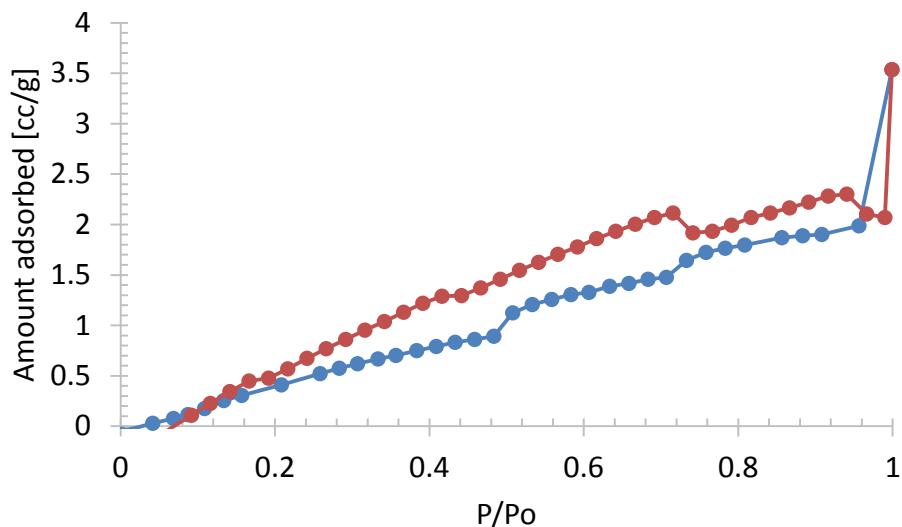
Figure 7-3. The graph of adsorption-desorption isotherm of the polymer sample in Fig. 7-2 after 20hr. Surface Area = 4.282 m²/g and total pore volume = 0.00547 cc/g.

7.2.2. Effect of monomer concentration

The monomer/water ratio can also be an important parameter that affects the polymer particle morphology. We used two different acrylic acid monomer concentrations: [M] = 3.01 mol/L) and 5.44 mol/L.

Low [M](=3.01 mol/L):

At this relatively low monomer concentration, discrete polymer particles were not formed until 11 hr of reaction time and after 12 hr, polymer particles were formed. Figure 7-4 show that the polymer particles obtained after 12 hr of reaction have no surface wrinkles but some particles

116

have surface dents, probably due to the collision with other particles. After 21 hr, perfectly spherical and smooth particles were obtained and the final monomer conversion was 99.6%.

| 12 hr | 14 hr | 15 hr |
| 21 hr | 22 hr | 25hr |
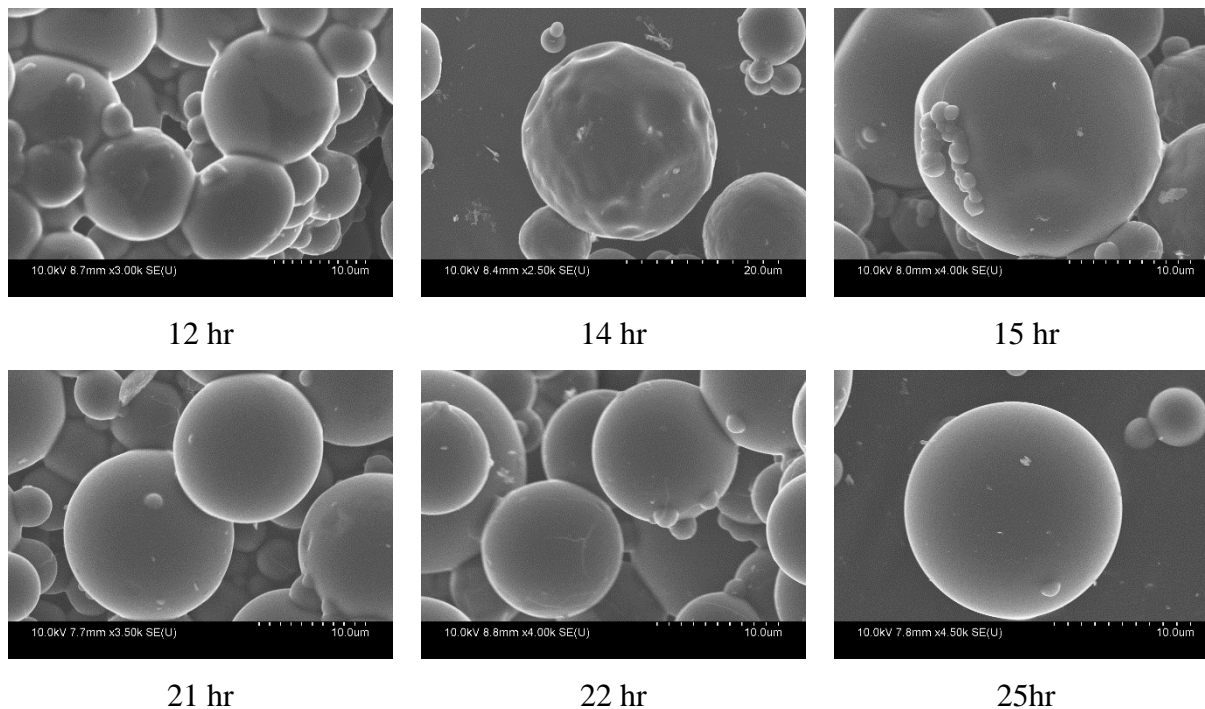
Figure 7-4. The SEM images of sodium polyacrylate particles from the same reactor (water/AA ratio = 20 vol.% of AA, neutralization ratio = 0.7, SPS = 0.09 mole% of AA, PEGDA= 0.06 mole% of AA, cyclohexane, Span 80 = 0.74 w% in oil, T = 65°C, and washing method 3).

High [M]=5.44 mol/L:

When the higher monomer concentration was used, wrinkle-free particles were obtained much earlier than in the case of low monomer concentration. Figure 7-5 shows that when the conversion reached 99.5% (t = 9 hr), all the polymer microparticles became wrinkle free. Thus, from the observations in Figures 7-5 and 7-6, the monomer concentration is an important reaction parameter that affect the surface morphology. Figure 7-6 shows the calculated conversion vs. time

curves for three different monomer concentrations. The difference may not look quite significant, but the time to reach certain high conversions above which the surface wrinkles disappear varies quite significantly with the initial monomer concentration. Figure 7-7 compares the actual experimental conversion data for [M] = 4.39 mol/L with the model-predicted conversion. We can see that very good fit of the experimental conversion data were obtained.

| 1hr | 3hr | 5hr |

| 6hr | 9hr | 11hr |
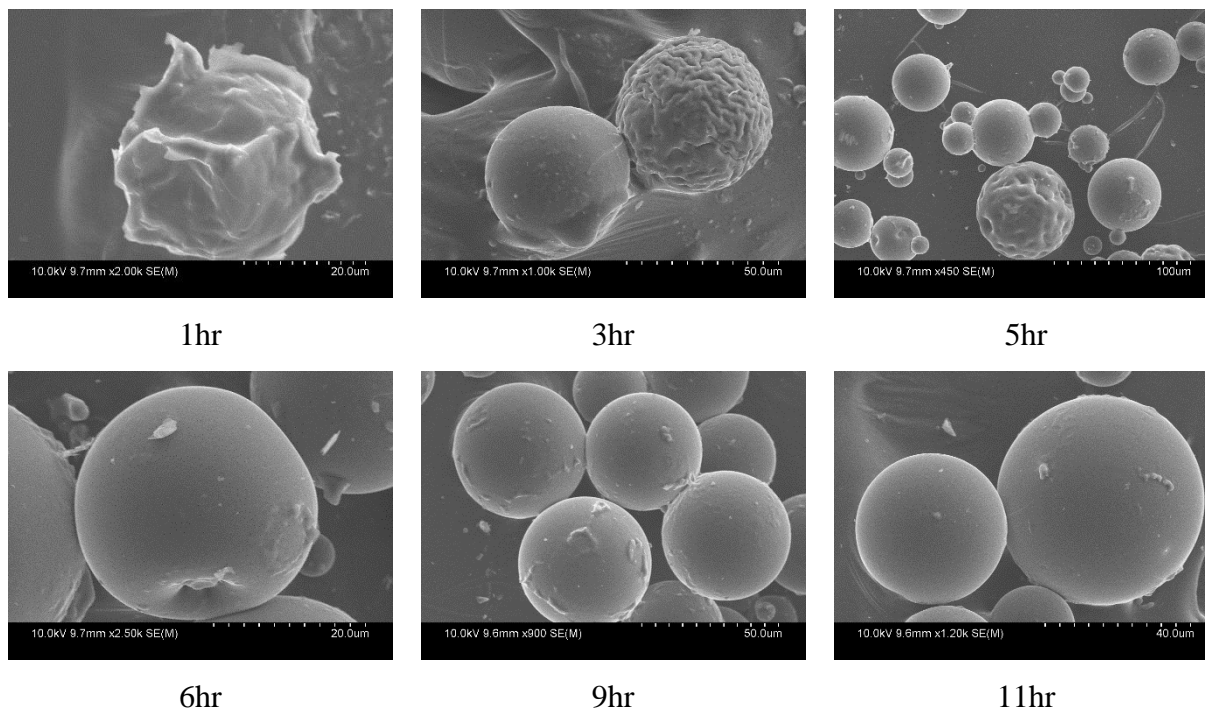
Figure 7-5. The SEM images of sodium polyacrylate particles from the same reactor (water/AA ratio = 37 vol.% of AA, neutralization ratio = 0.7, SPS = 0.09 mole% of AA, PEGDA= 0.06 mole% of AA, cyclohexane, Span 80 = 0.74 w% in oil, T = 65°C, and washing method 3).
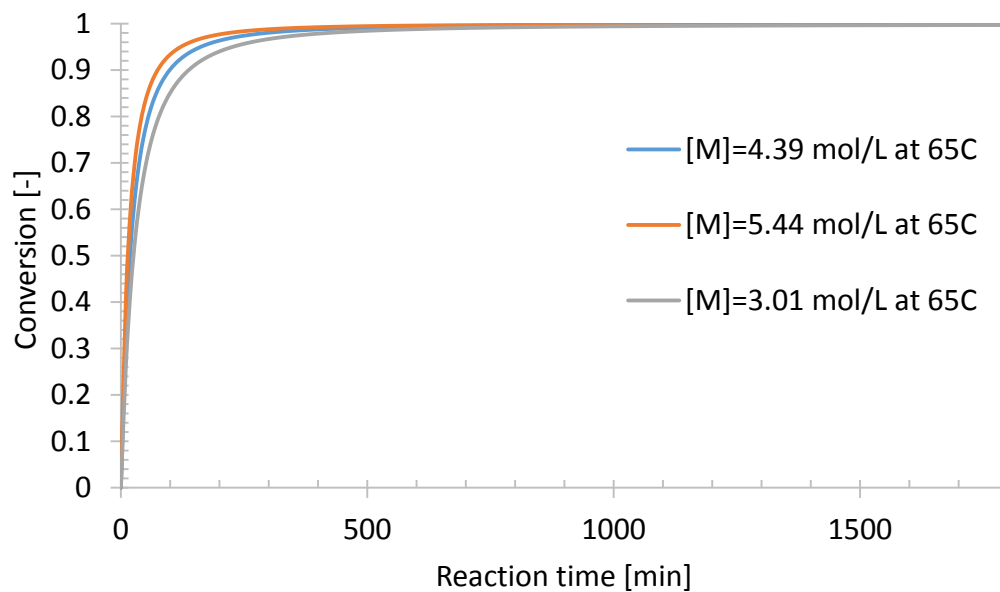
Figure 7-6. Conversion curve as monomer concentration varies.
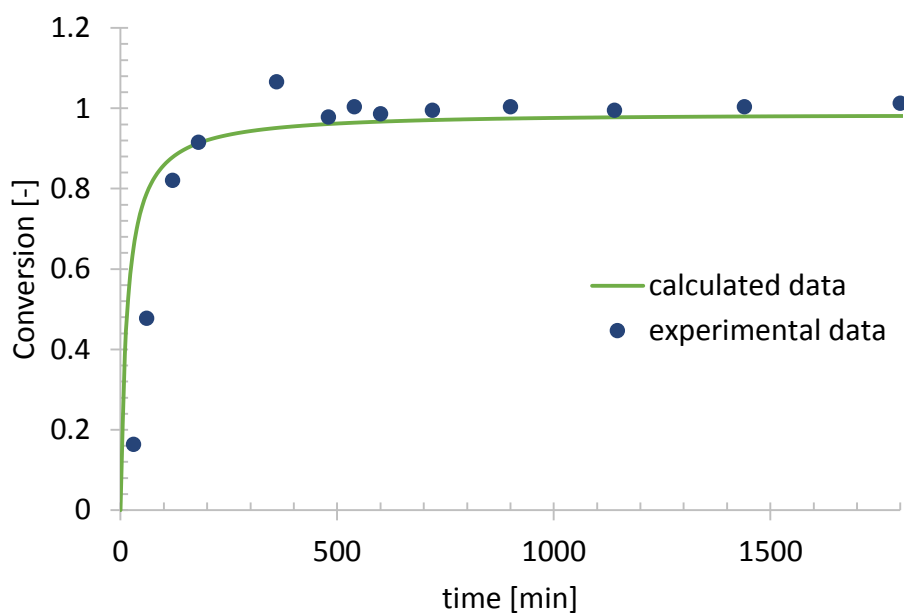
Figure 7-7. Plotted experimental conversion data with calculated conversion.

119

7.3. Conclusion

In this chapter, we investigated the effect of monomer conversion on the particle surface. When the conversion of acrylic acid was higher than 99.6%, polymer particles were perfectly spherical with no surface wrinkles. This result suggests that sodium polyacrylate particle morphology can be varied by controlling the monomer concentration. It should be noted that the experiments were limited with a fixed crosslinker concentration (PEGDA = 0.06 mol% of AA), and it is possible that both monomer concentration and crosslinker concentration can be optimized to obtain wrinkle-free microparticles of sodium polyacrylate.

List of Publications and Presentations

Publications

1. Carla V. Luciani, Kyu Yong Choi, Joong Jin Han, Yunju Jung, Polymer particles with a pomegranate-like internal structure via micro-dispersive polymerization in a geometrically confined reaction space I. Experimental study, Polymer 52 (2011) 942-948

2. Yunju Jung, Carla Vanesa Luciani, Joong Jin Han, Kyu Yong Choi, Polymerization of Methyl Methacrylate in the Presence of a nonpolar Hydrocarbon Solvent. I. Construction of a Complete Ternary Phase Diagram Through an In Situ Polymerization, Journal of Applied Polymer Science,Vol. 116, 3648–3658 (2010)

Conferences/Presentations

1. Yunju Jung, Carla V. Luciani, Joong Jin Han, and Kyu Yong Choi, Synthesis of Structured Polymer Particles by Micro Dispersive Suspension Polymerization, AICHE, Fall 2008

2. Carla V. Luciani, Yunju Jung, Joongjin Han, Kyu Yong Choi, Modeling of Dispersion Polymerization in a Confined Reaction Space, AICHE, Fall 2008

3. Yunju Jung, Joong Jin Han, and Kyu Yong Choi, Multi-Hollow Polymer Particles by Dispersive Suspension Polymerization, AICHE, Fall 2007

4. Yunju Jung, Joong Jin Han, and Kyu Yong Choi, Synthesis of Multi-Hollow Polymer Particles by Dispersive Suspension Polymerization, 9th International Workshop Polymer Reaction Engineering, 7 – 10 October 2007, University of Hamburg

Invention disclosure

1. Preparation of porous or multihollow micron size polymer particles by dispersive suspension polymerization, University of Maryland, 2007.

Manuscripts in preparation

1. Inverse suspension polymerization of sodium acrylate to superabsorbent polymer microparticles (in preparation).

2. Micropolymer particle morphologies via inverse suspension polymerization under different mixing conditions (in preparation).

3. Morhological control of micropolymer particles of partially crosslinked sodium polyacrylate (in preparation).

Bibliography

1. Im, S. H.; Jeong, U. Y.; Xia, Y. N. "Polymer hollow particles with controllable holes in their surfaces." *Nature Materials* 2005, *4*, 671-675.

2. Xu, X.; Asher, S. A. "Synthesis and utilization of monodisperse hollow polymeric particles in photonic crystals." *Journal of the American Chemical Society* 2004, 126, 25, 7940-7945.

3. He, X. D.; Ge, X. W.; Liu, H. R.; Wang, M. Z.; Zhang, Z. C. "Synthesis of cagelike polymer microspheres with hollow core/porous shell structures by self-assembly of latex particles at the emulsion droplet interface." *Chemistry of Materials* 2005, *17*, 5891-5892.

4. Kobayashi, H.; Miyanaga, E.; Okubo, M. "Preparation of multihollow polymer particles by seeded emulsion polymerization using seed particles with incorporated nonionic emulsifier" *Langmuir* 2007, 23, 17, 8703-8708.

5. Emmerich, O.; Hugenberg, N.; Schmidt, M.; Sheiko, S. S.; Baumann, F.; Deubzer, B.; Weis, J.; Ebenhoch, J. "Molecular boxes based on hollow organosilicon micronetworks." *Advanced Materials* 1999, *11*, 1299-1303.

6. ODonnell, P. B.; McGinity, J. W. "Preparation of microspheres by the solvent evaporation technique." *Advanced Drug Delivery Reviews* 1997, *28*, 25-42.

7. Zhu, K. J.; Jiang, H. L.; Du, X. Y.; Wang, J.; Xu, W. X.; Liu, S. F. "Preparation and characterization of hCG-loaded polylactide or poly(lactide-co-glycolide) microspheres using a modified water-in-oil-in-water (w/o/w) emulsion solvent evaporation technique." *Journal of Microencapsulation* 2001, *18*, 247-260.

8. Langer, R. "Drug delivery and targeting." *Nature* 1998, *392*, 5-10.

9. Bergbreiter, D. E. "Self-assembled, sub-micrometer diameter semipermeable capsules." *Angewandte Chemie-International Edition* 1999, *38*, 2870-2872.

10. Ruiters; Marcel; Herman; Josef "Protection of biologically active molecules using amphiphiles", WO2006/043809 A1, 2006.

11. Wu, H. S.; Sun, F.; Dimonie, V. L.; Klein, A. "Expandable hollow particles", US 5,834,526, 1998.

12. Itou, N.; Masukawa, T.; Ozaki, I.; Hattori, M.; Kasai, K. "Cross-linked hollow polymer particles by emulsion polymerization." *Colloids and Surfaces a-Physicochemical and Engineering Aspects* 1999, *153*, 311-316.

13. Okubo, M.; Ito, A.; Nakamura, M. "Effect of molecular weight on the production of multi-hollow polymer particles by the alkali/cooling method." *Colloid and Polymer Science* 1997, *275*, 82-85.

14. McDonald, C. J.; Bouck, K. J.; Chaput, A. B.; Stevens, C. J. "Emulsion polymerization of voided particles by encapsulation of a nonsolvent." *Macromolecules* 2000, *33*, 1593-1605.

15. Gross, J. R. "Process for forming a porous particles of an absorbent polymer", US 5,403,870, 1995.

16. Adebajo, M. O.; Frost, R. L.; Kloprogge, J. T.; Carmody, O.; Kokot, S. "Porous materials for oil spill cleanup: A review of synthesis and absorbing properties." *Journal of Porous Materials* 2003, *10*, 159-170.

17. Mu, G. H.; Shen, H. G.; Qiu, J. X.; Gu, M. Y. "Microwave absorption properties of composite powders with low density." *Applied Surface Science* 2006, *253*, 2278-2281.

18. Mu, G. H.; Pan, X. F.; Chen, N.; He, C. H.; Gu, M. Y. "Synthesis and characterization of hard magnetic composites - Hollow microsphere/titania/barium ferrite." *Applied Surface Science* 2008, *254*, 2483-2486.

19. Okubo, M.; Minami, H.; Komura, T. "Preparation of micrometer-sized, monodisperse, magnetic polymer particles." *Journal of Applied Polymer Science* 2003, *88*, 428-433.

20. Kim, J. W.; Chang, I. S.; Kang, H. K. "Application of polymers in the field of high functional cosmetics." *Polymer Science & Technology* 2002, *13*, 422-4300.

21. Li, G. L.; Yang, X. Y.; Wang, B.; Wang, J. Y.; Yang, X. L. "Monodisperse temperature-responsive hollow polymer microspheres: Synthesis, characterization and biological application." *Polymer* 2008, *49*, 3436-3443.

22. Qian, J.; Wu, F. P. "Synthesis of thermosensitive hollow spheres via a one-pot process." *Chemistry of Materials* 2007, *19*, 5839-5841.

23. Glinel, K.; Sukhorukov, G. B.; Mohwald, H.; Khrenov, V.; Tauer, K. "Thermosensitive hollow capsules based on thermoresponsive polyelectrolytes." *Macromolecular Chemistry and Physics* 2003, *204*, 1784-1790.

24. Boh, B.; Knez, E.; Staresinic, M. "Microencapsulation of higher hydrocarbon phase change materials by in situ polymerization." *Journal of Microencapsulation* 2005, *22*, 715-735.

25. Zhang, X.X.; Tao, X. M.; Yick, K.I.; Wang, X.C. "Structure and thermal stability of microencapsulated phase-change materials." *Colloid Polym. Sci*. 2004, 282, 330-336.

26. Soane, D. S.; Houston, M. R. "Method for synthesizing thermo-expandable polymeric microspheres", US 6,617,364 B2, 2003.

27. Jonsson, M.; Nordin, O.; Malmstrom, E.; Hammer, C. "Suspension polymerization of thermally expandable core/shell particles." *Polymer* 2006, *47*, 3315-3324.

28. Okubo, M.; Minami, H.; Yamamoto, Y. "Release of toluene from micron-sized, monodispersed, cross-linked, hollow polymer particles." *Colloid and Polymer Science* 2001, *279*, 77-81.

29. Okubo, M.; Konishi, Y.; Inohara, T.; Minami, H. "Production of hollow polymer particles by suspension polymerizations for ethylene glycol dimethacrylate/toluene droplets dissolving styrene-methyl methacrylate copolymers." *Journal of Applied Polymer Science* 2002, *86*, 1087-1091.

30. Jiang, B. B.; Gao, C. Y.; Shen, J. C. "Polylactide hollow spheres fabricated by interfacial polymerization in an oil-in-water emulsion system." *Colloid and Polymer Science* 2006, *284*, 513-519.

31. Park, J. H.; Oh, C.; Shin, S. I.; Moon, S. K.; Oh, S. G. "Preparation of hollow silica microspheres in W/O emulsions with polymers." *Journal of Colloid and Interface Science* 2003, *266*, 107-114.

32. He, X. D.; Ge, X. W.; Liu, H. R.; Wang, M. Z.; Zhang, Z. C. "Cagelike polymer microspheres with hollow core/porous shell structures." *Journal of Polymer Science Part a-Polymer Chemistry* 2007, *45*, 933-941.

33. He, X. D.; Ge, X. W.; Wang, M. Z.; Zhang, Z. C. "The preparation of composite microsphere with hollow core/porous shell structure by self-assembling of latex particles at emulsion droplet interface." *Journal of Colloid and Interface Science* 2006, *299*, 791-796.

34. He, X. D.; Ge, X. W. W.; Wang, M. Z.; Zhang, Z. C. "Polystyrene/melamine-formaldehyde hollow microsphere composite by self-assembling of latex particles at emulsion droplet interface." *Polymer* 2005, *46*, 7598-7604.

35. Dinsmore, A. D.; Hsu, M. F.; Nikolaides, M. G.; Marquez, M.; Bausch, A. R.; Weitz, D. A. "Colloidosomes: Selectively permeable capsules composed of colloidal particles." *Science* 2002, *298*, 1006-1009.

36. Xu, X. L.; Asher, S. A. "Synthesis and utilization of monodisperse hollow polymeric particles in photonic crystals." *Journal of the American Chemical Society* 2004, *126*, 7940-7945.

37. Fu, G. D.; Shang, Z. H.; Hong, L.; Kang, E. T.; Neoh, K. G. "Preparation of cross-linked polystyrene hollow nanospheres via surface-initiated atom transfer radical polymerizations." *Macromolecules* 2005, *38*, 7867-7871.

38. Kim, B. S.; Kim, J. W.; Suh, K. D. "Poly(methyl methacrylate) multihollow particles by water in oil in water emulsion polymerization." *Journal of Applied Polymer Science* 2000, *76*, 38-44.

39. Kim, J. W.; Joe, Y. G.; Suh, K. D. "Poly(methyl methacrylate) hollow particles by water-in-oil-in-water emulsion polymerization." *Colloid and Polymer Science* 1999, *277*, 252-256.

40. Kim, J. W.; Ko, J. Y.; Jun, J. B.; Chang, I. S.; Kang, H. H.; Suh, K. D. "Multihollow polymer microcapsules by water-in-oil-in-water emulsion polymerization: morphological study and entrapment characteristics." *Colloid and Polymer Science* 2003, *281*, 157-163.

41. Bao, Y. Z.; Huang Z. M.; Weng Z. X. "Particle features of a poly(methyl methacrylate) resin prepared by a new emulsion polymerization process", *Journal of Applied Polymer Science*, Vol. *94*, 1905–1911 (2004).

42. Cohen, C.; Tanny, G.B.; Prager, S. "Diffusion-controlled formation of porous structures in ternary polymer systems", *Journal of Polymer Science: Polymer physics Edition*, Vol. 17, 477-489 (1979).

43. Soh, Y. S.; Kim J. H.; Gryte C. C., "Phase behavior of polymer/solvent/non-solvent systems", *Polymer*, Vol. 36, 3711-3717 (1995).

44. Lai, J. Y.; Lin, S. F.; Lin. F. C.; Wang, D. M. "Construction of ternary phase diagrams in nonsolvent/solvent/PMMA system", *Journal of Polymer Science Part B: Polymer Physics,* Vol. 36, 607-615 (1998).

45. Young, T. H.; Cheng, L. P. "Phase behavior of EVAL polymers in water-2-propanol cosolvent", *Macromolecules* 1998, 31, 1229-1235.

46. Wang, D.; Li, K.; Teo, W. K. "Phase separation in polyetherimide/solvent/nonsolvent systems and membrane formation", *Journal of Applied Polymer Science,* vol. 71, 1789-1796 (1999).

47. Lin, K. Y.; Wang, D. M.; Lai, J. Y. "Nonsolvent-induced gelatin and its effect on membrane morpnology", *Macromolecules* 2002, 35, 6697-6706.

48. Meira, G.R., Luciani, C.V., Estenoz, D.A. "Continuous Bulk Process for the Production of High-Impact Polystyrene: Recent Developments in Modeling and Control", *Macromolecular Reaction Engineering* 2007, 1, 25-39.

49. Alexopoulos, A.H., Kiparissided, C. "On the prediction of internal particle morphology in suspension polymerization of vinyl chloride. Part I: The effect of primary particle size distribution", *Chemical Engineering Science* 2007, 62, 3970-3983.

50. Dong, R., Zhao, J., Zhang, Y., Pan, D. "Morphology Control of Polyacrylonitrile (PAN) Fibers by Phase Separation Technique", *Journal of Polymer Science Part B: Polymer Physics* 2009, 47, 261-275.

51. Wang, B.; Dar, Y.; Shi, L.; Caneba, G. T. "Polymerization control through the free-radical retrograde-precipitation polymerization process", *Journal of Applied Polymer Science* 1999, *71*, 761-774.

52. Tao, C. T.; Young, T. H. "Phase behavior of poly(N-isopropylacrylamide) in water-methanol cononsolvent mixtures and its relevance to membrane formation", *Polymer* 2005, *46*, 10077-10084.

53. Barzin, J.; Sadatnia, B. "Theoretical phase diagram calculation and membrane morphology evaluation for water/solvent/polyethersulfone systems", *Polymer* 2007, *48*, 1620-1631.

54. Young, T. H.; Tao C. T.; Lai, P. S. "Phase behavior of poly (ether imide) in mixtures of *N*-methyl-2-prrolidinone and methylene chloride", *Polymer* 2003, 44, 1689-1695.

55. Cheng, L. P.; Shaw, H. Y. "Phase behavior of a water/2-propanol/poly (methyl methacrylate) cosolvent system", *Jouranl of Polymer Science Part B: Polymer Physices* 2000, 38, 747-754.

56. Aggarwal, A.; Saxena, R.; Wang, B.; Caneba, G. T. "Studies of the polymerization of methacrylic acid via free-radical retrograde precipitation polymerization process", *Journal of Applied Polymer Science* 1996, 62, 2039-2051.

57. http://www.photocor.com/dls-instrument/

58. Flory, "Principles of polymer chemistry"; Cornell University Press: Ithaca, 1953.

59. Mayoux, C; Dandurand, J.; Ricard, A.; Lacabanne, C. "Inverse suspension polymerization of sodium acrylate: synthesis and characterization", *Journal of Applied Polymer Science*, Vol. 77, 2621–2630 (2000).

60. Zohuriaan-Mehr, M. J.; Kabiri, K. "Superabsorbent Polymer Materials_ A Review", *Iranian Polymer Journal* 17 (6), 2008, 451-477.

61. Arshady, R. "Suspension, emulsion, and dispersion polymerization: A methodological survey", *Colloid and Polymer Science* 270 717~732 (1992).

62. Luciani, C. V.; Choi, K. Y.; Han, J. J.; Jung, Y. "Polymer particles with a pomegranate-like internal structure via micro-dispersive polymerization in a geometrically confined reaction space 1. Experimental study", *Polymer* 52 (2011) 942-948.

63. Jung, Y.; Luciani, C. V.; Han, J. J.; Choi, K. Y.; "Polymerization of methyl methacrylate in the presence of a nonpolar hydrocarbon solvent. 1. Construction of a complete ternary phase diagram through an *in situ* polymerization." *Jouranl of Applied Polymer Science,* Vol. 116, 3648–3658 (2010).

64. Buchholz & Graham, "Modern Superabsorbent Polymer Technology", New York, Wiley-VCH, Chapter 1~7 (1998).

65. Buchholz et al., American Chemical Society (1994), "In Superabsorbent Polymers", chapter 8 ~ 10.

66. J.W. Gooch, "Biocompatible Polymeric Material and Tourniquets for Wounds", *Topics in applied chemistry.*

67. Zohuriaan-Mehr, M. J.; Omidian, H.; Doroudiani, S.; Kabiri, K. "Advances in non-hygienic applications of superabsorbent hydrogel materials", *Journal of Material Science* (2010) 45 5711–5735.

68. Transparency Market Research, "Superabsorbent Polymers Market - Global Industry Analysis, Size, Share, Growth, Trends and Forecast, 2014 – 2020.

69. Buchholz, "Keeping dry with Superabsorbent Polymers", *Chemtech article* (1994).

70. Liu, Z.; Brooks, B. W. "A study of inverse dispersion polymerization of acrylic acid using water-soluble redox initiators", *Journal of Applied Polymer Science*, Vol. 66, 2191–2197 (1997).

71. Liu, Z.; Brooks, B. W. "Inverse dispersion polymerization of acrylic acid initiated by a water-soluble redox pair: the role of drop mixing", *Polymer* 40 (1999) 2181–2188.

72. Liu, M.; Guo, T. "Preparation and Swelling Properties of Crosslinked Sodium Polyacrylate", *Journal of Applied Polymer Science*, Vol. 82, 1515–1520 (2001).

73. Benda D.; Snuparek, J.; Cermak, V. "Inverse suspension polymerization of the hydrophilic acrylic monomers in the static continuous phase", *Journal of Dispersion Science and Technology*, 18(2), 115-121 (1996).

74. Kiatkamjornwong S.; Phunchareon, P. "Influence of Reaction Parameters on Water Absorption of Neutralized Poly(acrylic acid-co-acrylamide) Synthesized by Inverse Suspension Polymerization", *Journal of Applied Polymer Science*, Vol. 72, 1349–1366 (1999).

75. Griffin, "Classification of surface active agents by "HLB"", *Journal of the society of cosmetic chemists*, Vol. 1, No. 5, December 1949.

76. Sannino, A.; Esposito, A.; Rosa, A. D.; Cozzolino, A.; Ambrosio, L.; Nicolais, L. "Biomedical application of a superabsorbent hydrogel for body water elimination in the treatment of edemas", *Journal of Biomedical Materials Research Part A*, 67A:1016 (2003).

77. Chen, J.; Blevins, W. E.; Park, H.; Park, K. "Gastric retention properties of superporous hydrogel composites", *Journal of Controlled Release* 64 (2000) 39–51.

78. Wang, M.; Gao, Y.; Cao, C.; Chen, K.; Wen, Y.; Fang, D.; Li, L.; Guo, W. "Binary Solvent Colloids of Thermosensitive Poly(N-isopropylacrylamide) Microgel for Smart Windows", *Industrial and Engineering Chemistry Research*, 2014, 53 (48), 18462–18472.

79. Dabhi, R.; Bhatt, N.; Pandit, B.; "Super absorbent polymers-an innovative water saving technique for optimizing crop yield", *International Journal of Innovative Research in Science, Engineering and Technology,* Vol. 2, 2013, 5333-5340.

80. Kiatkamjornwong S., "Superabsorbent Polymers and Superabsorbent Polymer Composites", *ScienceAsia 33 Supplement 1* (2007) 39-43.

81. "http://www.dryprocessing.com/super-absorbent-polymer.php" from LIST technology.

82. Dobi'c, S. N.; Filipovic, J. M.; Tomic, S. L. "Synthesis and characterization of poly(2-hydroxyethyl methacrylate/itaconic acid/poly(ethylene glycol) dimethacrylate) hydrogels", *Chemical Engineering Journal* 179 (2012) 372–380.

83. Ge, J. F.; Lu, F. J.; Ding, W. "Investigation on the Inverse Emulsion Polymerization of Acrylic Acid", *Chinese Chemical Letters* Vol. 13, No. 10, 993 – 996 (2002).

84. Kriwet, B.; Walter, E.; Kissel, T. "Synthesis of bioadhesive poly(acrylic acid) nano and microparticles using an inverse emulsion polymerization method for the entrapment of hydrophilic drug candidates", *Journal of Controlled Release* 56 (1998) 149 –158.

85. Wang, G.; Li, M.; Chen, X. "Inverse suspension polymerization of sodium acrylate", *Journal of Applied Polymer Science*, vol. 65, 789–794 (1997).

86. Ye, Q.; Zhang, Z.; Ge, X. "Formation of monodisperse polyacrylamide particles by dispersion polymerization: particle size and size distribution", *Polymer International* 52:707–712 (2003).

87. Minami, H.; Kimura, A.; Kinoshita, K.; Okubo, M. "Preparation of Poly(acrylic acid) Particles by Dispersion Polymerization In an Ionic Liquid", *Langmuir*, 2010, 26 (9), 6303–6307.

88. Dotson, N. A.; Galvan, R.; Laurence, R.; Tirrell, M. "Polymerization process modeling", Chapter 7: Heterogeneous polymerization. New York: VCH; 1996.

89. Vivaldo-Lima, E.; Wood, P. E.; Hamielec, A. E. "An updated review on suspension polymerization", *Industrial and Engineering Chemistry Research* 1997, 36, 939-965.

90. Ramirez, J. C.; Herrera-Ordonez, J. "Kinetics of styrene minisuspension polymerization using a mixture PVA–SDS as stabilizer", *Polymer* 47 (2006) 3336–3343.

91. "Emulsions and Emulsification", *Particle sciences, Technical Brief*, 2009, vol. 9.

92. Lee, Y.; Hahm, Y. M. "Evaluation on the Possibility of Preparation of Nanosized Alumina Powder under W/O Emulsion Method Using Homogenizer", *Applied Chemistry Engineering* Vol. 21, No. 5, October 2010, 488-494.

93. Björkegren, S.; Karimi, R. F.; Martinelli, A.; Jayakumar, N. S.; Hashim, M.A. "A new emulsion liquid membrane based on a palm oil for the extraction of heavy metals", *Membranes* 2015, 5, 168-179.

94. Mark Elliott, "Superabsorbent Polymers", Product Development Scientist for SAP, BASF Aktiengesellschaft, 1997.

95. Whitten, K.W.; Davis, R. E.; Peck, L.; Stanley, G. G. "Chemistry", 10th edition, Brooks/Cole (2010)

96. Tjipangandjara, K. F.; Somasundaran, P. "Effects of the conformation of poly acrylic acid on the dispersion-flocculation of alumina and kaolinite fines", *Advanced Powder Technology*, Vol. 3, 119-127 (1992).

97. Brannon-Peppas and Harland, "Studies in polymer science", Volume 8, (1995).

98. Cutie et al., Journal of Polymer Science Part B Polymer Physics, Vol. 35, 2029–2047 (1997), Acrylic acid polymer kinetics.

99. Manickam et al., *Eur. Polym. J.,* 16, 483 (1979).

100.   Kabanov et al. *Eur. Polym. J*., 11, 153 (1975).

101.   Elliott et al., Polymer 45 (2004) 1503–1510, Structure and swelling of poly(acrylic acid) hydrogels: effect of pH, ionic strength, and dilution on the crosslinked polymer structure.

102.   Mechtcherine and Reinhardt, "Application of super absorbent polymers in concrete construction" 2012.

103.   Nagorsky, ACS Symposium, 1994, In Super Absorbent Polymers" Chapter 8, ACS Symposium, 1994, In Super Absorbent Polymers" Chapter 8.

104. Lee et al., Journal of Applied Polymer Science, Vol. 106, 1992–1999 (2007), Swelling and Antibacterial Properties for the Superabsorbent Hydrogels Containing Silver Nanoparticles.

105. Lee et al., KR patent 10-200-0022813 (2005), Synthesis of Superabsorbent polymer beads.

106. Lee and Hahm, *Appl. Chem. Eng*., Vol. 21, No. 5, October 2010, 488-494.

107. Sannino et al., Journal of Applied Polymer Science, Vol. 91, 3791–3796 (2004), Water and synthetic urine sorption capacity of cellulose-based hydrogels under a compressive stress field.

108. Sannino et al., *Materials* 2009, *2*, 353-373, Biodegradable Cellulose-based Hydrogels: Design and Applications.

109. Mabilleau et al., *Journal of Biomedical Materials Research Part A*, Vol. 77A, Issue 1, 35–42, 2006.

110. Belmares, M.; Blanco, M.; Goddard, W. A.; Ross, R. B.; Caldwell, G.; Chou, S. h.; Pham, J.; Olofson, P. M.; Thomas, C. "Hildebrand and Hansen Solubility Parameters from Molecular Dynamics with Applications to Electronic Nose Polymer Sensors", *Journal of Computational Chemistry* 25, 1814-1826, 2004.

111. http://www.sigmaaldrich.com/

112. Chen, Z.; Liu, M; Qi, X. "Synthesis and Properties of a Superabsorbent Polymer Prepared by Copolymerization of sodium acrylate with sodium 1-(acryloyloxy)propan-2-yl phosphate", *Macromolecular Reaction Engineering*, 2007, 1, 275-283.

113. IUPAC Definition in Compendium of Chemical Terminology (IUPAC Gold Book).

114. https://en.wikipedia.org/wiki/Degree_of_polymerization.

115. Huang, Y.; Zeng, M.; Ren, J.; Wang, J.; Fan, L.; Xu, Q. "Preparation and swelling properties of graphene oxide/poly(acrylic acid-co-acrylamide) super-absorbent hydrogel nanocomposites", *Colloids and Surfaces A: Physicochemical and Engineering Aspects* 401 (2012) 97– 106.

116. Raju, K. M.; Raju, P.; Mohan, Y. M. "Synthesis and Water Absorbency of Crosslinked Superabsorbent Polymers", *Journal of Applied Polymer Science*, Vol. 85, 1795–1801 (2002).

117. Kabiri, K.; Omidian, H.; Hashemi, S.A.; Zohuriaan-Mehr, M. J. "Synthesis of fast-swelling superabsorbent hydrogels: effect of crosslinker type and concentration on porosity and absorption rate", *European Polymer Journal* 39 (2003) 1341–1348.

118. Hirakata, H. A.; Takatsuki, T. M.; Kyoto, S. K. "Process for preparing porous and water absorbent resin", US patent 5210159.

119. Stanley, Jr., F. W.; Lamphere, J. C.; Chonde, Y. "Suspending agent for the suspension polymerization of water soluble monomers (DOW)", US patent 4708997 (1987).

120. Kakogawa, M. N.; Akashi, S. O.; Himeji; T. Y.; Kyoto, N.; Tanaka, H.; Sakamoto, Y. "Process for producing a water absorbent resin (Seitetsu Kagaku Co., Ltd.)", US patent 4683274 (1987).

121. Omidian, H.; Hashemi, S. A.; Sammes, P. G.; Meldrum, I. "Modified acrylic-based superabsorbent polymers (dependence on particle size and salinity)", *Polymer* 40 (1999) 1753–176.

122. Omidian, H.; Zohuriaan-Mehr, M. J.; Bouhendi, H. "Polymerization of sodium acrylate in inverse-suspension stabilized by sorbitan fatty esters", *European Polymer Journal* 39 (2003) 1013–1018.

123. Choudhary, M. S. "Inverse suspension polymerization of partially neutralized and lightly cross-linked acrylic acid: effect of reaction parameters", *Macromolecular Symposium* 2009, 277, 171–176.

124. Omidian, H.; Rocca, J. G.; Park, K. "Advances in superporous hydrogels", *Journal of Controlled Release* 102 (2005) 3-12.

125. Kabiri, K.; Zohuriaan-Mehr, M. J. "Porous superabsorbent hydrogel composites: Synthesis, morphology and swelling rate", *Macromolecular Materials and Engineering* 2004, 289, 653–661.

126. Silva, J. M.; Bautista, F.; Sanchez-Dı´az, J. C.; Nuno-Donlucas, S. M.; Puig, J. E.; Hernandez, E. "Synthesis of poly (sodium acrylate) nanogels via semicontinuous inverse heterophase polymerization", *Macromolecular Reaction Engineering* 2015, 9, 125–131.

127. Zhou, W.; Zhang, Y.; Jin, K.; Qiu, X.; Ren, X.; Hu, S.; Zhang, F. "Synthesis and Characterization of Functionalized Acrylic-Acrylamide-Based Superabsorbent Gels", *Journal of Applied Polymer Science*, Vol. 114, 2828–2836 (2009).

128. Zhiquiang, S.; Huigen, Y.; Zuren, P. "Studies on the rheological behavior of high-impact polystyrene prepolymerizing systems", *Journal of Applied Polymer Science* 1986, 32, 3349-3369.

129. Lazrak, N.; Le Bolay, N.; Ricard, A. "Droplet stabilization in high holdup fraction suspension polymerization reactors", *European Polymer Journal* 1998, 34, 1637-1647.

130.   Fenouillot, F.; Terrisse, J.; Rimlinger, T.; "Experimental study and simulation of the polymerization of methyl methacrylate at high temperature in a continuous reactor", *Journal of Applied Polymer Science* 2001, 79, 2038-2051.

131.   Keramopoulos, A.; Kiparissides, C. "Mathematical modeling of diffusion-controlled free-radical terpolymerization reactions", *Journal of Applied Polymer Science* 2003, 88, 161-176.

132.   Marten, F. L.; Hamielec, A. E. "High-conversion diffusion-controlled polymerization of styrene", *Journal of Applied Polymer Science* 1982, 27, 489-505.